

Young researchers

Engineering Applications

Proceedings T-1

MARROQUÍN-DE JESÚS, Ángel
CASTILLO-MARTÍNEZ, Luz Carmen
OLIVARES-RAMÍREZ, Juan Manuel
ÁLVAREZ-ORTEGA, Annel Angelia

Coordinators

ECORFAN®

Coordinators

MARROQUÍN-DE JESÚS, Ángel. PhD
CASTILLO-MARTÍNEZ, Luz Carmen. PhD
OLIVARES-RAMÍREZ, Juan Manuel. PhD
ÁLVAREZ-ORTEGA, Annel Angelia. PhD

Editor in Chief

VARGAS-DELGADO, Oscar. PhD

Executive Director

RAMOS-ESCAMILLA, María. PhD

Editorial Director

PERALTA-CASTRO, Enrique. MsC

Web Designer

ESCAMILLA-BOUCHAN, Imelda. PhD

Web Designer

LUNA-SOTO, Vladimir. PhD

Editorial Assistant

TREJO-RAMOS, Iván. BsC

Philologist

RAMOS-ARANCIBIA, Alejandra. BsC

ISBN: 978-607-8948-16-1

ECORFAN Publishing Label: 607-8534

PJIAI Control Number: 2023-01

PJIAI Classification (2023): 10262723-0101

©ECORFAN-México, S.C.

No part of this writing protected by the Federal Copyright Law may be reproduced, transmitted or used in any form or by any means, graphic, electronic or mechanical, including, but not limited to, the following: Quotations in articles and bibliographic commentaries, of radio or electronic journalistic data compilation. For the effects of articles 13, 162,163 fraction I, 164 fraction I, 168, 169,209 fraction III and other relative of the Federal Copyright Law. Violations: Being compelled to prosecution under Mexican copyright law. The use of general descriptive names, registered names, trademarks, in this publication does not imply, even in the absence of a specific statement, that such names are exempt from the relevant protection in laws and regulations of Mexico and therefore free for general use by the international scientific community. PJIAI is part of Ecorfan-Mexico, S.C., E: 94-443.F:008-(www.ecorfan.org).

Proceedings

Definition of Proceedings

Scientific Objectives

To support the International Scientific Community in its written production of Science, Technology and Innovation in the CONAHCYT and PRODEP research areas, respectively, in the following sub-disciplines: Tourism Business Administration-Health Institutions Administration-Project Management and Evaluation-Sustainable and Protected Agriculture-Agro-Food-Agrobiotechnology-Agroforestry-Agroindustrial-Agronomy-Agrotechnology-Anthropology-. Archaeology-Architecture-Art and Design-Biology-Marine Biology and Watershed Management-Biomedical-Biotechnology-Botany-Cardiology - Communication Sciences -Earth Sciences-Business Sciences-Food Science and Technology-Dental Surgeon- Accounting-Criminalistics and Biochemistry -Criminology and Biotechnology -Biomedical and Biomedical-Biotechnology-Botany-Cardiology Accounting-Criminalistics and Forensic Sciences-Civil Law-Tax Law-Human Rights-Business Development-Diabetes-Graphic Design-Industrial Design and Fashion-Econometry-Physical Education and Sports Science-Education and Teaching-Electronics and Telecommunications- Renewable Energies-Nursing-Pharmacobiology-Finance-Food Genomics-Food Genomics-Geosciences-Gerontology-SMEs Management-Urban Management-Humanities-Food Industries-Computer Science Administrative Informatics-Aeronautical Engineering- Biochemical Engineering-Pharmacobiology-Finance-Food Genomics-Geosciences-Gerontology-Aeronautical Engineering- Biochemical Engineering-Petrochemical Engineering- Biochemical Engineering-Pharmaceutical Engineering Biochemical Engineering-Petroleum Engineering-Agribusiness Engineering-Forestry Engineering-Industrial Engineering-Chemical Engineering-Chemical Engineering-Agricultural Sustainable Innovation-Language and Culture-Logistics and Transportation-Industrial Maintenance-Petroleum Maintenance-Aeronautical Manufacturing-Applied Mathematics-Automotive Mechanics-Mechatronics-Medicine-Marketing-Industrial Metrology-Mining-Nanotechnology-Nephrology-International Business-Nutrition-Pediatrics-Industrial Processes-Industrial Chemistry-Industrial Chemistry- Chiropractic-Natural Resources-Robotics-Industrial Safety and Ecology-Public Safety and Forensic Sciences-Industrial Safety and Automation-Automotive Systems-Computer Systems-Quality Systems-Agricultural Production Systems-Sociology-Environmental Technology-Pharmaceutical Technology-Bio-food Technologies-Information Technologies-Information and Communication Technologies-Manufacturing Technologies-Telematics-Physical Therapy-Topography and Hydrology-Tourism and Zootechnics.

ECORFAN-Mexico, S.C. is a Scientific and Technological Company in contribution to the formation of Human Resources focused on the continuity in the critical analysis of International Research and is attached to the RENIECYT of CONAHCYT with number 1702902, its commitment is to disseminate research and contributions of the International Scientific Community, academic institutions, agencies and entities of the public and private sectors and contribute to the linkage of researchers who perform scientific activities, technological developments and training of specialized human resources with governments, businesses and social organizations.

Encourage the dialogue of the International Scientific Community with other study centers in Mexico and abroad and promote a wide incorporation of academics, specialists and researchers to the serial publication in Science Niches of Autonomous Universities - State Public Universities - Federal IES - Polytechnic Universities - Technological Universities - Federal Technological Institutes - Teacher Training Colleges - Decentralized Technological Institutes - Intercultural Universities - S&T Councils - CONAHCYT Research Centers.

Scope, Coverage and Audience

Proceedings is a product edited by ECORFAN-Mexico, S.C. in its Holding with repository in Mexico, it is a refereed and indexed scientific publication. It admits a wide range of contents that are evaluated by academic peers by the Double-Blind method, on topics related to the theory and practice of the CONAHCYT and PRODEP research areas respectively with diverse approaches and perspectives, which contribute to the dissemination of the development of Science, Technology and Innovation that allow arguments related to decision making and influence the formulation of international policies in the field of Sciences. The editorial horizon of ECORFAN-Mexico® extends beyond academia and integrates other segments of research and analysis outside this field, as long as they meet the requirements of argumentative and scientific rigor, in addition to addressing issues of general and current interest of the International Scientific Society.

Editorial Board

CENDEJAS - VALDEZ, José Luis. PhD
Universidad Politécnica de Madrid

DE LA ROSA - VARGAS, José Ismael. PhD
Universidad París XI

HERNÁNDEZ - PRIETO, María de Lourdes. PhD
Universidad Gestalt

LÓPEZ - LÓPEZ, Aurelio. PhD
Syracuse University

VEGA - PINEDA, Javier. PhD
University of Texas

VAZQUEZ - MARTINEZ, Ernesto. PhD
University of Alberta

ROBLEDO - VEGA, Isidro. PhD
University of South Florida

ROCHA - RANGEL, Enrique. PhD
Oak Ridge National Laboratory

LAGUNA, Manuel. PhD
University of Colorado

DIAZ - RAMIREZ, Arnoldo. PhD
Universidad Politécnica de Valencia

Arbitration Board

RODRÍGUEZ - DÍAZ, Antonio. PhD
Centro de Investigación Científica y de Educación Superior de Ensenada

JUAREZ - SANTIAGO, Brenda. PhD
Universidad Internacional Iberoamericana

CUAYA - SIMBRO, German. PhD
Instituto Nacional de Astrofísica, Óptica y Electrónica

INZUNZA - GONÁLEZ, Everardo. PhD
Universidad Autónoma de Baja California

AVILÉS - COYOLI, Katia Lorena. PhD
Instituto Tecnológico de Pachuca

CASTRO - ENCISO, Salvador Fernando. PhD
Universidad Popular Autónoma del Estado de Puebla

CALDERÓN - PALOMARES, Luis Antonio. PhD
Universidad Popular Autónoma del Estado de Puebla

MARTÍNEZ - RAMÍRES, Selene Marisol. PhD
Universidad Autónoma Metropolitana

NAVARRO - ÁLVEREZ, Ernesto. PhD
Centro de Investigación y de Estudios Avanzados

AMARO - ORTEGA, Vidblain. PhD
Universidad Autónoma de Baja California

Assignment of Rights

By submitting a Scientific Work to ECORFAN Proceedings, the author undertakes not to submit it simultaneously to other scientific publications for consideration. To do so, the author must complete the Originality Form for his or her Scientific Work.

The authors sign the Authorisation Form for their Scientific Work to be disseminated by the means that ECORFAN-Mexico, S.C. in its Holding Mexico considers pertinent for the dissemination and diffusion of their Scientific Work, ceding their Scientific Work Rights.

Declaration of Authorship

Indicate the name of 1 Author and a maximum of 3 Co-authors in the participation of the Scientific Work and indicate in full the Institutional Affiliation indicating the Unit.

Identify the name of 1 author and a maximum of 3 co-authors with the CVU number - PNPC or SNI-CONAHCYT - indicating the level of researcher and their Google Scholar profile to verify their citation level and H index.

Identify the Name of 1 Author and 3 Co-authors maximum in the Science and Technology Profiles widely accepted by the International Scientific Community ORC ID - Researcher ID Thomson - arXiv Author ID - PubMed Author ID - Open ID respectively.

Indicate the contact for correspondence to the Author (Mail and Telephone) and indicate the Contributing Researcher as the first Author of the Scientific Work.

Plagiarism Detection

All Scientific Works will be tested by the PLAGSCAN plagiarism software. If a Positive plagiarism level is detected, the Scientific Work will not be sent to arbitration and the receipt of the Scientific Work will be rescinded, notifying the responsible Authors, claiming that academic plagiarism is typified as a crime in the Penal Code.

Refereeing Process

All Scientific Works will be evaluated by academic peers using the Double-Blind method. Approved refereeing is a requirement for the Editorial Board to make a final decision which will be final in all cases. MARVID® is a spin-off brand of ECORFAN® specialised in providing expert reviewers all of them with PhD degree and distinction of International Researchers in the respective Councils of Science and Technology and the counterpart of CONAHCYT for the chapters of America-Europe-Asia-Africa and Oceania. The identification of authorship should only appear on a first page, which can be removed, in order to ensure that the refereeing process is anonymous and covers the following stages: Identification of ECORFAN Proceedings with their author occupancy rate - Identification of Authors and Co-authors - PLAGSCAN Plagiarism Detection - Review of Authorisation and Originality Forms-Assignment to the Editorial Board - Assignment of the pair of Expert Referees - Notification of Opinion - Statement of Observations to the Author - Modified Scientific Work Package for Editing - Publication.

ECORFAN Science Engineering Applications

Volume I

The Proceedings will offer volumes of selected contributions from researchers who contribute to the scientific dissemination activity of the Knowledge Society for their area of research in the role of the institution to the challenges of the Knowledge Society. In addition to having a total evaluation, in the hands of the directors of the Knowledge Society collaborates with quality and timeliness in their chapters, each individual contribution was refereed to international standards (RENIECYT - LATININDEX - DIALNET - ResearchGate - DULCINEA - CLASE - Sudoc - HISPANA - SHERPA - UNIVERSIA - REBID -e REVISTAS - Scholar Google - DOI - Mendeley), the Proceedings thus proposes to the academic community, recent reports on new developments in the most interesting and promising areas of research on the role of the institution in the challenges of the Knowledge Society.

For future volumes:

<http://www.ecorfan.org/proceedings/>

MARROQUÍN-DE JESÚS, Ángel. PhD
CASTILLO-MARTÍNEZ, Luz Carmen. PhD
OLIVARES-RAMÍREZ, Juan Manuel. PhD
ÁLVAREZ-ORTEGA, Annel Angelia. PhD

Coordinators

Young Researchers
Engineering Applications
Proceedings

T-I

CIERMMI - Mexico.

October 2023.

DOI: 10.35429/P.2023.1.1.116

Prologue

As part of human evolution and with the desire to have a healthy and sustainable planet, the use and automation of renewable energies is becoming a practice that is here to stay, not only in large sectors but also as a way of life for individuals. At present, solar energy has an exponential growth above any other renewable source because by its nature it is abundant and inexhaustible, capable of supplying the earth. enough to become a powerful industry. Let's promote positive changes to the energy transition, through projects that have as a key factor the use of renewable energies. key factor in the use of clean economies and thus ensure the sustainability of people and companies. sustainability of people and companies. The future of renewable energies is promising, and innovation will be fundamental to continue advancing. continue to move forward.

CIERMMI 2023, thank you for creating spaces where knowledge and experiences are shared experiences.

ALVAREZ ORTEGA - Annel Angelia
Universidad Tecnológica de San Juan del Río

It contains ten refereed chapters dealing with these issues in Engineering Applications.

As the first chapter, *ORTEGA, HERNÁNDEZ, ALVARADO and GÓMEZ* introduce us to the design and construction of CanSat educational satellites. *BARRERA, VAQUERO, JAEN and MARROQUÍN* present the design of an automated cleaning system for 79.2 KW photovoltaic power plant panel. *JAEN, VAQUERO, BARRERA and MARROQUIN* innovate design of a circuit for an automated system used for cleaning the panels of the 79.2KW photovoltaic power plant. *RIVAS, GAMBOA and VERÁSTEGUI* introduce us to the educational mechatronics and applied to the design of an automated prototype for obtaining thin films. *SÁNCHEZ, HERNÁNDEZ, CASTILLO and ÁLVAREZ* present the mobile laboratory for FVM analysis. *MURGUIA, LANDEROS, REYES and PEREZ* present the evaluation of obtaining biohydrogen by different fermentation methods. *REYES, REYES, MURGUIA and PEREZ* introduce us to the evaluation of substrates for biopolymer processing. *CASTAÑÓN, CUENCA and HERNÁNDEZ* review the annual emissions of greenhouse gases of motor vehicles in the Academic Unit Valle de las Palmas UABC. *GARCÍA, ONTIVEROS, MADRID and ALVAREZ* perform the comparison of gasoline, hybrid and electric vehicles. Finally, *SUAREZ, GONZALEZ, SANCHEZ and GARCIA* present the Importance of the development of companies that manage government administrative services in support of the senior citizens of Villa Guerrero.

We would like to thank the anonymous reviewers for their reports and many others who contributed greatly to the publication in these proceedings by reviewing the manuscripts that were submitted. Finally, we wish to express our gratitude to the CIERMMI in the process of preparing this edition of the volume.

*Marroquín-De Jesús, Ángel
Castillo-Martínez, Luz Carmen
Olivares-Ramírez, Juan Manuel
Álvarez-Ortega, Annel Angelia*

Volume Coordinators

Content	Page
Engineering Sciences	
Design and construction of CanSat educational satellites	1-16
Design of an automated cleaning system for 79.2 KW photovoltaic power plant panel	17-23
Design of a circuit for an automated system used for cleaning the panels of the 79.2KW photovoltaic power plant	24-36
Educational mechatronics and applied to the design of an automated prototype for obtaining thin films	37-45
Mobile laboratory for FVM analysis	46-60
Evaluation of obtaining biohydrogen by different fermentation methods	61-70
Biotechnology and Agricultural Sciences	
Evaluation of substrates for biopolymer processing	71-78
Physics-Mathematics and Earth Sciences	
Annual emissions of greenhouse gases of motor vehicles in the Academic Unit Valle de las Palmas UABC	79-88
Comparison of gasoline, hybrid and electric vehicles	89-106
Social Sciences	
Importance of the development of companies that manage government administrative services in support of the senior citizens of Villa Guerrero	107-116

Design and construction of CanSat educational satellites

Diseño y construcción de satélites educativos CanSat

ORTEGA-ALVAREZ, Eduardo†*, HERNÁNDEZ-TORRES, Martha, ALVARADO-ANTÚNEZ, José Alfredo and GÓMEZ-ROA, Antonio

Instituto Politécnico Nacional, México.

Universidad Autónoma de Baja California, México.

ID 1st Author: *Eduardo, Ortega-Alvarez* / **ORC ID:** 0000-0002-3142-360X

ID 1st Co-author: *Martha, Hernández-Torres* / **ORC ID:** 0000-0003-3490-8255

ID 2nd Co-author: *José Alfredo, Alvarado-Antúnez* / **ORC ID:** 0009-0004-2258-7452

ID 3rd Co-author: *Antonio, Gómez-Roa* / **ORC ID:** 0000-0002-3548-0740, **CVU CONAHCYT ID:** 395899

DOI: 10.35429/P.2023.1.1.16

E. Ortega, M. Hernández, J. Alvarado and A. Gómez

* eortegaa1500@alumno.ipn.mx

Á. Marroquín, L. Castillo, J. Olivares and A. Álvarez (AA. VV.). Young Researchers. Engineering Applications - Proceedings-©ECORFAN-México, Queretaro, 2023.

Abstract

Artificial satellites play a key role in research and modern communications serving the purpose of gathering data and transmitting it back to Earth. However, due to its complexity and strict quality standards, the design and construction of a satellite can span up to six years, making it challenging to teach this process to university students. Which is why the development of pico-satellites like CanSats provides students with the opportunity to learn the operation and basic systems of a satellite and their common launch vehicles on a small scale and in a short period of time. This paper explains the design and manufacturing process of a CanSat and a model rocket and their launch in the Mexican desert to gather data on the atmosphere throughout its descent, including height, pressure, air quality, latitude, and longitude. Additionally, it gives a brief explanation of the interface and database using Lab VIEW and Excel to plot all the collected variables.

Satellite, CanSat, Launch vehicle, Model rockets, Data, Atmosphere, Complexity, Variables, Systems, Communications, Standards, Creation, Drones, Latitude

Resumen

Los satélites artificiales juegan un importante papel en la investigación y las comunicaciones modernas, sirviendo el propósito de recolectar datos y enviarlos de vuelta a la Tierra. Sin embargo, debido a su complejidad y estrictos estándares de calidad, el desarrollo de un satélite puede durar hasta seis años, lo que dificulta enseñar este proceso a estudiantes universitarios. Es por eso por lo que el desarrollo de pico-satélites como CanSats brinda a los estudiantes la oportunidad de aprender el funcionamiento y los sistemas básicos de un satélite y sus vehículos de lanzamiento comunes a pequeña escala y en un corto periodo de tiempo. Este artículo describe cómo se construyeron un modelo de cohete y un CanSat y cómo se lanzaron en el desierto mexicano para recopilar datos sobre la atmósfera a lo largo de su descenso, incluida la altura, la presión, la calidad del aire, la latitud y la longitud. Adicionalmente, proporciona una breve explicación de la interfaz y la base de datos usando LabVIEW y Excel para graficar todas las variables.

Satélite, CanSat, Vehículo de lanzamiento, Cohete modelo, Datos, Atmósfera, Complejidad, Variables, Sistemas, Comunicaciones, Estándares, Creación, Drones, Latitud

1.1 Introduction

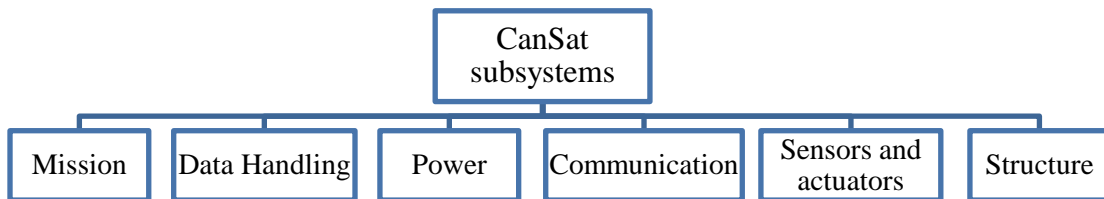
Artificial satellites hold significant importance in today's world. The main objective of these systems is data collection and signal transmission while placed in Earth orbit. Nonetheless, due to their remote location, providing maintenance and addressing repair issues is an arduous and unfeasible task. Hence, in their design, they must be able to withstand extreme temperatures, guarantee their survival in the case of space debris impact, and have a useful life of at least fifteen years (Maral, Bousquet, & Sun, 2020).

Given its complexity and intricate nature, the manufacturing of a satellite typically requires around six years, posing challenges for its incorporation into university-level education. For this reason, the development of a pico-satellite such as a CanSat represents an easily accessible option that enables students to acquire hands-on experience in conducting a space project. They can choose their mission objectives, design and integrate subsystems, prepare for a launch and collect, analyze and process the gathered data, all within a short period of time.

A CanSat (Can-Satellite) is a pico-satellite with dimensions like those of a 350 ml soda can and a weight of under 350 grams. Because of its small scale and weight, its primary purpose is to provide students with an opportunity to acquire fundamental concepts related to the design and construction of pico-satellites. Professor Robert Twiggs from Stanford University first proposed the CanSat project during the University Space Systems Symposium (USSS) held in Hawaii in November 1998.

Opposed to traditional satellites, CanSats typically function within the Earth's atmosphere and their release altitude varies depending on the mission goals. Along this descent trajectory, they execute specific missions, which usually involve tasks such as capturing images and/or video, collecting stored data, or transmitting information to an Earth station, among other functions. (University Space Engineering Consortium (UNISEC), 2017). In order to meet mission requirements, the CanSat system needs to be divided into distinct subsystems. Figure 1.1 provides a visualization of the CanSat's subsystems.

Figure 1.1 Main subsystems of a CanSat



Source: Own elaboration

The Mission subsystem holds significant importance, as it defines the main objective of the CanSat during both launch and descent, it also communicates the intended investigation, measurement, capture, observation, or analysis. Therefore, it becomes essential to establish three success criteria: minimal, medium, and complete success. Determining the mission involves considering factors based on feasibility and available resources, such as tools, laboratories, test systems, experience levels, components, in addition to the constraints commonly imposed in competitions, like cost, dimensions, energy consumption, weight, atmospheric variables, and more. The command and data subsystem relies on physical components that facilitate the deployment of data at the software level of picosatellite operation. It comprises a flight computer that presents collected data through an interface, a data reception system, and, in some instances, the transmission of commands. The power subsystem focuses on providing the energy requirements to the system in compliance with a power budget depending on the different modes of operation. The main components are usually controllers, switches, power sources such as photovoltaic cells and batteries. The communication subsystem consists of a receiver, transmitter, channel, antenna, and communication protocol. In summary, it enables the transmission and reception of data or commands essential for the mission. It aids in understanding the operational status and recovery point of the CanSat. The attributes of internal components, such as weight, dimensions, temperature, humidity, current, and radio wave permeability, establish the materials, volume, and dimensions of the CanSat structure responsible for carrying them throughout the mission. (Agencia Espacial Mexicana (AEM), 2018)

Currently, the launch system is not only based on high-powered model rockets, other alternatives for launch vehicles are also weather balloons, model aircraft and quad copters. The type of launch device is dependent on factors such as the mission, height, weather conditions, and structure. Table 1.1 gives a description of some of the common launch devices used for pico-satellites.

Table 1.1 Typical launch devices for CanSat

Launch device	Description
Rocket model	It is a scale rocket made of lightweight and heat resistant materials that uses an engine of a liquid or solid fuel to be propelled during launch. The classification of the engine is based on the thrust it provides to the rocket.
Weather balloons	These latex or synthetic rubber balloons are inflated with hydrogen or helium. For CanSats, they are launched to attain a minimum height of 200 meters and a maximum of 4000 meters, ensuring the maintenance of stable and optimal conditions during ascent.
Model Aircraft.	Small scale aircraft consisting of a transmitter, receiver and servos, the maximum flight height is dependent on the range of the radio signal.
Quadcopters	Multi-rotor capable of lifting and propelling with 4 rotors, 2 rotating clockwise and the other pair counterclockwise.

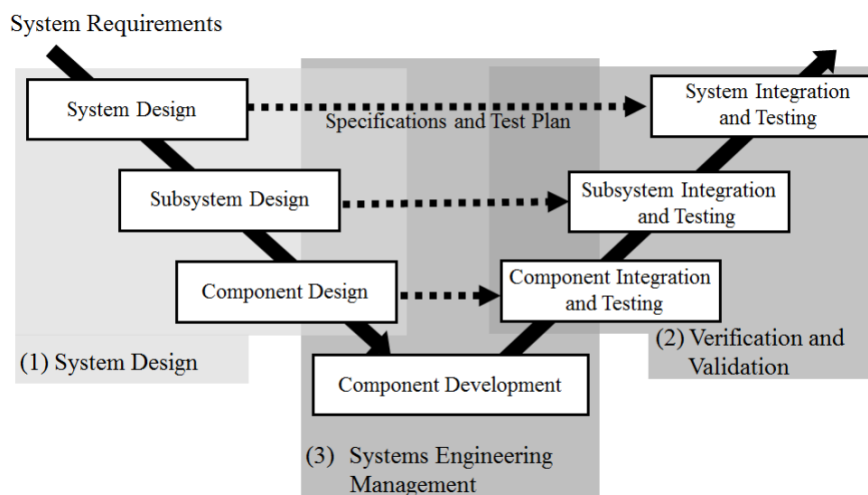
Source: Own elaboration

This article explains the process of designing and constructing a CanSat, along with detailing the model rocket employed for launch. To begin with, Section 1.2 describes the mission and main goals, as well as the Concept of Operation. Subsequently, Section 1.3 gives details about the characteristics of the BME680, NEO-7M, MQ-135, GY-91 sensors, which measure altitude, temperature, pressure, latitude, longitude, acceleration, position, among other atmospheric variables. Moving on to Section 1.4, it shows the communication subsystem and the main properties of the transceivers, such as their frequency and protocol. Transitioning to Section 1.5, it addresses the programming and integration of the microcontroller with the sensors. In Section 1.6, it illustrates the connection diagram for the electronic components, and Section 1.7 explains their physical integration to fit within the structure of the pico-satellite. Turning attention to Section 1.8, the article provides an explanation of the structure, the materials employed, and the underlying reasons for its architecture. Transitioning to Section 1.9, it details the design and manufacturing of the launch vehicle. Lastly, Section 1.10 elaborates on the process of development of the interface. Finally, the article gives a brief explanation of the results and conclusions of the project.

1.2 Mission objectives, success criteria and concept of operation

To achieve a comprehensive project perspective and maximize the likelihood of success, it is important to apply the principles of Systems Engineering throughout the development process. Different approaches exist for depicting and planning project lifecycles. The approach adopted for this project's development utilizes the V Model, as illustrated in Figure 1.2.

Figure 1.2 V-model in systems engineering



Source: (University Space Engineering Consortium (UNISEC), 2017)

The initial stage of project development involves defining the mission objectives and three success criteria: minimum success, medium success, and full success.

First, the mission objectives are defined. These objectives are to reach a height of 500 meters, release the CanSat to begin the descent and collect data, and process and transmit atmospheric readings from sensors to the ground base.

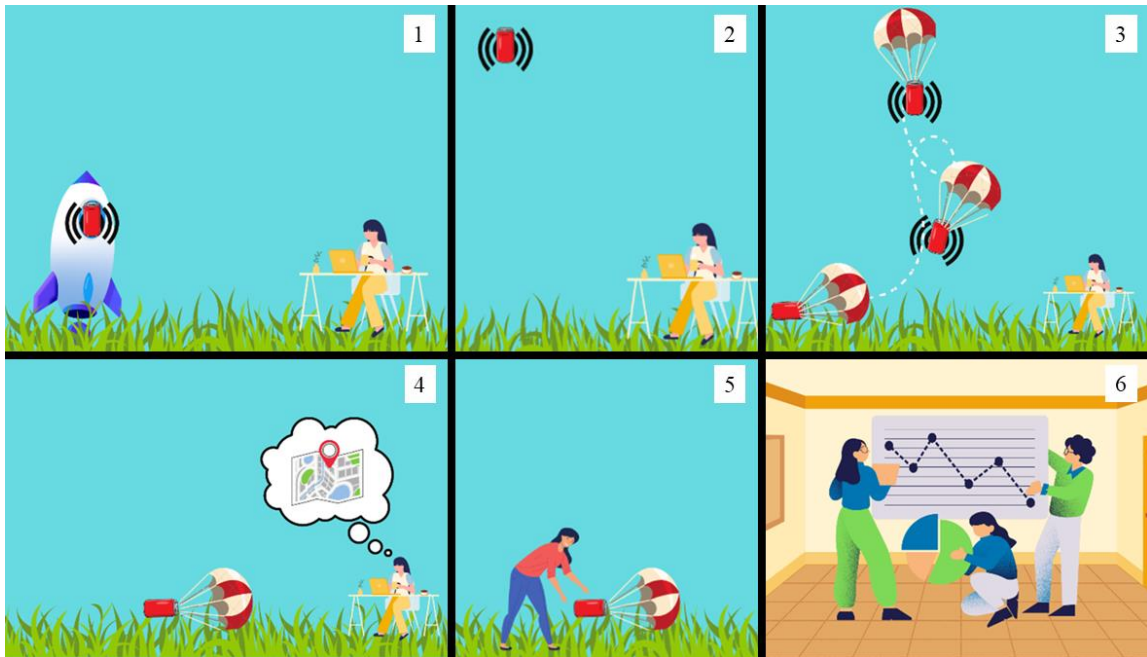
Second, the three success criteria are defined. The minimum success criteria is to reach a height of 500 meters, release the CanSat from the lifting device, and successfully deploy the parachute. The medium success criteria is to begin taking atmospheric readings periodically upon descent, transmit readings to ground base, and retrieve the CanSat. The full success criteria is to obtain readings with true data, useful evidence, and preserve the integrity of the CanSat upon recovery.

The Concept of Operation is illustrated in Figure 1.3 and it is described as follows:

- First, the CanSat is energized, initiating data transmission.
- Next, it is mounted onto the lifting device, which in this instance is a model rocket.

- Then, the CanSat is elevated to a height of 500 meters and deployed at its peak altitude.
- At this point, the parachute is deployed, initiating the descent phase. The ground computer receives transmitted data from the CanSat throughout its descent. The CanSat lands safely.
- Finally, the coordinates of the final recorded position are verified. The CanSat is retrieved and the collected data is analyzed.

Figure 1.3 Concept of operation



Source: Own elaboration

1.3 Sensors

The pico-satellite's mission requirements dictated the selection of its sensors, including the NEO-7M, GY-91, BME-680, and MQ-135. These sensors measure a range of atmospheric parameters, such as air quality, atmospheric pressure, humidity, altitude, latitude, orientation, acceleration, and magnetic fields. The following sections provide the main features and characteristics of each sensor.

1.3.1 BME680

The BME6880 is a sensor that can measure air quality by integrating the measurement of several atmospheric variables, such as gas, humidity, relative humidity, barometric pressure, air quality, and temperature from $-40\text{ }^{\circ}\text{C}$ to $85\text{ }^{\circ}\text{C}$. It offers several advantages, including its compact size, low power consumption, stability, and strong electromagnetic compatibility performance. (Bosch Sensortec GmbH, 2022).

In addition, the device can identify a broad spectrum of gases, primarily volatile organic compounds (VOCs), by absorbing them into its sensitive layer of metal oxide. The sensor reacts to most VOCs and other pollutants and can measure their cumulative presence in the surrounding air. The sensor displays the VOC values using the Air Quality Index (AQI), which ranges from 0 (clean air) to 500 (very polluted air). Table 1.2 shows the AQI values and their corresponding descriptions based on the air quality scale (Secretaría del Medio Ambiente, 2018).

Finally, the most common uses of the sensor are to measure and indicate air quality and well-being in indoor environments.

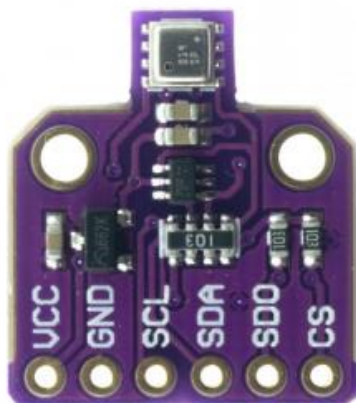
Table 1.2 Air quality classification index and color coding

Index Value	Classification	Precautions to protect yourself from ozone
0 – 50	Good	None
51 – 100	Moderate	Extremely sensitive individuals should consider limiting prolonged exertion outdoors.
101 – 150	Harmful to the health of sensitive groups	The elderly, children, active adults, and people with respiratory conditions such as asthma should avoid prolonged outdoor exertion and the rest of the population should limit their exposure.
151 – 200	Harmful to health	The elderly, children and people with respiratory diseases should avoid prolonged exertion in the open air and the rest of the population should limit their exposure.
201 – 300	Very harmful to health.	The entire population should avoid any outdoor effort.

Source: (Secretaría del Medio Ambiente, 2018)

The BME680 pin configuration is illustrated in Figure 4. The following are the pin descriptions:

- VCC: The supply voltage pin, which provides power to the sensor. The voltage range is 3.3-5 VDC.
- GND: The ground pin, which provides a common reference for all the signals.
- SCL: The clock pin, which is used to synchronize the data transfer between the sensor and the microcontroller. The SCL pin can be used with both the I2C and SPI protocols.
- SDA: The data pin, which is used to transmit and receive data between the sensor and the microcontroller. The SDA pin can be used with both the I2C and SPI protocols.
- SDO: The serial data output pin, which is used to transmit data from the sensor to the microcontroller. The SDO pin is only used with the SPI protocol.
- CS: The chip select pin, which is used to select the BME680 chip when communicating with multiple sensors. The CS pin is only used with the SPI protocol.

Figure 1.4 BME680 sensor module

Source: (Bosch Sensortec GmbH, 2022)

1.3.2 NEO-7M

The NEO-7M is a GNSS (Global Navigation Satellite Systems) module that provides GPS satellite positioning. Moreover, its main features are high sensitivity with a maximum navigation update rate of 10 Hz. Additionally, it boasts high integration capacity in a compact system and great synergy between its elements. Furthermore, the module chips are certified, providing reliability, which is an important aspect of their choice in the project. (u-blox, 2014). The module has four pins: VCC, GND, TXD, and RXD that are shown in Figure 1.5 and are described below (techmake, 2022):

- VCC is the power supply pin, which provides 3.3V to 5V power to the module.
- GND is the ground pin, which provides a common reference voltage for the module.
- TXD is the serial port transmission pin, which is used to transmit data from the module to the microcontroller.
- RXD is the serial port receive pin, which is used to receive data from the microcontroller.

Figure 1.5 NEO-7M module



Source:(techmake, 2022)

1.3.3 MQ-135

The MQ-135, an electrochemical air quality sensor that changes its resistance in response to different chemical compounds in the air, offers versatile capabilities. Notably, it can detect ammonia (NH₃), nitrogen oxides (NO_x), alcohol, benzene (C₆H₆), smoke, carbon dioxide (CO₂), sulfides, carbon monoxide (CO), and other harmful gases.

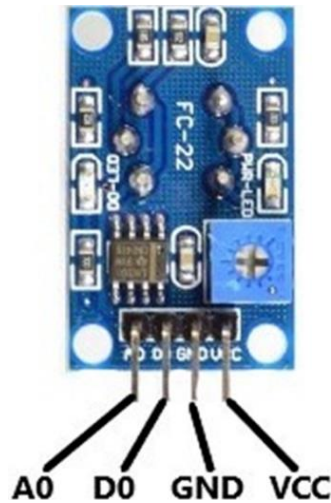
This module measures hazardous gases in parts per million (ppm), making it a valuable tool for air quality assessment. Its wide detection range of 10 to 1000 ppm makes it suitable for integration into air quality management systems across various settings, including residences, commercial buildings, offices, and industrial facilities dealing with hazardous gases. Additionally, the sensor operates effectively between -20 °C and 70 °C, ensuring reliable performance even in diverse environmental conditions. Remarkably, it weighs only 8 grams, enhancing its portability and ease of use.

In the specific project context, the MQ-135 was employed to record the air quality variable, which was quantified at ppm, demonstrating its adaptability and relevance for air quality monitoring.

The MQ-135 gas sensor has four connection pins, as shown in Figure 1.6. These pins are described below:

- Vcc: This pin is used to power the sensor. The operating voltage is typically 5V.
- Ground: This pin is used to connect the sensor to the system ground or reference.
- Digital output: This pin can be used to obtain a digital output from the sensor. The threshold value for the digital output can be set using the potentiometer.
- Analog output: This pin outputs an analog voltage of 0-5V, depending on the intensity of the gas.

Figure 1.6 MQ-135 module



Source: (Nawazi, 2021)

1.3.4 GY-91

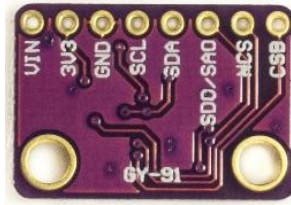
The GY-91 module incorporates two sensors, the IMU MPU9250 and the BMP280. The system integrates 10 degrees of freedom, which are manifested as a 3-axis gyroscope, a 3-axis accelerometer, a 3-axis magnetometer, and an altimeter. In addition, the implementation allowed for the acquisition of data from the gyroscope, accelerometer, temperature, pressure, and altitude. (Zago, 2017)

The IMU MPU9250 has a digital motion processor that accurately captures the fast and slow movements of 9 axes using complex algorithms. It has a programmable scale range of 250/500/1000/2000 degrees/s for the gyroscope, 2g/4g/8g/16g for the accelerometer, and $\pm 4800\mu\text{T}$ for the magnetometer.

Furthermore, the BMP280 is a barometric pressure sensor that is known for its exceptional accuracy and minimal power consumption. It operates within a range of 300 to 1100 hPa and offers impressive precision, linearity, long-term stability, high pressure resolution, high precision temperature, and digital filters. (Mechatronics, 2019).

The connection pins of the GY-91 are shown in Figure 1.7. They are described below:

- VIN: This pin supplies the GY-91 with 5V power.
- 3V3: This pin outputs 3.3V power.
- GND: This pin is the ground pin.
- SCL: This pin is the clock pin for the I2C and SPI protocols.
- SDA: This pin is the data pin for the I2C and SPI protocols.
- NCS: This pin is used to select the MPU-9250 chip when using the SPI protocol.
- CSB: This pin is used to select the BMP280 chip.

Figure 1.7 GY-91 module

Reference source: (Mechatronics, 2019)

1.4 Communication subsystem

Figure 1.8 showcases the XBee, a radio module utilized for establishing wireless connectivity among various devices. When implemented in the picosatellite, this module enables both data transmission and reception functionalities. The XBee module actively employs the IEEE 802.15.4 protocol operating at a frequency of 2.4Hz. This protocol facilitates the creation of either point-to-multipoint or point-to-point networks. These modules are particularly suited for applications demanding high data traffic, low latency, and precise communication timing. The module itself incorporates a reception and emission system for wireless data operation, commonly referred to as the coordinator and router (Digikey, 2009).

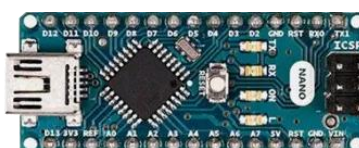
Figure 1.8 XBee module

Source: (Digikey, 2009)

For configuring, testing, and visualizing data on the XBee module, users typically turn to the cross-platform application known as XCTU. XCTU equips users with the essential tools needed for the effective operation of the XBee module. The primary objective behind the integration of the XBee module was to enable the wireless transmission of data collected from the sensors to a designated device, such as a computer.

1.5 Microcontroller

The pico-satellite uses the Arduino Nano microcontroller, as depicted in Figure 1.9. This electronic board measures 45mm x 18mm and is a practical choice given the size and weight constraints of the CanSat. It features an ATmega328P microchip and has 14 digital pins, 8 analog pins, 2 reset pins, and 6 power pins, offering similar power and connectivity capabilities as the Arduino Uno. The Arduino Nano also has a Mini-USB connector, Jack connector, and different header pins. It is worth noting that the Arduino Nano has the same memory space compared to the Arduino Uno. However, the Arduino Nano microcontroller is more than adequate to fulfill the memory requirements of the mission, which primarily focuses on data collection (Arduino, 2021).

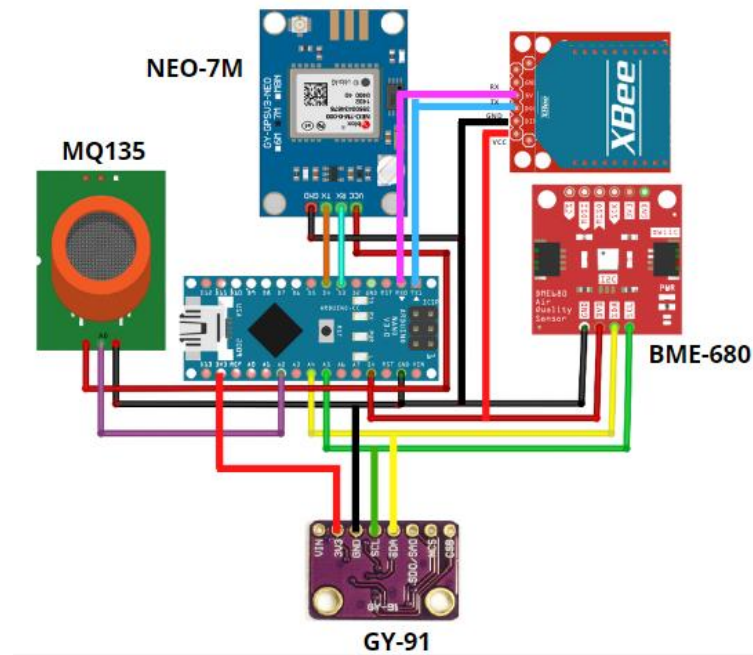
Figure 1.9 Arduino Nano

Source: (Arduino, 2021)

1.6 Electrical connections between modules

A proactive strategy was used to design the system integration of the CanSat, considering the individual descriptions of the sensor modules and the data transmission and reception components. This promoted seamless interaction. Figure 1.10 illustrates the schematic layout of the electrical connection network. The Arduino Nano Microcontroller was used to link all sensors and the XBee RF module, which facilitated programming.

Figure 1.10 Electrical connections of the wireless modules and sensors of the CanSat

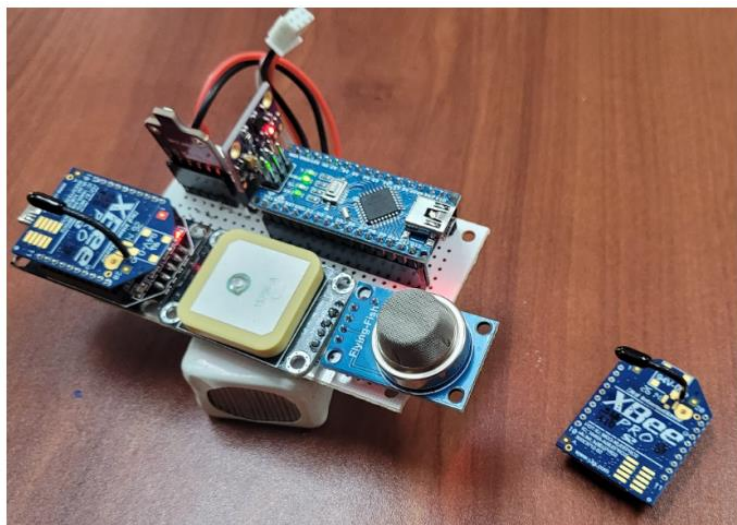


Source: Own elaboration. Fritzing v.0.9.3

1.7 Physical integration of electronic components

The physical integration of the components was made using a perforated board, as shown in Figure 1-11. The perforated board is ideal for this application as it already has pre-drilled holes which makes it easy to mount the components. The image shows the 12V Lipo battery as well, which is used to energize the system. The battery is connected to the Arduino Nano Microcontroller, which controls the operation of the sensors and the XBee RF module. The perforated board is an essential part of the CanSat, as it allows for the efficient and secure integration of all the components.

Figure 1.11 Integration of the sensors, microcontroller, battery and RF module in a perforated board



Source: Own elaboration

1.8 Structural subsystem

To facilitate the construction of the picosatellite, the utilization of PLA (polylactic acid) is essential. This material includes a slot for the insertion of a perforated card containing electronic components. In addition, the structural design incorporates a rectangular cavity specifically designed to accommodate the lithium polymer battery responsible for powering the system. Notably, for optimization, this structural model also integrates strategically placed holes within the external wall to effectively reduce weight (Figure 1.12).

Figure 1.12 PLA container used for the structural subsystem



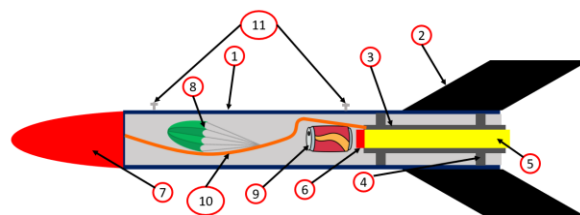
Source: Own elaboration

1.9 Launch vehicle

A launch vehicle assumes the responsibility of elevating the CanSat to a designated altitude and initiating its deployment. During the CanSat's development, a model rocket was designated to fulfill the role of the launch vehicle.

During the development of the CanSat, a model rocket was selected to serve as the launch vehicle. Model rockets are made of cardboard or fiberglass and have fins made of plastic, wood, cardboard, or fiberglass. The rocket's engine can be purchased commercially or made individually and can be disposable or reusable. The engine is fitted snugly within the engine mount, which transfers the thrust generated by the engine to the rocket's body. The upper segment of the engine houses the ejection charge, which is responsible for expelling the nose cone, recovery system, and payload. The recovery system helps to slow down the rocket's descent and typically uses a parachute. The payload is the CanSat itself. The nose cone is attached to the engine mount by a shock cord that must withstand the force from the ejection charge. Launch lugs are affixed along the rocket body's sides to secure the rocket to the launch rail. Figure 1.13 shows a visual representation of each component of a model rocket (Benson, 2021).

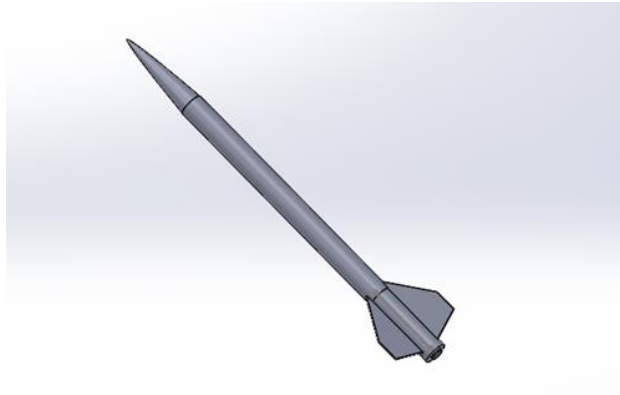
Figure 1.13 Parts of a model rocket. 1. Body of the rocket. 2. Fins. 3. Engine mount. 4. Washers to adjust engine. 5. Engine. 6. Engine explosive charge. 7. Nose cone. 8. Recovery system. 9. Payload. 10. Shock cord. 11. Rails of the rocket



Source: (Benson, 2021).

The rocket was designed using the OpenRocket software, a freely available program dedicated to model rocket design. This software allows users to distribute the weights of rocket components, specify the type of fins, and select the preferred engine brand. Figure 1.14 shows a CAD model of the rocket.

Figure 1.14 CAD model of the developed rocket



Source: Own elaboration. Solid Works, 2022

The rocket's construction involves the process of adhering layers of fiberglass with epoxy. To construct the rocket, fiberglass was applied to a PVC tube with the desired diameter, which had been enveloped in waxed paper. This allowed the fiberglass to be easily released. Flat components were then cut using band saws and jigsaws. These components were then refined to achieve the desired dimensions through sanding. The nose cone of the rocket was shaped using an existing mold. Figure 1.15 shows a visual representation of the manufacturing process.

Figure 1.15 Model rocket manufacturing process. From left to right: Applying epoxy to fiberglass in order to manufacture fins of the rocket. Cutting the fiberglass to the desired form. Body of the rocket. Rocket fully painted

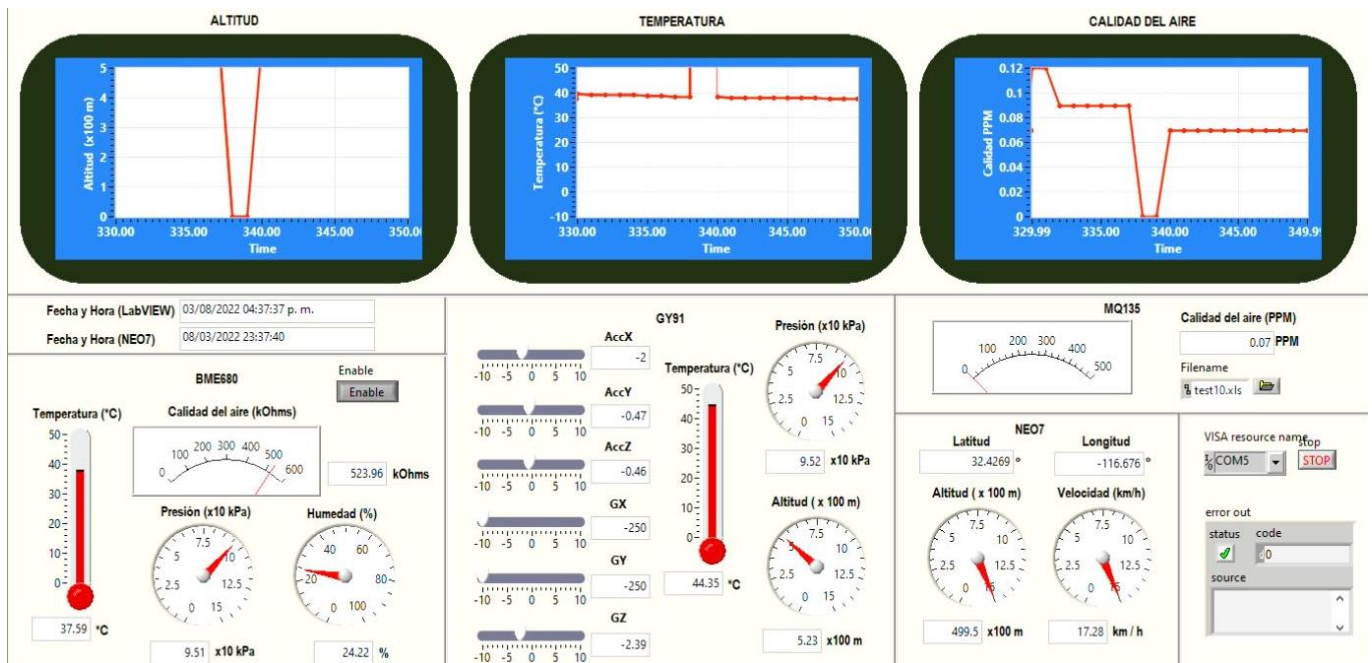


Source: Own elaboration.

1.10 Interface

To visualize and store the collected data from the sensors, an interface was created within LabVIEW. This environment is widely utilized in academic contexts for its user-friendly block programming approach, enabling the creation of graphical interfaces without the need for written code. Additionally, its extensive library collection facilitates the execution of a wide variety of functions. The data collected by the sensors is sent via serial communication by the XBEE module. This data is structured in a text line format and separated by semicolons, destined for the ground computer. LabVIEW interacts with the serial module through the I/O library. It categorizes the data based on variable names and presents it numerically on the interface, as well as plots it graphically. Additionally, LabVIEW displays the recorded timestamps for data transmission from the NEO-7M sensor and the time of reading by the computer, facilitating a comparison of the time delay between these two instances. For further examination, the data is stored in an Excel spreadsheet within the Microsoft Office suite.

Figure 1.16 Graphic interface developed in LabVIEW



Source: Own elaboration. LabVIEW, 2021

Figure 1.17 Data collected and stored in Excel

A	B	C	D	E	F	G	H	I	J	K	L	M	N	O	P
Time	Temperatura BME680	Presión kPa BME680	Humedad % BME680	Calidad del aire kohms BME680	AccX GY-91	AccY GY-91	AccZ GY-91	GX GY-91	GY GY-91	GZ GY-91	Altitud x100m GY-91	Presión kPa GY-91	Temperatura GY-91	Calidad aire MQ135	Latitud NEO-7
03/08/2022 16:23:49.073	0	0	0	0	0	0	0	0	0	0	0	0	0	0	0
03/08/2022 16:23:50.073	36	9.77	30.26	309.02	-2	-0.46	0.3	16.01	36.98	-2.33	3.11	9.76	36.95	0.02	0
03/08/2022 16:23:51.074	35.95	9.77	30.28	309.02	-2	-0.41	-0.06	-18.04	1.56	-2.17	3.11	9.76	36.97	0.02	0
03/08/2022 16:23:52.074	35.94	9.77	30.37	308.93	-2	-0.46	0.06	-14.83	-6.67	-2.31	3.11	9.76	36.98	0.02	0
03/08/2022 16:23:53.074	35.94	9.77	30.44	308.85	-2	-0.66	0.11	9.16	-7.45	-2.22	3.11	9.76	37.03	0.02	0
03/08/2022 16:23:54.074	35.94	9.77	30.56	308.93	-2	-0.72	0.04	-2.66	-12.66	-2.29	3.11	9.76	37.1	0.02	0
03/08/2022 16:23:55.112	35.96	9.77	30.61	308.93	-2	-0.73	0.09	-5.09	-9.73	-2.25	3.11	9.76	37.13	0.02	0
03/08/2022 16:23:58.027	35.98	9.77	30.62	309.02	-2	-0.78	0.06	-3.86	-3.12	-2.24	3.11	9.76	37.19	0.02	0
03/08/2022 16:24:00.296	35.97	9.77	30.62	309.02	-2	-0.73	0.07	-3.34	-5.91	-2.3	3.11	9.76	37.23	0.02	0
03/08/2022 16:24:02.690	35.99	9.77	30.6	308.93	-2	-0.83	0.01	12.17	-8.79	-2.43	3.11	9.76	37.23	0.02	0
03/08/2022 16:24:05.020	35.99	9.77	30.58	308.85	-2	-0.81	0.08	0.76	-6.98	-2.43	3.11	9.76	37.24	0.02	0
03/08/2022 16:24:07.289	35.97	9.77	30.68	308.85	-2	-0.78	0.08	-1.22	-1.32	-2.35	3.11	9.76	37.31	0.02	0
03/08/2022 16:24:09.714	35.99	9.77	30.66	308.93	-2	-0.84	0.19	12.79	-49.95	-2.29	3.12	9.76	37.36	0.02	0
03/08/2022 16:24:12.046	36	9.77	30.71	308.93	-2	-0.85	-0.44	10.83	1.35	-2.24	3.11	9.76	37.4	0.02	0
03/08/2022 16:24:14.298	35.99	9.77	30.56	308.93	-2	-0.84	-0.23	-22.77	-20.03	-2.36	3.12	9.76	37.44	0.02	0
03/08/2022 16:24:16.724	36.02	9.77	30.47	308.85	-2	-0.85	-0.32	5.62	-9.57	-2.32	3.11	9.76	37.39	0.02	0
03/08/2022 16:24:19.055	36.05	9.77	30.4	308.85	-2	-0.63	-0.64	-3.78	-11.65	-2.33	3.11	9.76	37.43	0.02	0
03/08/2022 16:24:21.307	36.04	9.77	30.24	308.76	-2	-0.46	-0.56	10.76	-20.32	-2.31	3.11	9.76	37.36	0.02	0
03/08/2022 16:24:23.702	36.05	9.77	30.25	308.85	-2	-0.41	-0.56	10.8	5.49	-2.34	3.12	9.76	37.38	0.02	0
03/08/2022 16:24:26.033	36.07	9.77	30.14	308.85	-2	-0.6	-0.66	18.52	-6.53	-2.36	3.12	9.76	37.37	0.02	0
03/08/2022 16:24:28.284	36.04	9.77	30.35	308.93	-2	-0.69	-0.24	-10.65	-58.9	-2.2	3.12	9.76	37.42	0.02	0
03/08/2022 16:24:30.695	36.04	9.77	30.52	309.02	-2	-0.67	-0.81	-44.88	-40.95	-2.44	3.12	9.76	37.47	0.02	0
03/08/2022 16:24:33.025	36.01	9.77	30.47	309.11	-2	-0.61	-0.76	-0.76	2.5	-2.38	3.12	9.76	37.39	0.02	0
03/08/2022 16:24:35.278	35.95	9.77	30.45	309.11	-2	-0.62	-0.77	0.4	-7.48	-2.21	3.12	9.76	37.44	0.02	0
03/08/2022 16:24:37.703	35.88	9.77	30.3	309.02	-2	-0.59	-0.8	-0.25	-7.61	-2.42	3.11	9.76	37.43	0.02	0
03/08/2022 16:24:40.034	35.78	9.77	30.27	309.11	-2	-0.56	-0.71	9.29	-6.22	-2.23	3.11	9.76	37.36	0.02	0

Source: Own elaboration. Excel, Version 2304.

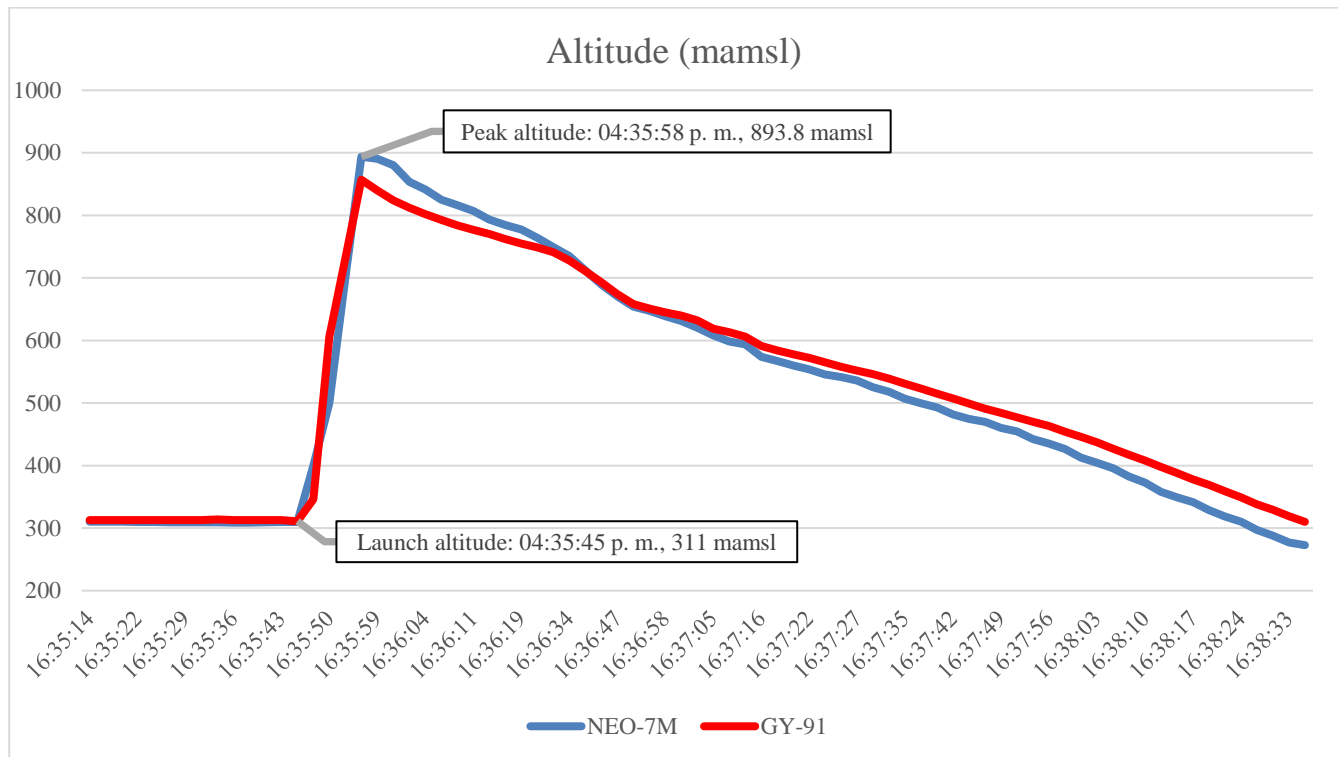
1.11 Results

Using a level L2 engine, a launch was made for data collection through the CanSat. The result for each recorded variable is presented as follows:

1.11.1 Height

The maximum elevation recorded on the rocket was 583.8 m, from 310 mamsl at the launch site to 893.8 mamsl. The total flight time between launch and maximum height was 14 seconds, and the fuel of the rocket burned in 2 seconds. Graphic 1.1 illustrates the height reached versus the time recorded by the CanSat.

Graphic 1.1 Altitude graph of the GY-91 and NEO-7M sensor on the CanSat during the mission and descent

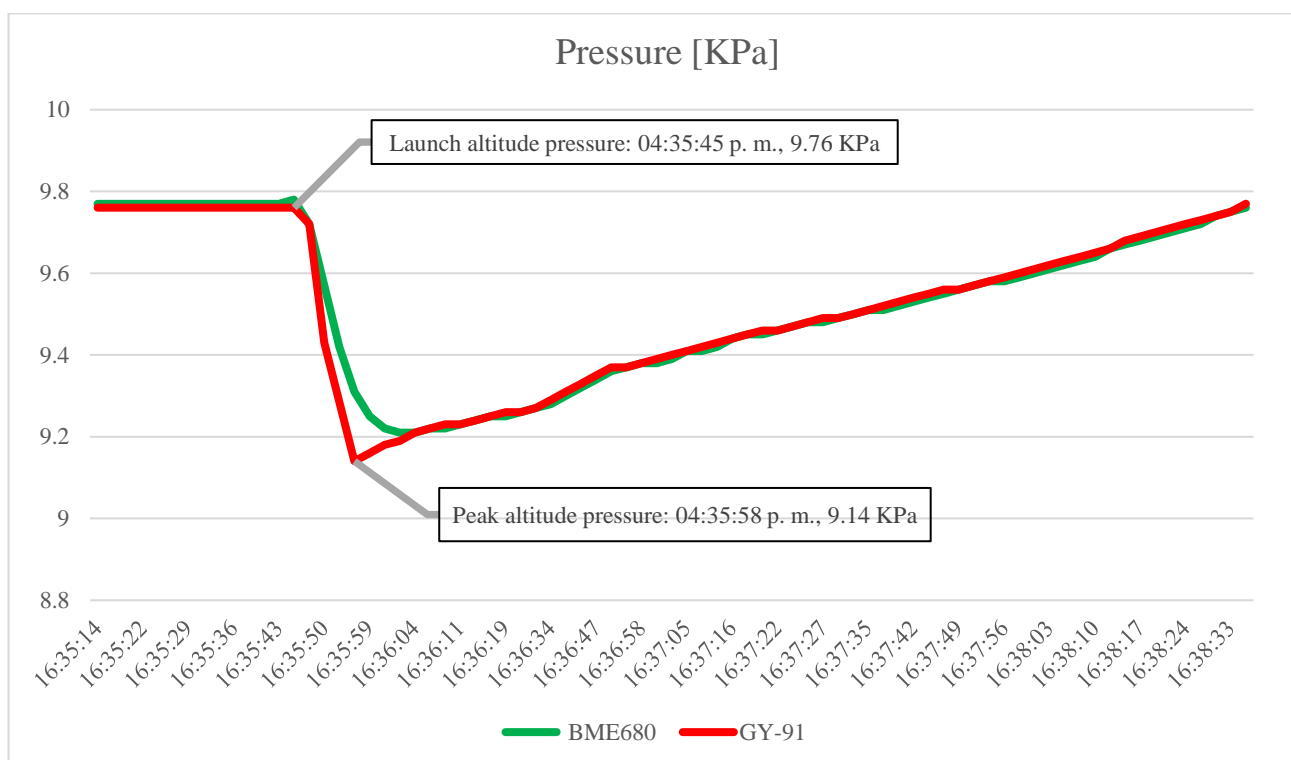


Source: Own elaboration. Excel, 2021

1.11.2 Pressure

The obtained data revealed a reduction in pressure as the rocket ascended. This phenomenon occurs due to the relationship between atmospheric pressure and the weight of the air column exerted on an object. As the altitude increases, the length of the air column decreases, resulting in a decreased amount and weight of air pressing on the object. Consequently, the overall pressure diminishes.

Graphic 1.2 Pressure graph of the BME680 and NEO-7M sensor on the CanSat during the mission and parachute descent

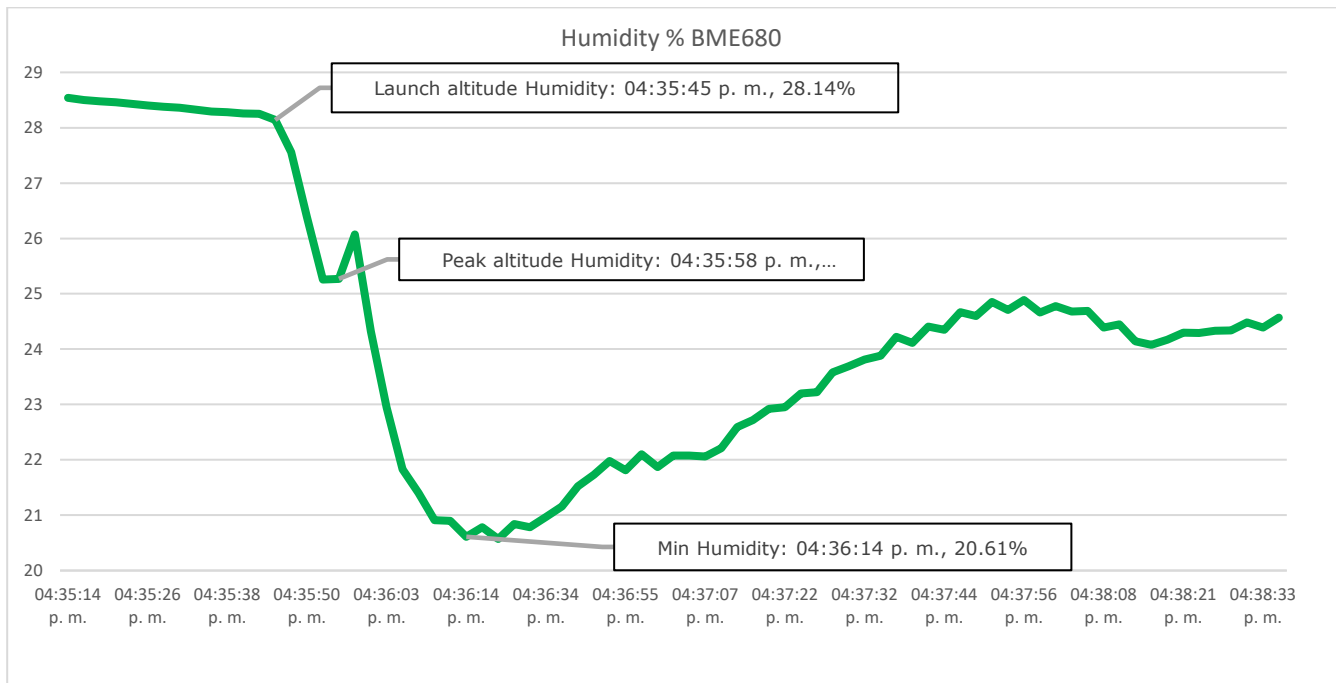


Source: Own elaboration. Excel, 2021

1.11.3 Humidity

The atmosphere contains water vapor, which is known as atmospheric humidity. The findings indicate a decline in atmospheric humidity as altitude increases. This phenomenon arises from the decrease in gas density within the concentrated atmospheric layers at higher altitudes, thereby limiting the atmosphere's water retention capacity.

Graphic 1.3 CanSat humidity graph during the mission until the parachute descent



Source: Own elaboration. Excel, 2021

1.12 Conclusions

The developed picosatellite and launch vehicle met the mission objectives based on the described success evaluation, obtaining all the data of the required variables during the launch and complied with the mission criteria of full success. The development of these systems opens the possibility of participating in competitions where construction limitations are defined, such as volume, weight and data to be obtained. The mission was carefully defined, setting clear and specific objectives to measure key variables and better understand our atmospheric environment, as well as objectives related to payload and launch vehicle survivability.

The design and manufacturing process required a meticulous approach and careful planning. From the concept, the specific development, the simulation, the selection of materials and the tools used for its manufacture. The CanSat was designed with essential parts based on the main subsystems scheme, including the microcontroller, communications subsystem, height, pressure, temperature, acceleration, gyroscope, and air quality sensors. Additionally, a power budget was made according to the modes of operation for the selection of the battery. In the design of the structural system, mechanical supports were also considered to secure the parachute cords that would fulfill the task of the recovery system.

Through launch tests, the CanSat demonstrated its functionality and ability to measure previously defined variables. The height, pressure, temperature, acceleration, rotation, and air quality were recorded and transmitted via telemetry, providing valuable information about the atmospheric environment of Laguna Salada, Mexicali in the state of Baja California. In conclusion, the design and manufacturing process of a CanSat allows the development of a project that starts from the design of a mission, the analysis of a system to meet a certain weight, power and dimensions, the integration of subsystems, the generation of an environment that allows the reception and transmission of data that are essential to study and analyze the environment with which the CanSat interacts, thus also fostering interest in science and technology, promoting practical learning and exploration of aerospace topics.

1.13 References

- Agencia Espacial Mexicana (AEM). (2018). *Ingeniería de Sistemas Espaciales. Aplicado a una misión CanSat*. Retrieved August 18, 2023, from Educación Espacial AEM: https://www.educacionespacial.aem.gob.mx/images_ise/pdf/05Sistemas%20Espaciales%20CanSat.pdf
- Arduino. (2021). *Arduino Nano*. Ivrea. Retrieved from <https://store.arduino.cc/products/arduino-nano>
- Benson, T. (2021, May 13). *Model Rockets*. Retrieved August 20, 2023, from NASA Glenn Research Center The Beginner's Guide to Aeronautics: <https://www.grc.nasa.gov/www/k-12/rocket/rktparts.html>
- Bosch Sensortec GmbH. (2022, August). BME680 Low power gas, pressure, temperature & humidity sensor. *BME680 – Datasheet*. Kusterdingen, Baden-Württemberg, Germany: Bosch. Retrieved August 18, 2023, from <https://www.bosch-sensortec.com/media/boschsensortec/downloads/datasheets/bst-bme680-ds001.pdf>
- Digikey, I. (2009). *Xbee /Xbee-PRO RF Modules*. USA: IEEE. Retrieved from <https://www.sparkfun.com/datasheets/Wireless/Zigbee/XBee-Datasheet.pdf>
- Maral, G., Bousquet, M., & Sun, Z. (2020). *Satellite Communications Systems: Systems, Techniques and Technology* (6th ed.). Chichester, West Sussex, UK: John Wiley & Sons Ltd. doi:10.1002/9781119673811
- Mechatronics, N. (2019). *Módulo GY-91*. Perú: SAC. Retrieved from <https://naylampmechatronics.com/sensores-posicion-inerciales-gps/356-modulo-gy-91-mpu9250-bmp280-acelerometro-giroscoPIO-magnetometro-altimetro-i2c.html>
- Nawazi, F. (2021, October 30). *MQ135 Air Quality Smoke Gas Sensor Module*. Retrieved August 20, 2023, from Circuits DIY: <https://www.circuits-diy.com/mq135-air-quality-smoke-gas-sensor/>
- Secretaría del Medio Ambiente. (2018, Noviembre 14). AVISO POR EL QUE SE DA A CONOCER LA NORMA AMBIENTAL PARA EL DISTRITO FEDERAL NADF009-AIRE-2017, QUE ESTABLECE LOS REQUISITOS PARA ELABORAR EL ÍNDICE DE CALIDAD DEL. *Gaceta Oficial de la Ciudad de México*(452). Retrieved August 19, 2023, from <http://www.aire.cdmx.gob.mx/descargas/monitoreo/normatividad/NADF-009-AIRE-2017.pdf>
- techmake. (2022). *techmake*. Retrieved August 20, 2023, from Módulo GPS Ublox NEO-7M con Antena: <https://techmake.com/products/gpsmod00563>
- u-blox. (2014, November 11). NEO-7 u-blox 7 GNSS modules. *Data Sheet(UBX-13003830)*. u-blox. Retrieved August 19, 2023, from https://content.u-blox.com/sites/default/files/products/documents/NEO-7_DataSheet_%28UBX-13003830%29.pdf
- University Space Engineering Consortium (UNISEC). (2017). *CanSat Pico Size Artificial Satellite. A Guidebook for Building Successful CanSat Project*. Retrieved from http://uniseC.jp/library/i-cansat/manual_CanSat_textbook_eng_v5.pdf
- Zago, R. (2017). *GY91-MPU9250-BMP280*. Sao Paulo: GitHub. Retrieved from <https://github.com/ricardoZago/GY91-MPU9250-BMP280>

Design of an automated cleaning system for 79.2 KW photovoltaic power plant panel

Diseño de un sistema automatizado de limpieza para paneles de central fotovoltaica de 79.2 KW

BARRERA-UGALDE, José Rafael†*, VAQUERO-GUTIERREZ, Maribel, JAEN-CUELLAR, Jesús Uriel and MARROQUÍN-DE JESÚS, Ángel

ID 1st Author: *José Rafael, Barrera-Ugalde* / **ORC ID:** 0009-0002-7353-1681, **CVU CONAHCYT ID:** 1295033

ID 1st Co-author: *Maribel, Vaquero-Gutiérrez* / **ORC ID:** 0009-0008-6053-4203, **CVU CONAHCYT ID:** 1294761

ID 2nd Co-author: *Jesús Uriel, Jaen-Cuellar* / **ORC ID:** 0009-0000-1112-9131, **CVU CONAHCYT ID:** 1295032

ID 3rd Co-author: *Ángel, Marroquín-de Jesús* / **ORC ID:** 0000-0001-7425-0625, **CVU CONAHCYT ID:** 81204

DOI: 10.35429/P.2023.1.17.23

J. Barrera, M. Vaquero, J. Jaen and A. Marroquín

Universidad Tecnológica de San Juan del Río / División de Mecatrónica, Desarrollo de Software e Ingeniería Civil. Av. La Palma no. 125. Col. Vista Hermosa. San Juan del Río, Querétaro, México.

* rafaebu.ma20

Á. Marroquín, L. Castillo, J. Olivares and A. Álvarez (AA. VV.). Young Researchers. Engineering Applications - Proceedings-©ECORFAN-México, Querétaro, 2023.

Abstract

In summary, the production of energy through photovoltaic panels is an efficient and sustainable technology. Its main objective is to generate electricity in a renewable way, reducing dependence on non-renewable resources and mitigating environmental impacts. As part of the methodology, the analysis of panel efficiency over time is included, highlighting the importance of regular cleaning to maintain optimal performance. A cleaning process is recommended, which includes visual inspection, selecting the appropriate method, and a post-cleaning inspection. Furthermore, the design of an automated cleaning system is addressed, considering ergonomic and environment- adaptive aspects. SolidWorks software is used to precisely model the system's components and optimize its structure and functionality. Finally, as a contribution, regular cleaning with an automated system can increase efficiency by a range of 2% to 5%, extending the lifespan of the panels and maximizing their performance over time. This implies that, with the use of appropriate cleaning systems, panels can regain some of their original efficiency, which is essential for ensuring optimal performance.

Design, Automated system, Photovoltaic panels

2 Introduction

Nowadays, energy production through photovoltaic panels has become an efficient and sustainable method of harnessing solar energy. This technology has become increasingly relevant in today's energy context due to its numerous benefits. Photovoltaic panels capture solar radiation and convert it into electricity directly, without generating greenhouse gas emissions.

The added value of photovoltaic panels lies in their ability to harness a renewable and inexhaustible source of energy, the sun. Unlike traditional energy sources, they do not rely on fossil fuels, which reduces dependence on non-renewable resources and the negative impacts associated with their extraction and burning. In addition, advances in more efficient solar panel technologies, such as thin film panels and concentrating solar panels, have made it possible to achieve higher efficiencies, exceeding 20% and even reaching 40% in some cases.

The problem to be solved centers on the efficiency of PV panels over time. As solar panels age and are exposed to environmental conditions, the accumulation of dirt and other contaminants on their surface can reduce their ability to capture solar radiation and convert it into electricity. The central hypothesis is that periodic cleaning of the panels, using appropriate and safe methods, can help minimize the efficiency losses caused by dirt and extend the lifetime of the solar panels.

The chapter is divided into three main sections. In the first section, energy production through photovoltaic panels is discussed, highlighting its benefits, such as its renewable nature and its ability to convert solar energy into usable electricity. In addition, advances in more efficient solar panel technologies are mentioned.

The second section focuses on the efficiency of PV panels over time and the influence of dirt on their performance. It explains how the accumulation of dust and other pollutants can gradually decrease the efficiency of the panels and highlights the importance of periodic cleaning to minimize these efficiency losses.

In the third section, the process of cleaning photovoltaic panels is discussed. Recommended steps are described, such as the visual pre-inspection, selection of the appropriate cleaning method, the actual cleaning and the post-cleaning inspection. Important considerations, such as avoiding damage to the panel surfaces and ensuring proper access and maintenance of the cleaning system, are also mentioned.

2.1 Energy production through photovoltaic panels

Energy production through photovoltaic panels is an efficient and sustainable method of harnessing solar energy. According to the document "Harnessing Solar Energy in the Tropics: Photovoltaic Energy for Bolivian Engineers", this technology has become increasingly relevant in today's energy context. Photovoltaic panels capture solar radiation and convert it into electricity directly, without generating greenhouse gas emissions.

The use of photovoltaic panels for energy production offers numerous benefits. First, it is a renewable source, since the sun is an inexhaustible source of energy. Furthermore, unlike traditional energy sources, it does not require fossil fuels, which reduces dependence on non-renewable resources and the negative impacts associated with their extraction and burning. If production is focused in general on crystalline silicon solar panels, which are the most common in the industry, they have an average efficiency ranging between 15% and 20%. This means that they convert about 15% to 20% of the solar energy they receive into usable electricity.

In recent years, however, thanks to advances in more efficient solar panel technologies, such as thin-film panels and concentrating solar panels. These panels can achieve higher efficiencies, exceeding 20% and even reaching 40% in some cases.

Figure 2.1 Photovoltaic power plant



Source: Own elaboration

Efficiency of photovoltaic panels over time

The analysis of the efficiency of PV panels over time shows part of the performance and maintenance of PV plants. As solar panels age and are exposed to environmental conditions, it is important to evaluate how their efficiency may be affected over time.

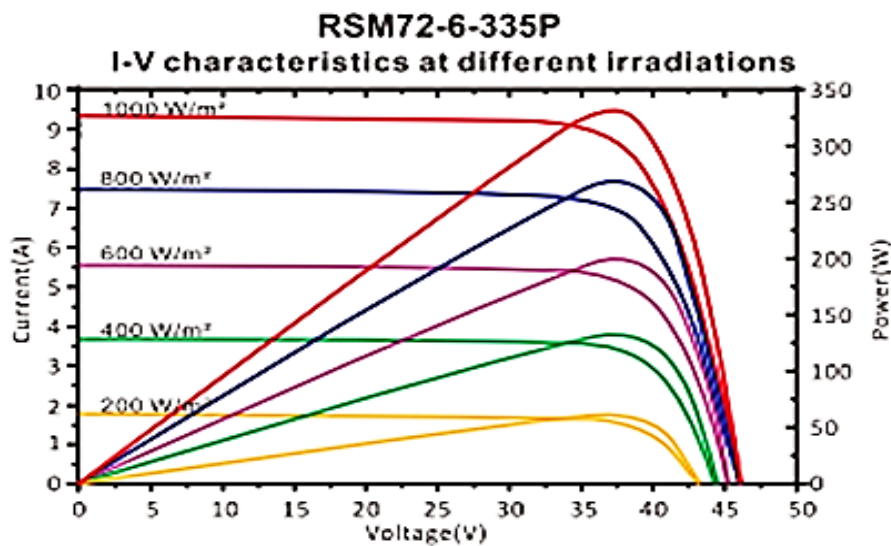
The study conducted in the paper "Analysis of Dirt Losses in PV Plants" examines the influence of dirt on the efficiency of solar panels over their lifetime. The accumulation of dust, dirt and other contaminants on the surface of panels can reduce their ability to capture solar radiation and convert it into electricity.

The analysis reveals that as solar panels become dirty, their efficiency gradually decreases. The layer of dirt acts as a barrier that blocks some of the solar radiation, which reduces the amount of power the panels can generate. In addition, dirt can cause partial shading of the panels, which also negatively affects their performance.

Periodic cleaning of the panels, using appropriate and safe methods, can help minimize efficiency losses caused by soiling and extend the life of the solar panels.

This analysis highlights the importance of considering proper maintenance and cleaning of PV panels as an integral part of PV plant management, in order to ensure optimal performance and sustained efficiency over time.

Graphic 2.1 Characteristics at different irradianations



Source: Prepared by the company

2.2 Risen product data sheet

The 2011 study "Effect of module cleaning in photovoltaic plants" provides relevant information on the cleaning process of solar panels and its impact on the performance of photovoltaic installations.

Regular maintenance of PV panels includes periodic cleaning of their surface to remove the accumulation of dirt and other contaminants that can reduce power generation efficiency where the solar panel cleaning process is discussed in detail, highlighting best practices and important considerations where the following steps are involved as a recommendation:

Visual inspection: prior to cleaning, a visual inspection of the panels is performed to identify any damage or problems that may require additional attention. This includes checking for loose wires, cracks in the panels or faulty connections.

Selection of cleaning method: The appropriate cleaning method is selected based on the specific conditions of the installation and the solar panels. This may include the use of pressurized water, soft brushes, specific cleaning products or automated cleaning systems.

Actual cleaning: Cleaning of the solar panels is performed using the selected method. Care is taken not to apply excessive pressure or use abrasive chemicals that may damage the panel surfaces or anti-reflective materials.

Post-cleaning inspection: After cleaning, an additional inspection is performed to verify that there is no additional damage and that the panels are in good working order.

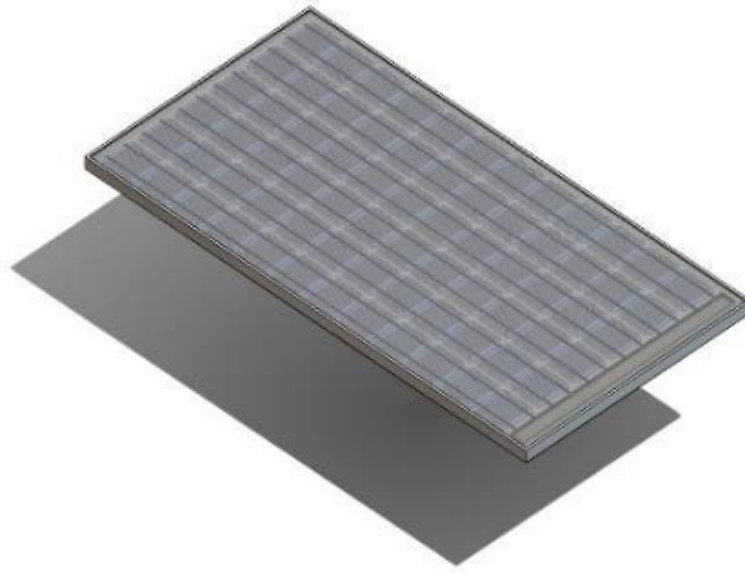
2.3 Parameters for the design of an automated cleaning system

When designing an automated cleaning system, ergonomically so that it is easy to use for operators, minimizing the physical load where controls and elements should be located in an accessible and ergonomic manner.

The method of maintenance and cleaning of the system should facilitate access and periodic maintenance of the system with easily replaceable components and parts and be designed to minimize the accumulation of dirt or debris on its surface.

Design adapted to the working environment and surface to be cleaned by adjusting parameters such as speed, pressure or type of cleaner used, so that it can be adapted to different needs and situations.

Figure 2.2 3D solar panel model



Source: Own elaboration

2.4 Design of parts of the automated cleaning system

Precise modeling using the tools and functions provided by SolidWorks, where an accurate three-dimensional model of each of the parts of the cleaning system was created. This involved defining the shapes, dimensions and geometric characteristics according to the specific requirements based on the measurements of a Risen solar panel.

So that the measurements of the design are precise and specific to meet the requirements of operation and assembly of the automated cleaning system giving the process of automated cleaning system giving the proper assembly process of the system within a slotted design or other elements that allow a correct assembly and ensure the structural integrity of the system.

As optimization evaluation within the SolidWorks software in order to optimize the form and function of each designed part where it is important to verify the structural efficiency, performance and functionality of the parts to make adjustments if necessary.

Table 2.1 Mechanical data

MECHANICAL DATA	
Solar cells	Polycrystalline 156.75*156.75 mm, 5BB
Cell configuration	72 cells (6*12)
Module dimensions	1956*992*40 mm
Weight	22 kg
Superstrate	3.2 mm, High transmission, low iron, tempered ARC glass
Substrate	White back-sheet
Frame	Anodized aluminum alloy type 6063T5, silver color
J-Box	Potted, IP67, 1500VCD, 3 Schottky bypass diodes
Cables	4.0 mm ² (12AWG), 120 mm length
Connector	Risen twinsel PV-SY02, IP67

Source: Elaborated by the company Risen, technical data sheet of its product

2.5 Methodology

In this case, the objective aspects of the methodology will fall on what are considered as three variables of the project, which are the design, the automated systems and the photovoltaic panels. On the other hand, the subjective aspects will have to do with the particularities of efficiency in particular, its long-term function and energy production.

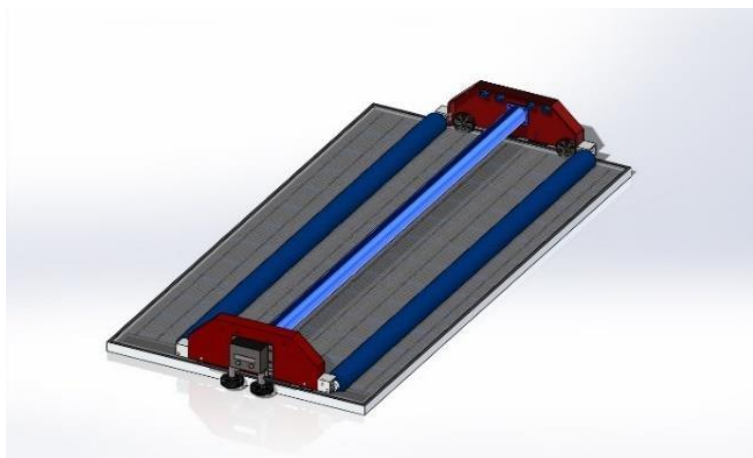
2.6 Results

The efficiency of energy production through photovoltaic panels provides sustainability with an average efficiency between 15% and 20% of solar energy into usable electricity.

In terms of efficiency over time, regular maintenance and cleaning of the PV panels in the face of accumulation of dirt and other contaminants on the surface of the panels, it can be estimated that cleaning with an automatic system can increase efficiency in the range of approximately 2% to 5%.

This means that after a long period of use these systems can recover between 2% and 5% of their original efficiency.

Figure 2.3 3D model of the automatic cleaning system assembly



Source: Own elaboration

2.7 Conclusions

In conclusion, the efficiency of a solar panel is affected by dirt as it acts as a barrier that reduces the capacity to capture solar radiation, decreasing the amount of energy generated. Therefore, periodic cleaning of the panels is crucial to minimize efficiency losses and prolong their useful life, as the efficiency recovered after cleaning with an automatic system can range between 2% and 5%, although these values are approximate and depend on various factors.

In addition, keeping the panels clean and performing regular cleaning contributes to maximize the performance and efficiency of the solar panels over time.

2.8 References

Cajas Chicaiza, M. E., & Montaluisa Ipiales, D. F. (August 20, 2012). *Diseño y Construcción de un Sistema Automático para la Limpieza de Paneles Solares*. Quito, Ecuador: QUITO/EPN/2012. Retrieved June 09, 2023, from <http://bibdigital.epn.edu.ec/handle/15000/4842>

Castro Martínez, J. (July 03, 2019). *Análisis de pérdidas por suciedad en plantas fotovoltaicas*. Master's thesis. Retrieved June 09, 2023, from <http://hdl.handle.net/10016/29375>

García Mendoza, R. (May, 2023). *SISTEMA FOTOVOLTAICO DE BAJA POTENCIA PARA INVERNADEROS INTELIGENTES*. Master's thesis. Chihuahua, Chihuahua, Mexico. Retrieved on June 09, 2023, from <http://cimav.repositorioinstitucional.mx/jspui/handle/1004/456>.

Iranzu Balbuena, A. (July 10, 2018). Diseño de equipamiento automatizado para la limpieza de paneles solares fotovoltaicos. Trabajo Fin de Grado. Tudela, España. Retrieved June 09, 2023, from: <https://hdl.handle.net/2454/29115>

Núñez García, W. B., Calla Durandal, E., & Fernández Fuentes, M. (November 2021). Desarrollo de un prototipo de limpieza de paneles fotovoltaicos. Artículo Científico, 10. scielobo. DOI:ISSN 1683-0789

Risen. (08 of 2018). HIGH PERFORMANCE POLYCRYSTALLINE MODULE RSM72-6325P-345P. Polycrystalline Photovoltaic Module [Datasheet]. Retrieved 06/09/2023, from https://solardistri.nl/wp-content/uploads/2018/08/Datasheet-RSM72_6_325P_345P.pdf.

Design of a circuit for an automated system used for cleaning the panels of the 79.2KW photovoltaic power plant

Diseño de un circuito para un sistema automatizado utilizado para la limpieza de paneles de la central fotovoltaica de 79.2KW

JAEN-CUELLAR, Jesús Uriel†, VAQUERO-GUTIÉRREZ, Maribel, BARRERA-UGALDE, José Rafael and MARROQUIN-DE JESÚS, Ángel

Universidad Tecnológica de San Juan del Río / División de Mecatrónica y Energías Renovables Av. La Palma no. 125. Col. Vista Hermosa. San Juan del Río, Querétaro, México.

ID 1st Author: *Jesús Uriel, Jaen-Cuellar* / **ORC ID:** 0009-0000-1112-9131, **CVU CONAHCYT ID:** 1295032

ID 1st Co-author: *Maribel, Vaquero-Gutiérrez* / **ORC ID:** 0009-0008-6053-4203, **CVU CONAHCYT ID:** 1294761

ID 2nd Co-author: *José Rafael, Barrera-Ugalde* / **ORC ID:** 0009-0002-7353-1681, **CVU CONAHCYT ID:** 1295033

ID 3rd Co-author: *Ángel, Marroquín-De Jesús* / **ORC ID:** 0000-0001-7425-0625, **CVU CONAHCYT ID:** 81204

DOI: 10.35429/P.2023.1.24.36

J. Jaen, M. Vaquero, J. Barrera and Á. Marroquin

Á. Marroquín, L. Castillo, J. Olivares and A. Álvarez (AA. VV.). Young Researchers. Engineering Applications - Proceedings-©ECORFAN-México, Querétaro, 2023.

Abstract

Solar panel cleaning is an important practice to ensure the performance and efficiency of solar energy systems. This brief description discusses the usefulness of cleaning solar panels and their impact on renewable energy production. The accumulation of dirt and other contaminants on the surface of solar panels can greatly reduce their ability to capture sunlight and convert it into electricity. Therefore, regular cleaning of panels is critical to maintaining their efficiency and maximizing energy production. The benefits of cleaning solar panels are substantial. By removing impurities, better penetration of sunlight is ensured, which translates into higher power generation. This ensures stable performance and increased power generation over time. In addition, regular cleaning prolongs the life of solar panels by preventing damage caused by the accumulation of dirt and other corrosive elements. Clean panels are less susceptible to damage and are less prone to failure.

Automated system, Photovoltaic panel, Renewable energy

3 Introduction

Good cleaning of solar panels is very important to ensure that they achieve maximum efficiency and effectiveness during power generation. Accumulation of dirt, grime and other contaminants can significantly reduce the amount of sunlight reaching the panels, reducing their energy efficiency. Keeping panels clean and free of obstructions provides optimal solar radiation, which increases energy efficiency and generates more efficient electricity. In addition, good cleaning also helps to extend the life of the panel, avoiding damage and problems caused by dirt accumulation in the long run.

The challenge is to clean the solar panels regularly and efficiently with an automated robot that does the job at least twice a month. Solar panels are exposed to various contaminants, such as dirt, leaves and bird droppings, which affects their efficiency and reduces power output. Manual cleaning of the panels is laborious and requires a lot of time and effort.

The main hypothesis is that by developing an automatic cleaning robot for solar panels that cleans regularly, it will be possible to keep the panels in optimal condition, maximizing their efficiency and power output. It is expected that this robot will be able to effectively and completely cover large areas of solar panels, ensuring uniform cleaning without the need for manual intervention. This will allow for more frequent and efficient cleaning, improving the overall efficiency of the PV system and extending the life of the panels.

There are several reasons why a robot might be better than manual labor:

Efficiency and speed. The cleaning robot is designed for fast and efficient cleaning. They can cover large areas of solar panels in a short time, resulting in faster cleaning and less panel downtime.

Accuracy and consistency: the cleaning robot is programmed to follow fixed routes and use specific cleaning methods. This ensures thorough and consistent cleaning of each panel, avoiding missed or poorly cleaned areas.

Hard-to-reach locations: some solar panels can be placed in hard-to-reach locations or on elevated structures. Cleaning robots are designed to move and work in confined spaces and difficult terrain, allowing them to reach panels in places where manual labor cannot reach. They also reduce the risk of accidents or injuries associated with working at height.

Long-term cost savings: while the initial investment in a robot vacuum cleaner may be higher, in the long run it can be more cost-effective than manual labor. Cleaning robots require less labor and can operate independently, which reduces labor costs in the long run. Therefore, using a robot vacuum cleaner to clean solar panels offers advantages in efficiency, accuracy, reach to hard-to-reach places, safety and cost reduction. These advantages make automatic cleaning an attractive and effective alternative to manual cleaning.

Regular cleaning of solar panels is essential to ensure optimal performance and maximize power generation. Dirt, leaves or other contaminants that accumulate on the surface of the panels can reduce their ability to capture sunlight efficiently. This reduces the efficiency of the panel and therefore reduces the amount of electricity generated.

With regular cleaning, at least twice a month, dirt does not build up and adhere to the solar panels. This helps keep the surface clean and transparent, allowing the panels to capture the maximum amount of available sunlight and generate power more efficiently.

Regular cleaning also contributes to the durability and longevity of the solar panels. By removing dirt and other contaminants, it prevents staining, corrosion or other damage that could negatively affect the integrity and performance of the panel.

3.1.1 Ergonomic design

When developing an ergonomic design for a solar panel cleaning robot, there are several features to consider to ensure ease of use and efficiency.

First, the robot should be compact and lightweight for ease of handling and movement around the solar panels. In addition, strategic handles or grips should be placed on the robot to ensure a secure and comfortable grip during transport and handling.

It is important that the design includes an intuitive and user-friendly interface for the operator. This means convenient buttons or controls that are properly positioned and labeled, as well as an easy-to-read display that shows up-to-date information on the robot's cleaning status and progress.

The robot should also have an automatic navigation system to avoid collisions and navigate the solar panels smoothly. Proximity sensors and obstacle detection technology can be integrated to ensure safe and efficient driving.

In addition, quick and easy access to robot parts for maintenance and repair must be provided. This means that parts are located for easy access, and the modular construction facilitates the replacement of damaged or worn parts.

3.1.2 Navigation system

An efficient navigation system is the basis for the development of solar panel cleaning robots. The positioning system will allow the robot to navigate automatically and accurately over the surface of the solar panels. Proximity sensors can also be used to avoid obstacles and ensure safe driving.

Navigation systems can also include obstacle avoidance by detecting and avoiding objects. As a result, the robot can move safely and efficiently without damaging the solar panels or other environmental elements.

A navigation system for a PV cleaning robot should combine vision sensors, proximity sensors.

3.1.3 Efficient cleaning mechanism

Developing an efficient cleaning mechanism is essential for solar panel cleaning robots. The cleaning mechanism must be able to effectively remove dirt and debris from the surface of the solar panels. A popular option is to use a soft brush or special cloth that is gentle enough not to damage the solar panels but effective enough to remove stubborn dirt and debris. These brushes or rags can be attached to a movable frame, ensuring constant and even movement over the surface of the panels. Another alternative is to use a pressure-controlled sprayer. This can help remove stubborn dirt and debris that clings to the panels. Water can be supplied through properly located taps on the robot, and the pressure should be carefully adjusted to avoid damaging the panels.

3.1.4 Pressure and temperature control

Effective pressure and temperature control is essential when designing a solar panel cleaning robot. This control ensures that the pressure and temperature used during the cleaning process are sufficient to avoid damage to the solar panels. For effective pressure control, a pressure sensor can be used to measure the force applied to the control panel. These sensors can be integrated into a brush system, allowing the pressure to be adjusted in real time according to the characteristics of the panel and the level of soiling. When it comes to temperature control, the temperature and environmental conditions of the solar panels must be taken into account when cleaning them. In addition, automatic control systems can be used to automatically adjust the pressure and temperature according to the characteristics of the panel and the level of soiling.

Automatically adjust the pressure and temperature according to the set parameters. This ensures efficient and safe cleaning without constant operator intervention. As a result, the effective control of pressure and temperature in the solar panel cleaning robot allows the cleaning parameters to be adjusted according to the characteristics of the panels, preventing damage and ensuring an efficient cleaning process.

3.1.5 Power and autonomy

When it comes to power, you can choose a combination of power sources. One option is to use a high-capacity battery that can provide the power needed to run the robot while cleaning. In addition, it is possible to build an automatic charging system that allows you to recharge the battery if necessary using the solar energy available from the photovoltaic panels. For autonomy, the energy consumption of the robot and the time it takes to perform the cleaning tasks must be taken into account. To optimize the use of the energy stored in the battery, an efficient energy management system can be implemented. This can include intelligent planning of cleaning routes and control of various parts of the robot to minimize energy consumption. In addition, a battery level monitoring and notification system can be activated so that operators can take preventive measures and recharge the batteries as needed.

Therefore, the correct development in terms of energy and autonomy of solar panel cleaning robots involves the use of batteries, automatic charging systems and efficient energy management to ensure long-term and efficient robot operation in cleaning tasks.

3.1.6 Safety

Safety is a key factor in the development of solar panel cleaning robots. Many measures must be taken to protect both the robot and the solar panels, as well as the environment. First, obstacle detection sensors and intelligent navigation systems can be activated to avoid collisions with objects and people. In addition, an emergency stop system can be implemented to quickly stop the robot in any dangerous situation. This could include strategically placed stop buttons or the ability to receive shutdown commands remotely.

It is also important to establish safe procedures for maintenance and cleaning of the robot, as well as ensuring that operators are properly trained to ensure that they follow established safety procedures. Therefore, safety developments in solar panel cleaning robots include the implementation of obstacle detection sensors, intelligent navigation systems, emergency shutdown systems, fire protection measures and related safety protocols. These measures ensure that people, solar panels and the environment are protected while the robot is in operation.

3.1.7 Resistance to environmental conditions

Environmental resilience is a critical aspect of the development of a solar panel cleaning robot, as it will operate in a variety of environments and weather conditions.

To ensure durability, durable and high quality materials and components can be used that can withstand adverse conditions such as high temperature, humidity, dirt, exposure to solar radiation. In addition, suitable sealing and protection rings can be used to prevent water, dust and other harmful elements from entering the internal components of the robot. This ensures long-lasting and reliable operation even under extreme conditions. Similarly, it is important to consider the design of the robot, which must be robust and resistant to shock and vibration. The components must be properly fixed and secured to avoid damage caused by sudden movements or vibrations during operation. In addition, efficient cooling systems, such as fans or heat sinks, can be used to avoid overheating of the robot electronics.

Therefore, improving the environmental resistance of solar panel cleaning robots requires the use of durable materials and components, proper sealing, protection, robust construction and effective cooling systems. These features ensure long and reliable operation of the robot in various environments and climatic conditions.

3.1.8 Integration with monitoring systems (Idea)

Integration with monitoring systems is a key feature in the development of PV cleaning robots, as it allows providing real-time information about the operation of the panels and the status of the robot.

Communication technologies such as Wi-Fi, Bluetooth and even cloud communication systems can be used for efficient integration. This allows the robot to interface with existing on-site monitoring systems, such as energy monitoring systems or property management systems.

Thanks to this integration, you can obtain data on the efficiency of your panels, energy production, the presence of contaminants or detect possible faults. This data can be viewed in real time and saved for later analysis.

In addition, integration with monitoring systems allows for scheduling and remote control of the robot. This means you can set cleaning schedules, customize your robot's settings and receive notifications when problems or maintenance are needed. In short, integration with monitoring systems on solar panel cleaning robots provides real-time access to relevant data on panel performance and robot status. This facilitates informed decision making, optimizes panel performance, and detects potential problems or service needs early.

3.1.9 Maintainability and serviceability

The development of a system that is easy to maintain and repair is essential for the development of solar panel cleaning robots to ensure optimal and uninterrupted long-term operation.

For ease of maintenance, the robot can be designed in a modular fashion with easily accessible and replaceable parts. This allows the operator to easily perform maintenance tasks, such as cleaning parts or replacing worn parts.

In addition, self-diagnostics and self-calibration systems can be integrated to help identify problems and perform automatic corrections. This simplifies the maintenance process and reduces robot downtime.

It is important to provide clear, detailed operating instructions and proper training to operators so that they can perform maintenance and repair tasks correctly. Similarly, you can set up a maintenance monitoring system that records activities performed and schedules periodic preventive maintenance. This helps prevent problems before they happen and prolongs the life of the robot. In the event of a breakdown or more complex repair, you can count on dedicated service and spare parts to ensure a quick solution to your problems.

Therefore, developing a maintenance and repair tool on a solar panel cleaning robot requires a modular design, a self-diagnostic system, clear operating instructions, operator training, maintenance monitoring and access to maintenance and spare parts. These measures ensure efficient maintenance and quick resolution of potential problems, maximizing the life and productivity of the robot.

3.2 What advantages and disadvantages can a solar panel cleaning robot have?

3.2.1 Advantages

- Efficiency: the automatic cleaning robot can clean solar panels efficiently and quickly without constant human intervention. This saves time and effort compared to manual cleaning.
- Increase productivity: Keeping the solar panels clean increases their efficiency and power. Regular vacuuming by the robot ensures optimal panel performance and thus greater energy savings.
- Safety: Using a robotic vacuum cleaner reduces the risks associated with manual cleaning of solar panels, such as injuries from falls or contact with hot surfaces. The operator can monitor and control the robot from a safe distance.
- Preventive maintenance: The cleaning robot can detect and report solar panel anomalies, such as cracks or damage, allowing you to take preventive maintenance measures to avoid serious long-term problems.
- Save water: with a solar cell cleaning robot, you can optimize your water usage as the system can use the right amount or may not even necessarily have water for efficient cleaning, avoiding waste and saving water.

3.2.2 Disadvantages

- Initial cost: purchasing and implementing a solar panel cleaning robot can be a significant investment, especially for systems with high performance and advanced functions.
- Maintenance and repairs. While cleaning robots are designed to last a long time, they may also require regular maintenance and repair, which means additional costs and potential downtime.
- Location and design limitations: Depending on the design of the robot, there may be limitations in its ability to clean some types of solar panels or hard-to-reach areas, such as slopes or non-flat surfaces.
- Technology dependent: The proper functioning of a cleaning robot depends on the proper functioning of its technologies, such as sensors, motors and navigation systems. Failure of these components can affect its performance.
- Adaptation to extreme weather conditions: In some adverse weather conditions, such as heavy rain, strong winds or sandstorms, it may be necessary to stop the robot to avoid damage or accidents.

Table 3.1 showing the estimated stress of a bipolar motor as a function of weight, which varies from 5 to 30 kilograms

Weight (kg)	Estimated motor stress (N)
5	49.03
10	98.06
15	147.09
20	196.12
25	245.15
30	294.18

Table 3.2 Voltage provided by a solar panel at different times of the day

Time of day	Average voltage (V)
6:00	0-2
9:00	10-20
12:00	20-30
15:00	30-40
18:00	10-20

3.3 Methodology to be developed

Define requirements: define the key requirements of the circuit, such as the ability to control the robot's movements, the sensors needed to detect dirt on the board, the ability to navigate automatically, etc. Research and select components: research the necessary components for circuits such as microcontrollers, sensors, actuators, power supplies, etc. Choose the ones that best suit your requirements.

Wiring design: use electronic design software (Proteus) to create a wiring diagram for the circuit. Connect the parts according to the manufacturer's specifications and the needs of the cleaning robot.

Circuit testing: On a breadboard, test the circuit made in the software used.

Printed circuit board (PCB) design: Change the electrical circuits to printed circuit boards. Place the components on the PCB and make the necessary connections with the PCB design software. Be sure to follow best design practices to ensure signal integrity and circuit performance.

PCB production: Send the PCB design to the manufacturer or produce it yourself if you have sufficient resources. Verify the manufacturer's specifications and perform a continuity and short circuit test before proceeding.

Assembly and test: Solder components to the PCB and perform functional tests to make sure the circuit works properly.

Make corrections and fix any problems identified during testing.

Cleaning robot integration: Integrate the circuit with the cleaning robot by making the correct connections and ensure compatibility with other parts of the robot.

Upgradeability

The possibilities for improvements to a solar panel cleaning robot are varied and new technologies are continually being researched to optimize its performance. Some areas of improvement include:

Energy efficiency: developing more efficient systems that use less energy during cleaning and maximize power generation from the solar panels.

Battery life and autonomy: Improving battery capacity and robot autonomy to perform longer cleanings without the need for recharging.

Advanced sensors and algorithms: Implement more sophisticated sensors and intelligent algorithms that allow better detection of dirt, obstacles and environmental conditions.

Self-cleaning system: Design a mechanism integrated in the robot that allows its own cleaning, avoiding the accumulation of dirt and increasing its efficiency.

Adaptability to different surfaces: Improve the robot's ability to adapt to different types of surfaces and angles of the solar panels, allowing effective cleaning in various configurations.

These improvements seek to optimize the efficiency, autonomy and adaptability of the solar panel cleaning robot, with the objective of facilitating cleaning and maintaining the optimal performance of the solar panels.

3.4 Results

Component compatibility: the circuit must ensure proper compatibility and connection of the components used, such as microcontrollers, sensors, actuators and power supplies.

Energy efficiency: the circuit design shall provide efficient power management to maximize the robot vacuum cleaner's battery life and make optimal use of the available power sources.

Reliability and stability: The chains must be designed to be stable and reliable, resistant to vibrations and temperature fluctuations occurring in the external environment.

Failure protection: the circuit design must include safety measures to prevent damage to components in the event of short circuit, overvoltage or overcurrent, to ensure circuit integrity and prolong circuit life.

Ease of maintenance and repair: The circuit design should allow easy access and replacement of parts in case of failure, facilitating theft maintenance and repair.

3.5 Annexes

This annex details additional aspects about the PV panel cleaning robot document, providing complementary information and relevant resources for its understanding.

Technical specifications:

ATPMEGA328 Function.

The ATmega328 is a microcontroller of the AVR family manufactured by Atmel (now part of Microchip Technology). The function of the ATmega328 is to act as the main brain or controller in various electronic devices. Some of the main functions of the ATmega328 include:

Data processing: The ATmega328 can execute instructions and perform mathematical, logic and control calculations to control the operation of an electronic system.

Peripheral control: The microcontroller can interface with a variety of peripherals, such as sensors, actuators, displays, and serial communication (such as UART, I2C, SPI), to receive and send data.

Memory management: The ATmega328 has an internal memory that can store program instructions, temporary data and variables.

Timing and counters: The microcontroller has built-in timers and counters that can be used to generate timing signals, measure time and control periodic events.

Ultrasonic sensor function to detect anomalies

An ultrasonic sensor is a device that uses high-frequency sound waves to detect objects and measure distances. In the context of altitude detection, ultrasonic sensors can be used to detect changes in the altitude or distance of an object relative to the surrounding surface. This is accomplished by emitting an ultrasonic pulse and measuring the time it takes to pick up the echo of that pulse after bouncing off an object.

The ultrasonic sensor, which detects drops, can provide information about the presence of an obstacle and the distance to it, or about the change in altitude from the original position. This information is useful in many applications, such as automatic leveling systems, mobile robots that need to avoid obstacles, and even safety systems that detect sudden changes in terrain.

Therefore, the role of ultrasonic sensors in impact detection is to use sound waves to measure and detect changes in the height or distance of an object from the surrounding surface, allowing decisions to be made or acted upon.

Function of L293D (H-Bridges)

Directional control: reverses the polarity of the motor poles, allowing the motor to rotate in both directions (forward and reverse). This is achieved by including suitable power transistors inside the L293D. **Speed control:** The L293D provides speed control via Pulse Width Modulation (PWM). By applying a PWM signal to the L293D speed control pin, you can change the speed of the motor by adjusting the duty cycle of the PWM signal. **Overcurrent protection:** The L293D has built-in thermal and protection diodes to help prevent circuit damage due to excessive current or power feedback generated by the motor.

Diagrams and drawings: Attached are technical diagrams and drawings of the robot, illustrating component layout, electrical circuits.

Figure 3.1 ATmega328

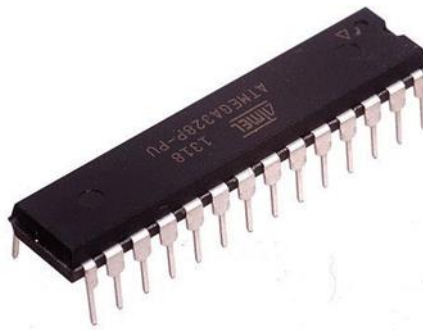


Figure 3.2 Ultrasonic Sensor



Figure 3.3 L293D



Figure 3.4 Stepper motor



Algorithms and programs: Algorithms and programs used to control the cleaning robot are provided, including navigation logic, obstacle detection, cleaning sequence and any other control processes implemented.

Figure 3.5 Arduino code used

```

Pruebasno | Arduino IDE 2.1.0
File Edit Sketch Tools Help
Arduino Uno

Pruebasno.ino
1 // librería para el sensor ultrasónico
2 #include <NewPing.h>
3
4 // Definición de los pines del sensor ultrasónico
5 const int buttonPin = 1; // Pin del botón
6 #define TRIGGER_PIN1 2
7 #define ECHO_PIN1 3
8 #define TRIGGER_PIN2 4
9 #define ECHO_PIN2 5
10
11
12 // Definición del pin del LED
13 // Definición de los pines del L293D
14 int motorPin1 = 6;
15 int motorPin2 = 7;
16 int motorPin3 = 8;
17 int motorPin4 = 9;
18
19 // Variables de control del motor
20 int velocidad1 = 500;
21 int velocidad2 = 500;
22 int ciclo = 0;
23 int again;
24
25 NewPing sonar1(TRIGGER_PIN1, ECHO_PIN1);
26 NewPing sonar2(TRIGGER_PIN2, ECHO_PIN2);
27
28 // Variables de distancia
29
30
31
32
33
34 int objetoAlejandose = 0;
35
36 void setup() {
37 // configurar los pines del L293D como salida
38 pinMode(motorPin1, OUTPUT);
39 pinMode(motorPin2, OUTPUT);
40 pinMode(motorPin3, OUTPUT);
41 pinMode(motorPin4, OUTPUT);
42 pinMode(buttonPin, INPUT_PULLUP);
43 }
44
45 void loop() {
46 // Leer el estado actual del botón
47 distanciaActual1 = sonar1.ping_cm();
48 distanciaActual2 = sonar2.ping_cm();
49
50 if (distanciaActual1 > distanciaAnterior1) {
51   objetoAlejandose = 1;
52 }
53 if (distanciaActual2 > distanciaAnterior2) {
54   objetoAlejandose = 2;
55   ciclo = ciclo + 1;
56 }
57 }
58
59
60
61
62
63
64
65
66
67
68
69
70
71
72
73
74
75
76
77
78
79
80
81
82
83
84
85
86
87
88
89
90
91
92
93
94
95
96
97
98
99
100

```

```

Arduino IDE 2.1.0
Pruebas no
45 void loop() {
46 // Leer el estado actual del botón
47 distanciaActual1 = sensor1.ping_cm();
48 distanciaActual2 = sensor2.ping_cm();
49
50 if (distanciaActual1 > distanciaAnterior1) {
51   objetoLejanose = 1;
52 }
53 if (distanciaActual2 > distanciaAnterior2) {
54   objetoLejanose = 2;
55   ciclo = ciclo + 1;
56 }
57 if (digitalRead(botonPin) == LOW) {
58   if (ciclo == 2) {
59     digitalWrite(motorPin1, LOW);
60     digitalWrite(motorPin2, LOW);
61     digitalWrite(motorPin3, LOW);
62     digitalWrite(motorPin4, LOW);
63     delay(500);
64     objetoLejanose = 3;
65     ciclo = 0;
66   } else {
67     // Controlar el motor en función del sentido de giro actual
68     switch (objetoLejanose) {
69       case 1:
70         digitalWrite(motorPin1, HIGH);
71         digitalWrite(motorPin2, LOW);
72         digitalWrite(motorPin3, LOW);
73         digitalWrite(motorPin4, LOW);
74         if (distanciaActual1 > distanciaAnterior1) {
75           velocidad1 = 5;
76         }
77         delay(velocidad1);
78         digitalWrite(motorPin1, HIGH);
79         digitalWrite(motorPin2, HIGH);
80         digitalWrite(motorPin3, LOW);
81         digitalWrite(motorPin4, LOW);
82         if (distanciaActual1 > distanciaAnterior1) {
83           velocidad1 = 5;
84         }
85         delay(velocidad1);
86         digitalWrite(motorPin1, LOW);
87         digitalWrite(motorPin2, HIGH);
88         digitalWrite(motorPin3, LOW);
89         digitalWrite(motorPin4, LOW);
90         if (distanciaActual1 > distanciaAnterior1) {
91           velocidad1 = 5;
92         }
93       }
94     }
95   }
96 }
97 }
98 }
99 }
100 }
101 }
102 digitalWrite(motorPin1, LOW);
103 digitalWrite(motorPin2, LOW);
104 digitalWrite(motorPin3, HIGH);
105 digitalWrite(motorPin4, LOW);
106 if (distanciaActual1 > distanciaAnterior1) {
107   velocidad1 = 5;
108 }
109 delay(velocidad1);
110 digitalWrite(motorPin1, LOW);
111 digitalWrite(motorPin2, HIGH);
112 digitalWrite(motorPin3, HIGH);
113 if (distanciaActual1 > distanciaAnterior1) {
114   velocidad1 = 5;
115 }
116 delay(velocidad1);
117 digitalWrite(motorPin1, LOW);
118 digitalWrite(motorPin2, LOW);
119 digitalWrite(motorPin3, LOW);
120 digitalWrite(motorPin4, HIGH);
121 if (distanciaActual1 > distanciaAnterior1) {
122   velocidad1 = 5;
123 }
124 delay(velocidad1);
125 digitalWrite(motorPin1, HIGH);
126 digitalWrite(motorPin2, LOW);
127 digitalWrite(motorPin3, LOW);
128 digitalWrite(motorPin4, HIGH);
129 }
130 }
131 }
132 }
133 }
134 }
135 }
136 }
137 }
138 }
139 }
140 }
141 }
142 }
143 }
144 }
145 }
146 }
147 }
148 }
149 }
150 }
151 }
152 }
153 }
154 }
155 }
156 }
157 }
158 }
159 }
160 }
161 }
162 }
163 }
164 }
165 }
166 }
167 }
168 }
169 }
170 }
171 }
172 }
173 }
174 }
175 }
176 }
177 }
178 }
179 }
180 }
181 }
182 }
183 }
184 }
185 }
186 }
187 }
188 }
189 }
190 }
191 }
192 }
193 }
194 }
195 }
196 }
197 }
198 }
199 }
200 }
201 }
202 }
203 }
204 }
205 }
206 }
207 }
208 }
209 }
210 }
211 }
212 }
213 }
214 }
215 }
216 }
217 }
218 }
219 }
220 }
221 }
222 }
223 }
224 }
225 }
226 }
227 }
228 }
229 }
230 }
231 }
232 }
233 }
234 }
235 }
236 }
237 }
238 }
239 }
240 }
241 }
242 }
243 }
244 }
245 }
246 }
247 }
248 }
249 }
250 }
251 }
252 }
253 }
254 }
255 }
256 }
257 }
258 }
259 }
260 }
261 }
262 }
263 }
264 }
265 }
266 }
267 }
268 }
269 }
270 }
271 }
272 }
273 }
274 }
275 }
276 }
277 }
278 }
279 }
280 }
281 }
282 }
283 }
284 }
285 }
286 }
287 }
288 }
289 }
290 }
291 }
292 }
293 }
294 }
295 }
296 }
297 }
298 }
299 }
300 }
301 }
302 }
303 }
304 }
305 }
306 }
307 }
308 }
309 }
310 }
311 }
312 }
313 }
314 }
315 }
316 }
317 }
318 }
319 }
320 }
321 }
322 }
323 }
324 }
325 }
326 }
327 }
328 }
329 }
330 }
331 }
332 }
333 }
334 }
335 }
336 }
337 }
338 }
339 }
340 }
341 }
342 }
343 }
344 }
345 }
346 }
347 }
348 }
349 }
350 }
351 }
352 }
353 }
354 }
355 }
356 }
357 }
358 }
359 }
360 }
361 }
362 }
363 }
364 }
365 }
366 }
367 }
368 }
369 }
370 }
371 }
372 }
373 }
374 }
375 }
376 }
377 }
378 }
379 }
380 }
381 }
382 }
383 }
384 }
385 }
386 }
387 }
388 }
389 }
390 }
391 }
392 }
393 }
394 }
395 }
396 }
397 }
398 }
399 }
400 }
401 }
402 }
403 }
404 }
405 }
406 }
407 }
408 }
409 }
410 }
411 }
412 }
413 }
414 }
415 }
416 }
417 }
418 }
419 }
420 }
421 }
422 }
423 }
424 }
425 }
426 }
427 }
428 }
429 }
430 }
431 }
432 }
433 }
434 }
435 }
436 }
437 }
438 }
439 }
440 }
441 }
442 }
443 }
444 }
445 }
446 }
447 }
448 }
449 }
450 }
451 }
452 }
453 }
454 }
455 }
456 }
457 }
458 }
459 }
460 }
461 }
462 }
463 }
464 }
465 }
466 }
467 }
468 }
469 }
470 }
471 }
472 }
473 }
474 }
475 }
476 }
477 }
478 }
479 }
480 }
481 }
482 }
483 }
484 }
485 }
486 }
487 }
488 }
489 }
490 }
491 }
492 }
493 }
494 }
495 }
496 }
497 }
498 }
499 }
500 }
501 }
502 }
503 }
504 }
505 }
506 }
507 }
508 }
509 }
510 }
511 }
512 }
513 }
514 }
515 }
516 }
517 }
518 }
519 }
520 }
521 }
522 }
523 }
524 }
525 }
526 }
527 }
528 }
529 }
530 }
531 }
532 }
533 }
534 }
535 }
536 }
537 }
538 }
539 }
540 }
541 }
542 }
543 }
544 }
545 }
546 }
547 }
548 }
549 }
550 }
551 }
552 }
553 }
554 }
555 }
556 }
557 }
558 }
559 }
560 }
561 }
562 }
563 }
564 }
565 }
566 }
567 }
568 }
569 }
570 }
571 }
572 }
573 }
574 }
575 }
576 }
577 }
578 }
579 }
580 }
581 }
582 }
583 }
584 }
585 }
586 }
587 }
588 }
589 }
590 }
591 }
592 }
593 }
594 }
595 }
596 }
597 }
598 }
599 }
600 }
601 }
602 }
603 }
604 }
605 }
606 }
607 }
608 }
609 }
610 }
611 }
612 }
613 }
614 }
615 }
616 }
617 }
618 }
619 }
620 }
621 }
622 }
623 }
624 }
625 }
626 }
627 }
628 }
629 }
630 }
631 }
632 }
633 }
634 }
635 }
636 }
637 }
638 }
639 }
640 }
641 }
642 }
643 }
644 }
645 }
646 }
647 }
648 }
649 }
650 }
651 }
652 }
653 }
654 }
655 }
656 }
657 }
658 }
659 }
660 }
661 }
662 }
663 }
664 }
665 }
666 }
667 }
668 }
669 }
670 }
671 }
672 }
673 }
674 }
675 }
676 }
677 }
678 }
679 }
680 }
681 }
682 }
683 }
684 }
685 }
686 }
687 }
688 }
689 }
690 }
691 }
692 }
693 }
694 }
695 }
696 }
697 }
698 }
699 }
700 }
701 }
702 }
703 }
704 }
705 }
706 }
707 }
708 }
709 }
710 }
711 }
712 }
713 }
714 }
715 }
716 }
717 }
718 }
719 }
720 }
721 }
722 }
723 }
724 }
725 }
726 }
727 }
728 }
729 }
730 }
731 }
732 }
733 }
734 }
735 }
736 }
737 }
738 }
739 }
740 }
741 }
742 }
743 }
744 }
745 }
746 }
747 }
748 }
749 }
750 }
751 }
752 }
753 }
754 }
755 }
756 }
757 }
758 }
759 }
760 }
761 }
762 }
763 }
764 }
765 }
766 }
767 }
768 }
769 }
770 }
771 }
772 }
773 }
774 }
775 }
776 }
777 }
778 }
779 }
780 }
781 }
782 }
783 }
784 }
785 }
786 }
787 }
788 }
789 }
790 }
791 }
792 }
793 }
794 }
795 }
796 }
797 }
798 }
799 }
800 }
801 }
802 }
803 }
804 }
805 }
806 }
807 }
808 }
809 }
810 }
811 }
812 }
813 }
814 }
815 }
816 }
817 }
818 }
819 }
820 }
821 }
822 }
823 }
824 }
825 }
826 }
827 }
828 }
829 }
830 }
831 }
832 }
833 }
834 }
835 }
836 }
837 }
838 }
839 }
840 }
841 }
842 }
843 }
844 }
845 }
846 }
847 }
848 }
849 }
850 }
851 }
852 }
853 }
854 }
855 }
856 }
857 }
858 }
859 }
860 }
861 }
862 }
863 }
864 }
865 }
866 }
867 }
868 }
869 }
870 }
871 }
872 }
873 }
874 }
875 }
876 }
877 }
878 }
879 }
880 }
881 }
882 }
883 }
884 }
885 }
886 }
887 }
888 }
889 }
890 }
891 }
892 }
893 }
894 }
895 }
896 }
897 }
898 }
899 }
900 }
901 }
902 }
903 }
904 }
905 }
906 }
907 }
908 }
909 }
910 }
911 }
912 }
913 }
914 }
915 }
916 }
917 }
918 }
919 }
920 }
921 }
922 }
923 }
924 }
925 }
926 }
927 }
928 }
929 }
930 }
931 }
932 }
933 }
934 }
935 }
936 }
937 }
938 }
939 }
940 }
941 }
942 }
943 }
944 }
945 }
946 }
947 }
948 }
949 }
950 }
951 }
952 }
953 }
954 }
955 }
956 }
957 }
958 }
959 }
960 }
961 }
962 }
963 }
964 }
965 }
966 }
967 }
968 }
969 }
970 }
971 }
972 }
973 }
974 }
975 }
976 }
977 }
978 }
979 }
980 }
981 }
982 }
983 }
984 }
985 }
986 }
987 }
988 }
989 }
990 }
991 }
992 }
993 }
994 }
995 }
996 }
997 }
998 }
999 }
1000 }

```

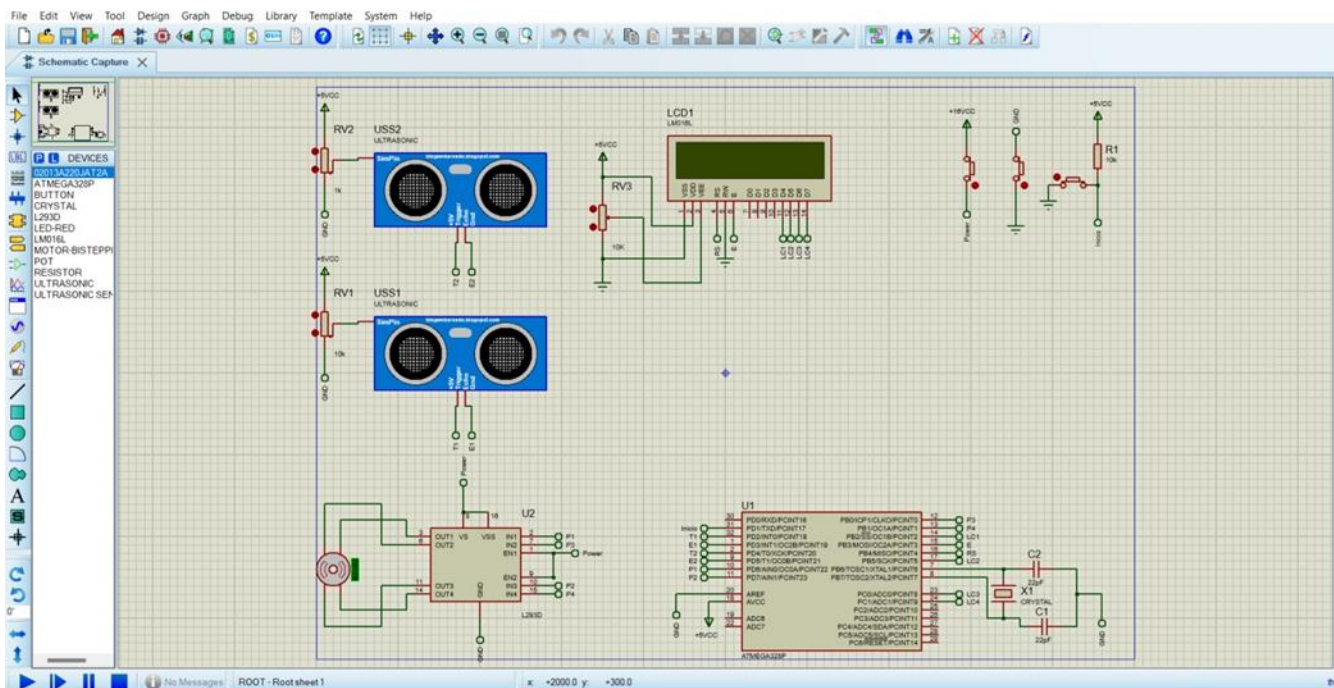
```

157
158 }
159 delay(velocidad2);
160 digitalWrite(motorPin1, LOW);
161 digitalWrite(motorPin2, LOW);
162 digitalWrite(motorPin3, HIGH);
163 digitalWrite(motorPin4, HIGH);
164 if ((distanciaActual2 > distanciaAnterior2) {
165   velocidad2 = 5;
166 }
167 delay(velocidad2);
168 digitalWrite(motorPin1, LOW);
169 digitalWrite(motorPin2, LOW);
170 digitalWrite(motorPin3, HIGH);
171 digitalWrite(motorPin4, HIGH);
172 if ((distanciaActual2 > distanciaAnterior2) {
173   velocidad2 = 5;
174 }
175 delay(velocidad2);
176 digitalWrite(motorPin1, LOW);
177 digitalWrite(motorPin2, HIGH);
178 digitalWrite(motorPin3, LOW);
179 digitalWrite(motorPin4, LOW);
180 if ((distanciaActual2 > distanciaAnterior2) {
181   velocidad2 = 5;
182 }
183 delay(velocidad2);
184 digitalWrite(motorPin1, LOW);
185 digitalWrite(motorPin2, HIGH);
186
187
188
189
190
191
192
193
194
195
196
197
198
199
200
201
202
203
204
205
206
207

```

Tests and results: The results of the tests performed (Circuit simulation) are presented.

Figure 3.6 Proteus circuit



Recommendations for use and safety: Recommendations for use of the cleaning robot are detailed, including safety considerations, preventive maintenance, component cleaning, and any other relevant precautions or guidelines for safe and efficient operation.

- Preliminary check: before cleaning the solar panels, perform a visual inspection to identify obstructions, loose wires, or anything else that may interfere with the safe operation of the robot.
- Maintain a safe environment: ensure that the area where the cleaning robot is being used is free of loose objects, wires or any obstructions that could damage the robot or solar panels.
- Continuous supervision: always monitor the operation of the robot vacuum cleaner during operation. Stay close by and watch for any unusual or unexpected behavior.

- Avoid bad weather: do not use the robot vacuum cleaner in bad weather, such as heavy rain, thunderstorms or strong wind. These conditions can affect the safety of the robot and damage both the robot and the solar panels.
- Routine maintenance: Perform routine maintenance on the robot vacuum cleaner according to the instructions correctly. This may include cleaning parts, lubricating moving parts, and checking cables and connections.
- Proper training: Ensure that personnel responsible for operating the robot vacuum cleaner have received proper training in operation, safety and maintenance. This will reduce the risk of errors or accidents during use.
- Turn off: Before performing any maintenance or repairs on your robot vacuum cleaner, turn it off and follow the manufacturer's recommended safety instructions.
- Report a problem: If you encounter any problems or malfunctions with your robot vacuum cleaner, notify the institution immediately so that they can provide technical support and resolve the problem in a timely manner.

3.6 Conclusions

In conclusion, designing a solar panel cleaning robot is a critical step in the development of this technology. With the right circuit design, positive results and functionality can be achieved that contribute to the efficient operation of the cleaning robot. By considering component compatibility, energy efficiency, circuit reliability and stability, fault protection, and ease of maintenance and repair, a robust and reliable design can be achieved.

Well-designed circuitry allows it to control the movement of the cleaning robot, detect contamination accurately, assist with automatic navigation, and ensure efficient cleaning of the solar panels. In addition, proper power management prolongs battery life and optimizes the use of available resources.

In summary, proper design of the solar panel cleaning robot is essential for efficient, reliable and sustainable operation. This robust design is the basis for the successful development of a solar panel cleaning robot capable of generating maximum power and extending the lifetime of the PV system.

3.7 References

- Núñez, A. M., et al. (2019). Impact of dust on solar photovoltaic (PV) performance: Research status, challenges, and recommendations. *Renewable and Sustainable Energy Reviews*, 107, 562-587.
- Kaldellis, J. K., et al. (2017). Review of dust effect on photovoltaic (PV) performance. *Renewable Energy*, 112, 296-305.
- Gürlek, A., et al. (2018). Analysis of soiling effect on photovoltaic systems in different climates. *Energy Reports*, 4, 381-387.
- Mekhilef, S., et al. (2020). Impact of soiling on the performance of solar photovoltaic (PV) systems: A review. *Renewable and Sustainable Energy Reviews*, 131, 109936.
- Hamzah, A., et al. (2017). Effects of dust accumulation on the performance of solar photovoltaic panels. *Journal of Advanced Research in Materials Science*, 39(1), 1-9.

Educational mechatronics and applied to the design of an automated prototype for obtaining thin films

Mecatrónica educativa y aplicada al diseño de un prototipo automatizado para la obtención de películas delgadas

RIVAS-OROZCO, Rafael†, GAMBOA-TORRES, Gerson A. and VERÁSTEGUI-DOMÍNGUEZ, Luz Hypatia*

Universidad Tecnológica Gral. Mariano Escobedo (UTE), México.

ID 1st Author: *Rafael, Rivas-Orozco* / **ORC ID:** 0009-0002-0791-4836

ID 1st Co-author: *Gerson A. Gamboa-Torres* / **ORC ID:** 0009-0004-56480397

ID 2nd Co-author: *Luz Hypatia Verástegui-Domínguez* / **ORC ID:** 0000-0003-1538-2825, **CVU CONAHCYT:** 589758

DOI: 10.35429/P.2023.1.37.45

R. Rivas, G. Gamboa and L. Verástegui

*ralvarez@upp.edu.mx

Á. Marroquín, L. Castillo, J. Olivares and A. Álvarez (AA. VV.). Young Researchers. Engineering Applications - Proceedings-©ECORFAN-México, Queretaro, 2023.

Abstract

This project presents the design and development of an automated prototype for the deposit of thin films on glass substrates, using the chemical immersion method (SILAR). The importance of the development of these films lies in their multiple applications such as electronic resistors, thin film transistors and capacitors. One of the objectives of the project is to promote scientific, technological and innovation interest so that higher education students understand real problems, in which solutions can be provided through the development and integration of mechatronic prototypes. The final device has a 500mm vertical axis, a 100mm stroke end piston, a clamp driven by a stepper motor, a temperature control bath, a resistive oven, LCD16X2 screen, its structure is made of aluminum profiles. 4040 extrusion with 10mm acrylic walls and its operation is carried out using software based on the Arduino platform.

Automated prototype, Arduino platform, Thin films, SILAR method

4 Introduction

At present, globalization implies that people acquire competitive skills, knowledge, and values to solve problems of high complexity. For such a motive, it is necessary to form students into integral citizens who could identify the challenges in their environment with a basis in its criteria and capture of decision (Anderson, Londoño, & Martínez, 2022). One of the objectives of the project in its first stage is to promote scientific, technological, and innovation interests so that students of higher education understand real problems for which they can provide solutions through the development and integration of mechatronic interactive prototypes, thus supporting the teaching and learning process.

This project presents the design and technological development of a prototype that allows the automation of a process that was previously done manually within the university. The process is known as chemical immersion (or SILAR method), which consists of immersing a glass substrate in different chemicals for some time for the formation of thin films.

4.1 Background

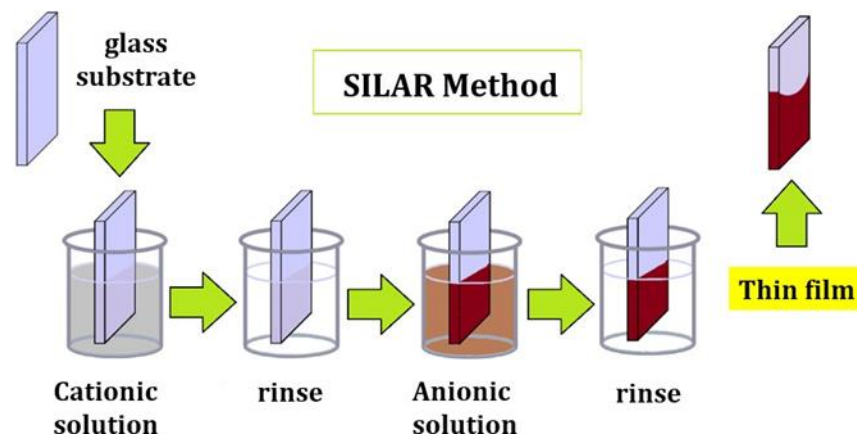
Thin films refer to a layer of material whose thickness ranges from fractions of a nanometer ($1\text{nm}=10^{-9}\text{m}$) to several micrometers thick. Controlled synthesis of materials such as thin films (process called deposition) is a fundamental step in many applications. A common example is the household mirror, which usually has a thin layer of metal on the back of a glass sheet to form a reflective interface.

Thin films have interesting properties that are quite different from those of bulk materials. As a film becomes thinner, the properties of the surface become more important than the thickness of the film. The other cause of interest is the miniaturization of elements such as electronic resistors, thin-film transistors, and capacitors. This is due to the fact that its properties depend on a number of interrelated parameters and also on the deposition technique. Despite the numerous strategies designed for the deposit of thin films, many of them require expensive specialized equipment, a fact that limits their use as an experimental tool in academic laboratories (Abengunde & et.al., 2019; Fayomi & et.al., 2019).

There are several deposition techniques to obtain thin films, including low-cost techniques such as chemical bath deposition, electrodeposition, and the SILAR method. To facilitate the work of obtaining thin films in the laboratory, developments aimed at the automation of the SILAR process have been carried out. For example, researcher Calixto-Rodríguez and collaborators built a prototype controlled through a man-machine interface. They used an HMI and state machine-based programming to control the SILAR process variables and number of cycles for the formation of thin films. This system consists of three stages: structural design, electronics and control programming, and HMI (Calixto-Rodríguez, Valdez-Martínez, & et.al., 2021). Subsequently, a group of researchers from the Veracruzana University developed an instrument composed of three different systems: a mobile platform with two degrees of freedom, an 8-bit microcontroller to adjust speeds over the XY axes, and free code software to program and monitor the main deposition parameters of the SILAR device (Woo García, Rodríguez Ibarra, & et.al., 2022).

This work focused on the deposition of thin films by means of the chemical immersion method, also known as SILAR, which consists of the adsorption and reaction of successive ionic layers to deposit films of different chemical precursors (Nkamuo, Okoli, & Igweze, 2021) but in an automated way. Figure 4.1 shows an outline of the SILAR process for the formation of thin films.

Figure 4.1 SILAR Process Outline



Source: (Calixto-Rodríguez, Valdez-Martínez, & et.al., 2021)

Our prototype is capable of handling glass substrates in a particular position, and by means of software, it is possible to control the time, position, speed, movement of the piston, and temperature monitoring. Another advantage of this tool is that this prototype is able to protect itself since it is completely closed. Furthermore, its software is capable of adapting to various requirements, offering greater flexibility to the user. Also, it has a system of emptying and filling of water containers that contain chemical solutions, which allows it to handle temperatures higher than the ambient temperature. This project has the main objective of impacting the training of mechatronics students in the automation area, because to build it, you will need to apply the skills and knowledge you have acquired in your subjects. It also allows the development of other skills such as leadership, resource management, time management, teamwork, problem-solving communication skills, as well as their professional and comprehensive training as engineers. In addition, the nanotechnology program will benefit from having a specialized tool for the development of new materials due to the versatility of the prototype, allowing students in this area to expand their competencies and enrich their educational learning.

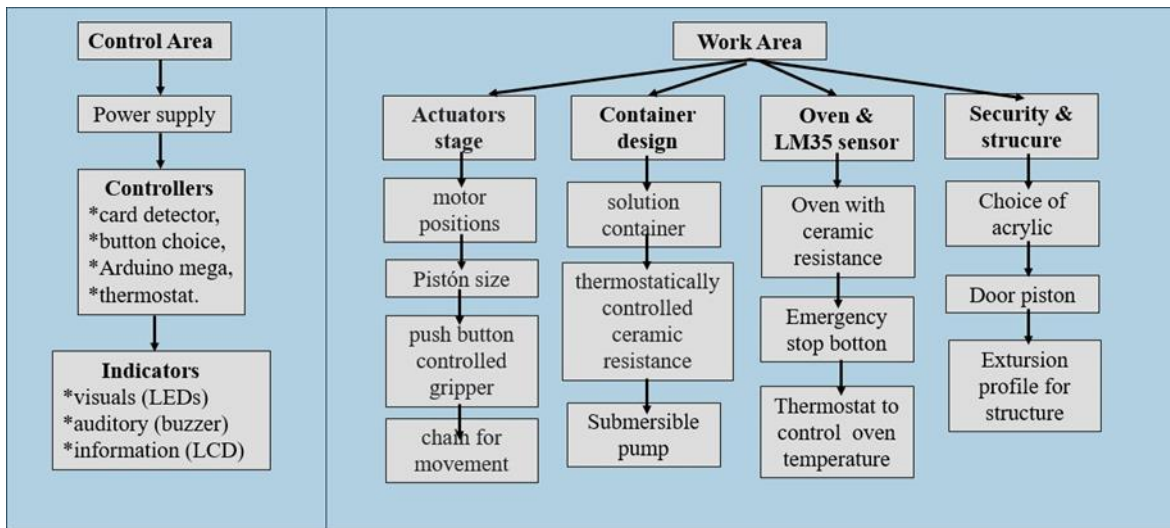
4.2 Methodology

This project consists of the design and construction of a prototype to develop thin films by chemical immersion deposition (SILAR method). The following specifications were proposed to design the equipment:

- That the prototype is closed to give greater security to the user.
- Have a water filling system with heating resistance to control the temperature of the solutions.
- Add a resistive oven to dry thin films after each immersion cycle is finished.
- Incorporate screens to monitor temperatures and process.
- Program a presence card that works as a key to operate the computer.

The design and construction of the equipment are divided into two areas: the control area and the work area. The control area consists of the power source, microcontrollers, user interface buttons, indicators, and card detector. The work area includes the stepped motor, 100-mm piston, vertical shaft, a heating resistance container to control the temperature of chemical solutions, and a resistive furnace for drying thin films between each cycle. In Figure 4.2, a block diagram is observed where each of these areas is briefly described.

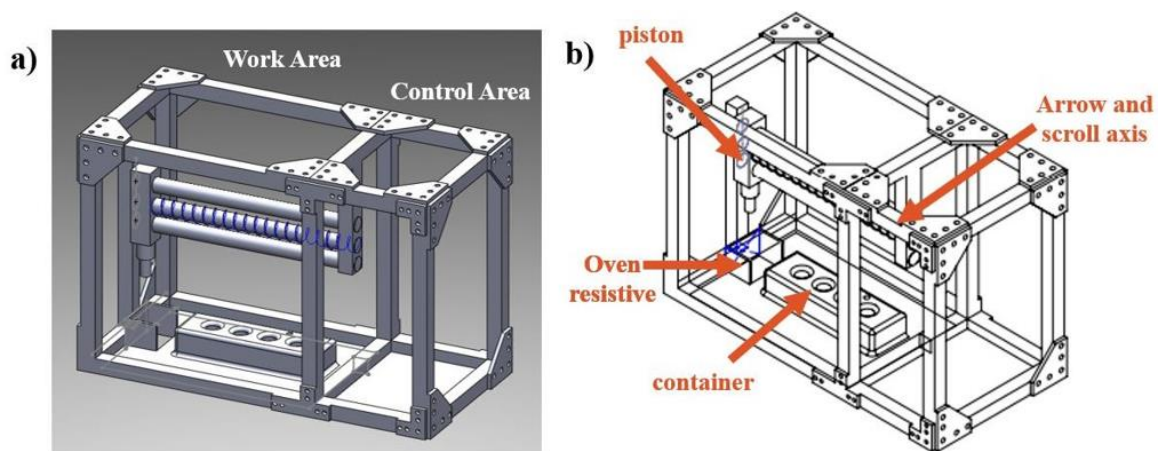
Figure 4.2 Block diagram with description of the work áreas.



Source: Own elaboration

The prototype was designed using SolidWorks software. Figure 4.3 shows the final design indicating the aforementioned work areas.

Figure 4.3 a) Areas of final prototype, b) description of elements of work area

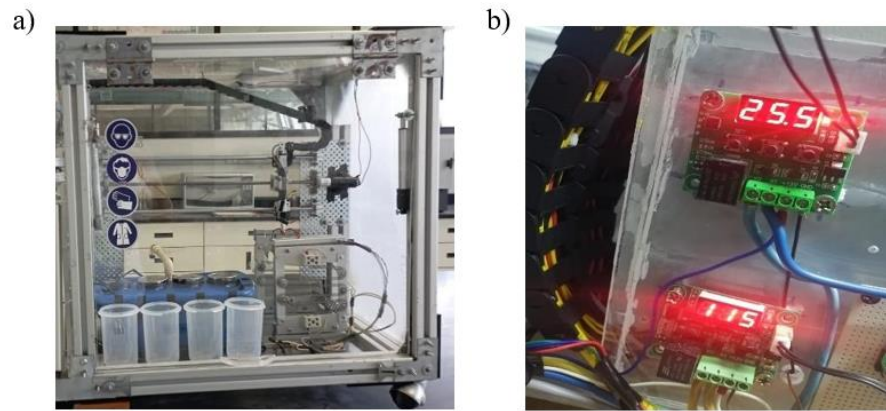


Source: Own elaboration

4.2.1 Works area

Within the working area is the mechanical module, which consists of a stepped motor, a piston, and a claw, which are limited to 480 mm of linear displacement, a maximum voltage of 12V for the piston with a height of 23 cm, and a clamp to control the pressure on the substrate. Also used were two thermostats with tolerances of $\pm 2^\circ\text{C}$ and $\pm 5^\circ\text{C}$, one intended to control the resistance of the container of water and the other to check the temperature of the resistive furnace, respectively. Figure 4.4 shows a) the working area of the finished prototype, and b) the thermostats used are also observed.

Figure 4.4 Work area of the final prototype and its thermostats



Source: Own photographs of the prototype

4.2.2 Control area

The RFID module (which allows reading the key code), visual and auditory indicators were incorporated. Libraries that are included within the software of the Arduino platform were used to be able to manipulate and give programming instructions independently; therefore, the engine was first programmed in steps for the shaft, the piston, the claw, and the RFID module. Also activating each independent function, we proceeded to migrate each part of the programs to join them in itself and to be able to combine all the actions by means of the conditions (if, else, for) that helped us to make use of the libraries together using a C++ programming language. Figure 4.5 shows the control area with its respective buttons and indicators, some of the libraries used for programming are also observed.

Figure 4.5 Control area of the final prototype and programming libraries



Source: Own photographs of the prototype

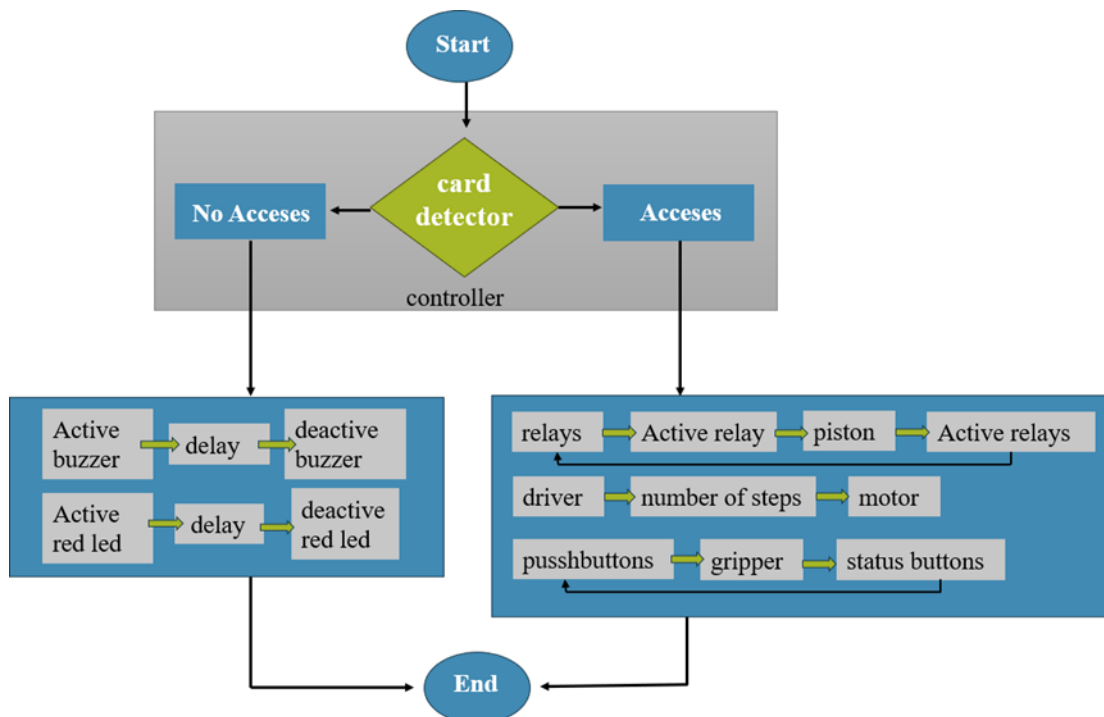
Figure 4.6 shows the final finished prototype, and Figure 4.7 shows the schedule flowchart, which serves to simplify the operator's execution actions when using the device.

Figure 4.6 Final prototype



Source: Own elaboration

Figure 4.7 Programming flowchart



Source: Own elaboration

4.3 Results

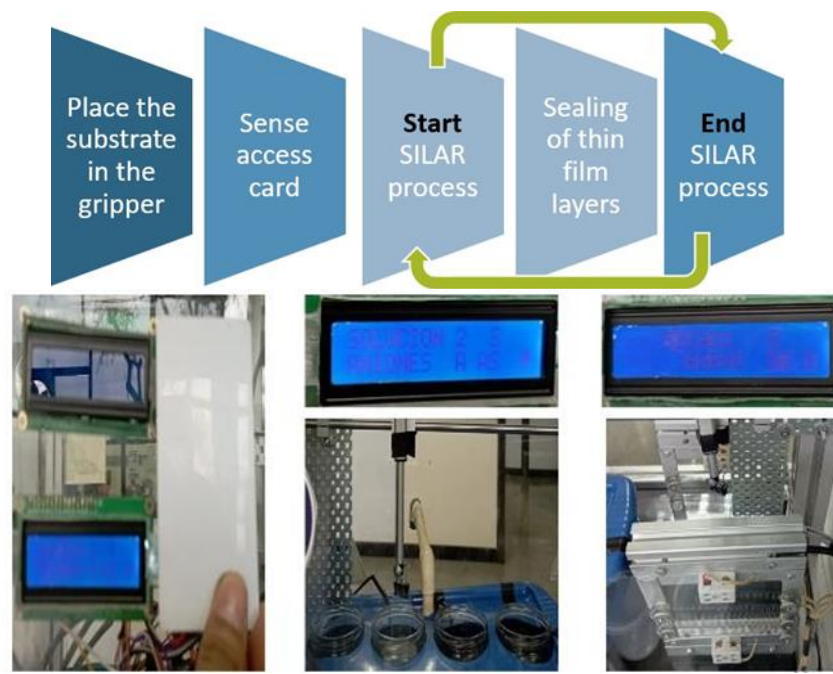
A prototype that meets the initial proposed requirements was obtained. Laboratory tests monitor the behaviour of this to check that everything works properly. Figure 4.8 shows a diagram that simply indicates the mode of operation of the prototype, and in the images, you can visually observe the stage of the process that is being executed.

Mode of operation:

1. The substrate is placed in the prototype clamp.
2. The card (key) is placed on the sensor to give access to the process and begin its execution.

3. Start the SILAR process. In this, you can vary initial parameters such as time, speed, and number of cycles depending on the specifications given by the user.
4. Once the substrate is immersed in the solutions with chemical precursors, the SILAR process ends until it passes to the stage of sealing or drying layers through the resistive furnace, then it starts again with the immersion in the solutions. Each time the substrate reaches the resistive furnace, it is counted as a complete cycle.
5. The process is complete until the device has completed all scheduled cycles.

Figure 4.8 Diagram of operation of the SILAR process



Source: Elaboration of diagram and own photographs

Tests were done to determine the time it takes for the water container to reach its maximum temperature (80 ° C). Table 4.1 shows information from independent tests performed, as well as the temperatures reached.

Table 4.1 Temperature monitoring in the container

Test	Temperature(°C)	Time (min)
1	35	11.9
2	35	11.6
3	40	13
4	40	12.7
5	50	16
6	50	16.3
7	60	20
8	60	19.8
9	80	26
10	80	26.2

Source: Own elaboration

From Table 4.1 it can be observed that the recorded temperatures are constant with respect to time. It was also concluded that above 40 ° C it will no longer be advisable to develop thin films in this device, since chemical solutions could begin to deliver toxic gases that could damage the prototype or even be harmful to the health of the user; however, this depends on the type of chemical precursor used to perform the film deposition process.

Table 4.2 shows the information collected from independent tests that monitor the time it takes for the resistive furnace to reach its maximum temperature.

Table 4.2 Temperature monitoring in the resistive furnace

Test	Temperature(°C)	Time(min)
1	80	34.3
2	80	35
3	90	38.8
4	90	39
5	105	39.7
6	105	39.4
7	120	45.1
8	120	45

Source: Own elaboration

From Table 4.2 it is again observed that the temperatures recorded in the tests are constant with respect to time. It was also concluded that the resistive furnace must reach its maximum temperature in order to dry thin films optimally and quickly.

In general, this prototype consumes 15A (amperes) when in maximum load (temperatures at their maximum range.) This data was obtained from the electrical tests carried out with the multimeter. Since the device is turned on, the ambient temperature is sensed, and the resistors start to heat, it can be used for 90 minutes and should be allowed to rest for 15 minutes before being used again.

Annexes Does not apply.

4.4 Acknowledgment

We thank the rector of our university, C.P. and Lic. Fernando Garza Rodríguez, for the support provided to this work, for the direction and rigor provided in its development.

We also thank the director of the Mechatronics -Automation Area, Engineer Juan José Gloria Puente, for the trust he gave us to develop this project.

We also thank the teacher Hilariona Martínez and all the teachers of the Mechatronics, Nanotechnology and Environmental Chemistry careers for all the ideas and suggestions provided during the design of the project.

4.5 Financing

This work has been financed by own resources of the Universidad Tecnológica General Mariano Escobedo.

4.6 Conclusions

An automated device was built to develop thin films by the chemical immersion deposition process (SILAR). This device allows you to control initial process parameters such as immersion time, speed, and number of cycles. The working temperature can be adjusted in solutions with chemical precursors, but it is necessary to consider that at temperatures above 40 ° C if these precursors are toxic or corrosive, they could damage the components of the prototype, so it is recommended to work at room temperature or check the technical sheets of the chemicals in order to keep the prototype in good condition.

This prototype is safe for the user as its work area is completely closed, plus with the access card, you can have greater control over people who want to manipulate it. It is important to take into account your working time so that they can function properly and films are developed optimally.

As a future work, it is intended to make an airtight system in order to control the characteristics and properties of thin films. It is also planned to add a grid with an extraction filter in the event of increasing the temperatures of the chemical solutions to avoid damaging the prototype. Another area for improvement is to separate the furnace section from the solutions to avoid any type of incident with the equipment.

4.7 References

Abengunde, O., & al., e. (2019). Overview of thin film deposition techniques. *AIMS Materials Science*, 6(2), 174-199. doi:10.3934/materci.2019.2.174.

Anderson, L., Londoño, D., & Martínez, G. (2022). Desarrollo de competencias en el ámbito educativo: definiciones conceptuales y operacionales. *Revista de investigaciones de la Universidad Le Cordon Bleu*, 9(1), 20-30. doi:10.36955/RIULCB.2022v9nl.002.

Calixto-Rodríguez, M., Valdez-Martínez, J., & al., e. (2021). Design and Development of Software for the SILAR Control Process Using a Low-Cost Embedded System. *Processes*, 967.

Fayomi, O., I., A., Abioye, O., & O., F. (2019). New tren in thin film composite coating deposition: a mini review. *Procedia Manufacturing*, 35, 1007-1012. doi:10.1016/j.promfg.2019.06.049.

Nkamuo, J., Okoli, N., & Igweze, C. (2021). Results of SILAR cycles variation on the optical structural and electrical properties of lead iodide thin films. *Applied Physics*, 4, 31-39. doi:10.31058/j.ap.2021.43003.

Woo García, R., Rodríguez Ibarra, I., & al., e. (2022). Automated instrument for the deposition of thin films using successive ionic layer adsorption and reaction. *Processes*, 10, 492. doi:10.3390/pr10030492.

Mobile laboratory for FVM analysis

Laboratorio móvil para análisis de MFV

SÁNCHEZ-VILLARREAL, Milagros del Rocío†, HERNÁNDEZ-SALAS, Carlos Manuel, CASTILLO-CAMPOS, Nohemí Alejandra and ÁLVAREZ-MACÍAS, Carlos*

Tecnológico Nacional de México, Departamento de Eléctrica, Electrónica y Energías Renovables, Campus Laguna, Coahuila, México.

ID 1st Author: *Milagros del Rocío, Sánchez-Villarreal* / **ORC ID:** 0009-0009-9272-5140

ID 1st Co-author: *Carlos Manuel, Hernández-Salas* / **ORC ID:** 0009-0002-7640-0767

ID 2nd Co-author: *Nohemi Alejandra, Castillo-Campos* / **ORC ID:** 0009-0001-2490-4325, **CVU CONACYT ID:** 1271718

ID 3rd Co-author: *Carlos, Álvarez-Macías* / **ORC ID:** 0000-0002-2263-0316, **CVU CONAHCYT ID:** 165872

DOI: 10.35429/P.2023.1.46.60

M. Sánchez, C. Hernández, N. Castillo and C. Álvarez

* Alu.18130747@correo.itlalaguna.edu.mx

Á. Marroquín, L. Castillo, J. Olivares and A. Álvarez (AA. VV.). Young Researchers. Engineering Applications - Proceedings-©ECORFAN-México, Queretaro, 2023.

Abstract

Due to its geographical location, different regions are rich in solar energy, which favors the use of solar panels, however, the installation is a process that involves taking different factors into account, and it is a recurring topic of study. In this project, a mobile unit was built for the transport of photovoltaic modules (MFV) and to study in a practical way the factors that affect their efficiency. The preliminary design of the mobile laboratory was carried out taking into account the measurements of a 410 W JaSolar module, from this consideration the pertinent calculations were made to size the laboratory, then the measurements obtained were scaled and a prototype was elaborated through a model to detail the necessary mechanisms and materials. Then proceeded with the construction of the laboratory based on the preliminary design and the prototype. Finally, the functionality of the mobile unit was verified by determining the efficiency of the 410 W JaSolar module at different inclination angles, on different floors, shading vertically and horizontally, and with ventilation cooling. It was concluded that the laboratory is practical and meets the desired characteristics.

Transport, Analysis, Photovoltaic module

5.1 Introduction

In recent years, population growth has caused energy demand to increase worldwide, the main source that satisfies this demand has been through the use of fossil fuels, which have a significant impact on the generation of greenhouse gases that damage the environment, this has led the world to set its sights on renewable energies, which is why in the last decade there has been a considerable increase in the use of these energies, as they generate less pollution and help reduce the use of fossil fuels. Urban environments, due to their high demand for energy consumption, are considered one of the most promising places for the installation of renewable technologies. Among the different types of technologies available, solar panels are the most promising in urban areas in order to meet the needs of the residential and commercial sector (Sukhatme and Nayak, 2009, p.71-108).

To understand how a photovoltaic cell works, it is essential to have a clear understanding of the concept of "radiation", defined as the energy emitted by the sun, which propagates in the form of electromagnetic waves through space in multiple directions. This energy originates from a series of nuclear fusion reactions that occur in the sun. Different types of radiation are differentiated by their wavelengths; ultraviolet rays, infrared rays, and visible rays (Duffie and Beckman, 1991, p. 747).

One of the ways to harness it is by converting solar radiation into electrical energy by means of the photoelectric effect, with the help of semiconductors. Photovoltaic devices are semiconductors that convert part of the incident solar radiation into direct current electrical energy (Goswami and Kreith, 2000, p.1-80).

The power generation of a solar cell is mainly affected by the variation in incident solar radiation and cell temperature (Tsai, Tu, and Su, 2008). This means that a PV cell works thanks to the presence of solar radiation with the minimum solar radiation they receive to start working. Figure 5.1 shows the earth's declination.

Figure 5.1 Earth's declination

Source: Goswami and Kreith, 2000

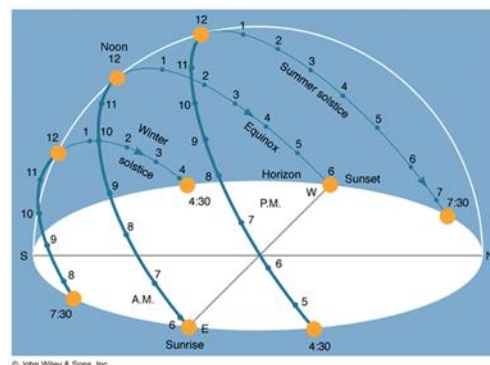
Not only radiation is fundamental, as it varies according to geographical location, but the theory of the apparent motion of the sun adds to these factors. To understand the apparent motion of the Sun, the actual motion of the Earth around the Sun and on its own axis must be taken into account. The nearly circular (it is slightly elliptical with the Sun at one of its foci) rotation of the Earth around the Sun takes place in a year in a plane called the ecliptic, and the rotation about its axis causes it to make one complete revolution every 24 hours. The Earth's axis is tilted 23.45° with respect to the ecliptic (see figure 1.1). Because of the tilt of the Earth's axis, the sun's rays strike the Earth's surface perpendicularly at a different point each day of the year. The Cooper equation for declination (degrees) where "n" is the day of the year is equation 1.

$$\delta = 23.45 * \text{sen} \left(360 \frac{284+n}{365} \right) \quad (1)$$

In addition to the above, there are angles that affect its functionality. The solar hour angle is the angular displacement of the sun in the apparent orbit (ecliptic) east or west of the local meridian, the morning is negative and the afternoon is positive, the solar hour angle is equal to zero at solar noon and varies by 15° per hour from solar noon, for example, at 7 a.m. (solar time) the hour angle is equal to -75° . At 7 p.m. (solar time) the hour angle is equal to 75° . The sunset hour angle (ω_s) is the solar hour angle corresponding to the time when the sun sets; it is given by the following equation:

$$\text{Cos}(\omega_s) = -\text{Tan} \psi \text{Tan} \delta \quad (2)$$

Where (δ) is the declination, calculated through equation 1 and ψ is the latitude of the site, specified by the user. The orientation of the solar collector is described by its tilt angle β and the "azimuthal" azimuth (γ), both related to the horizontal and considered optimal when facing south ($\gamma=0^\circ$) in the northern hemisphere. The optimum tilt angle depends on latitude λ , solar declination, or days of the year (J. Duffie and W. Beckman, 1991, p. 747), this is shown in Figure 5.1.

Figure 5.2 Apparent Motion of the Sun

Source of reference: Sukhatme and Nayak, 2009

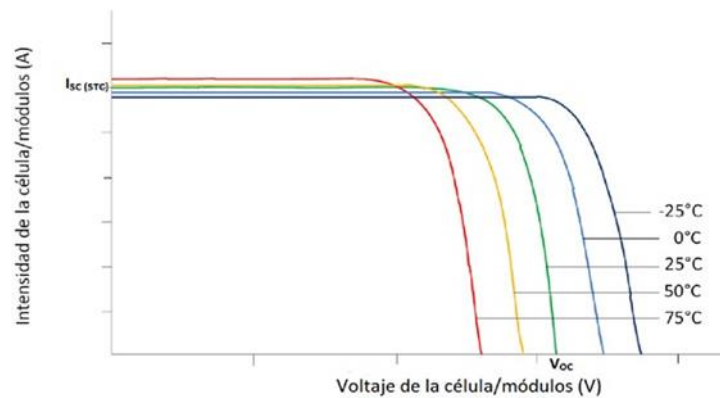
It was investigated that the daily solar energy collected was 19 % to 24 % higher with a solar PV panel, with a single-axis east-west tracking system than with a fixed system (Salmi et al, 2012). However, since solar tracking systems have high operating and maintenance costs and are not always applicable, it is often desirable to set the solar collector to a fixed value of an optimal tilt angle the standard recommended angle is $\pm 10^\circ$.

If you live in the northern hemisphere, you would point your panels to the south. If you live in the southern hemisphere, your panels should point north. Most homeowners with solar power systems mount their panels in a fixed position, where the panels can be manually tilted as needed (Tsai, Tu, and Su, 2008).

A. Factors affecting the performance of solar panels.

In the last decade, research has been carried out to identify the factors that affect the performance of photovoltaic panels in order to mitigate their effects and achieve significant improvements in terms of efficiency for this type of system (see Fig. 5.2).

Figure 5.3 Temperature Vs open circuit voltage graph



Source: Algarín, 2011

Among the factors that interfere with the optimal performance of solar panels is temperature, which plays a key role in the energy conversion process in these systems. Both the electrical performance and the power output of the module depend linearly on the operating temperature of the panel. Solar panels absorb on average 80% of the solar irradiation received. However, a part of this irradiance is converted into electricity and the remaining is converted into heat (Cepeda, 2017). The ideal operating temperature of a solar panel is often around 25°C (Algarín, 2011).

For solar panel installation, the tilt angle of the PVM is an important consideration that will have variations between regions, as this can benefit or affect the efficiency and energy yield of the entire system. The tilt angle of the panel affects the solar radiation reaching the surface of the cells. When the panel is positioned perpendicular to the sun, it receives the maximum radiation for a time interval, which is considered the optimum tilt angle. This angle is affected by factors such as latitude, solar radiation characteristics, period of use, shading effect and the distribution of sunny days representing climatic conditions (Cepeda, 2017).

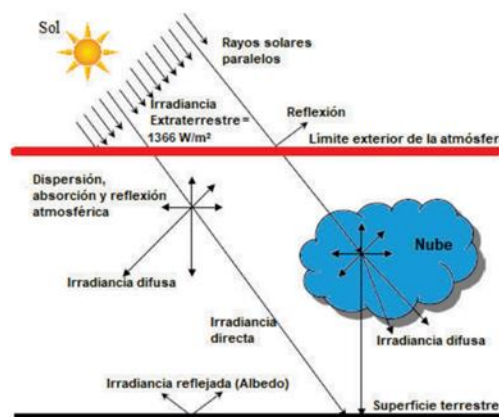
The shading effect is caused when the light hitting the panel surface is obstructed causing voltage and current mismatches in the system. This is mainly due to shadow formations produced by elements close to the panels such as trees, structures or external agents that prevent sunlight from reaching evenly over the panel surface. A solar panel that is under the effects of shading collects energy unevenly, which leads to fluctuations in the delivered power causing damage to the PV system components such as the inverter or batteries (Cepeda, 2017). Figure 5.3 shows the shading effect caused by tree branches.

Figure 5.4 Shading effect

Source of reference: Sukhatme and Nayak, 2009

Solar irradiance is an important monitoring parameter, used to evaluate the efficiency and performance of photovoltaic systems mainly, just as the operating temperature affects the performance of a panel, the irradiance to which the solar cells of a panel are exposed affects the efficiency of the system. Among the types of irradiance are (Cushicóndor, 2019):

- Direct irradiance: direct irradiance is the component of global irradiance, which is incident on a surface and comes directly from the sun, with no change in direction (Cushicóndor, 2019).
- Diffuse irradiance: It is the one that impacts on the earth's surface indirectly, since it goes through the atmosphere and clouds, which causes it to disperse, diffuse irradiance represents 15% of the global irradiance on sunny days and on cloudy days this percentage increases considerably (Cushicóndor, 2019).
- Reflected irradiance: This is the irradiance reflected by the earth's surface, and depends on the reflection coefficient of each surface or ground where the panels are installed. It is also known as albedo [10] (see figure 5.4 types of solar irradiance).

Figure 5.5 Types of solar irradiance

Source: Cushicóndor, 2019

The inclination and orientation will be factors that will directly influence the way in which the panel receives light and consequently its optimal performance. Table 1.1 shows the standard values for the recommended tilt for module installation. This will depend on the translational movement of the planet, since it will not always be the same orientation throughout the year due to seasonal changes, this is done in order to maintain a good energy production. In the specific case, Mexico is located in the northern hemisphere, therefore, the solar panels should be oriented towards the south (Tarifasdeluz, 2022).

- Solar panels in winter: At this time of the year, the sun is lower and its radiation has a more horizontal incidence. To make the most of this solar orientation, the angle of inclination of the solar panels is raised between 10° and 15° with respect to that calculated with the latitude, so that the solar panels are in a position close to total verticality (Tarifasdeluz, 2022).

- Solar panels in summer: In this season of the year, the sun is high and the radiation is vertical most of the day. To capture the most energy in this solar orientation, the tilt angle is reduced by 10° to 15° degrees to obtain a tilt close to total horizontality (Tarifasdeluz, 2022).

Table 5.1 Standard for angles

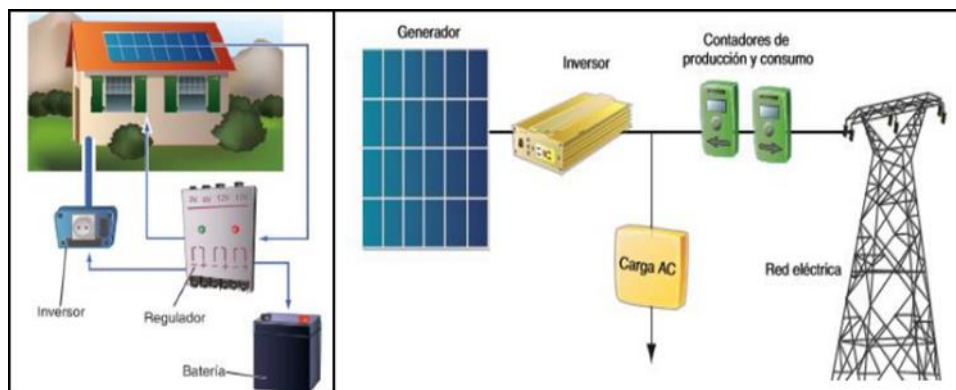
Latitude of location	Fixed angle of inclination
0° to 15°	15°
15° to 25°	Same latitude
25° to 30°	Latitude + 5°
30° to 35°	Latitude + 10°
25° to 40°	Latitude + 15°
40° or more	Latitude + 20°

Source: Arbona, 2022

B. Principle of photovoltaic operation.

A photovoltaic system is the set of electrical and electronic equipment that produces electrical energy from solar radiation through the photoelectric effect, which is the effect of generating electric current when the semiconductor materials of a solar cell are illuminated, causing the generation of pairs of electrons. Photovoltaic systems can be stand-alone systems and grid-connected systems. Autonomous systems by means of a solar panel produce energy, to be subsequently stored in batteries to be available at any time (Cepeda, 2017). This is shown in Figure 5.6.

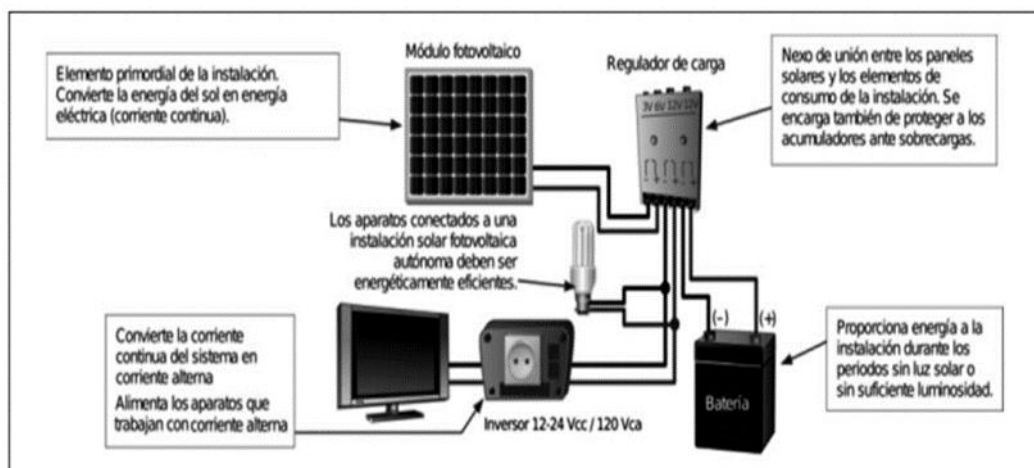
Figure 5.6 Stand-alone installation, grid-connected installation



Source: Cepeda, 2017

Solar cells or solar cells can be considered commercially as the smallest commercially available element to transform the sun's radiation into electricity. The combination of solar cells with similar characteristics allows increasing both the voltage and the current generated and make up what is known as a solar photovoltaic module or panel (Ortiz, 2013), (see Figure 5.7).

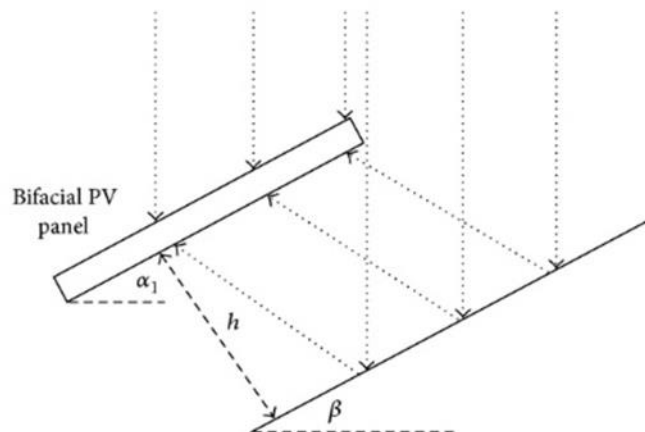
Figure 5.7 Diagram of a solar photovoltaic system



Source: Ortiz, 2013

On the other hand, bifacial modules are those with two layers of photovoltaic cells, generally with PERC technology. The cell located on the upper or front face has the objective of capturing direct solar irradiation, while the cell located on the lower or rear face takes advantage of the diffuse radiation reflected on the surface on which the modules are located. In addition, bifacial technology also seeks to use high-performance photovoltaic cells in order to maximize the flow of electrons. The great advantage of bifacial cells is the increase in module efficiency by up to 25% and even up to 30%. One of the most relevant factors of bifacial technology and that makes the big difference compared to single-facial modules is the albedo. This is defined as the percentage of incident sunlight -mainly diffuse radiation- reflected by a surface and determines in turn the amount of reflected radiation on the ground available to be used by the lower face of the panel (Martín, 2022). Figure 5.8. shows the use of light thanks to its two faces.

Figure 5.8 Bifacial panels



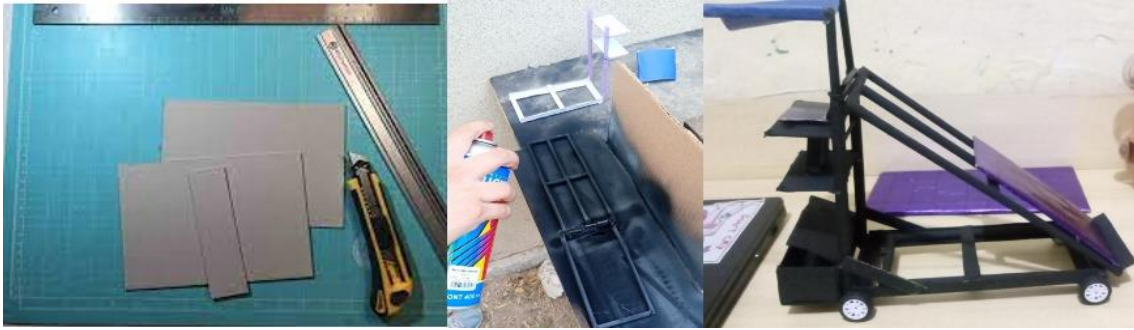
Source: Martín, 2022

The design and construction of this mobile laboratory arises from the need of students to analyze and work with photovoltaic modules, the main objective is to build a structure that facilitates the study of photovoltaic modules, to optimize the transport of the PVMs, and the investigation of the phenomena that affect the operation of a panel, as well as the variables that occur in the environment. Specifically, the aim is to design an ergonomic and comfortable system for the user who will carry out the study with PVMs, through the elaboration of a previous design using 2D drawing programs (AutoCAD), as well as a scale prototype. It is intended to build the mobile unit taking into account the durability and strength of the materials, as well as the ability to handle the module safely. As well as to evaluate the practicality of the mobile laboratory through the study of the efficiency of a module by performing various tests.

This paper deals with the design and construction of a mobile structure for the transport and analysis of photovoltaic modules, as well as the experimentation with it. The first chapter introduces the important topics and concepts for the understanding of the work, while the second chapter indicates the materials and procedures used to design and build both a prototype and the final structure, as well as the costs involved and the experimentation techniques used. On the other hand, Chapter 5.3 discusses the results obtained from the different measurements made with the use of the mobile laboratory, where inferences are made about the factors that affect the performance of a solar module. Finally, Chapter 5.4 contains the conclusions regarding the operation of the mobile laboratory and the evaluated performance of the photovoltaic module.

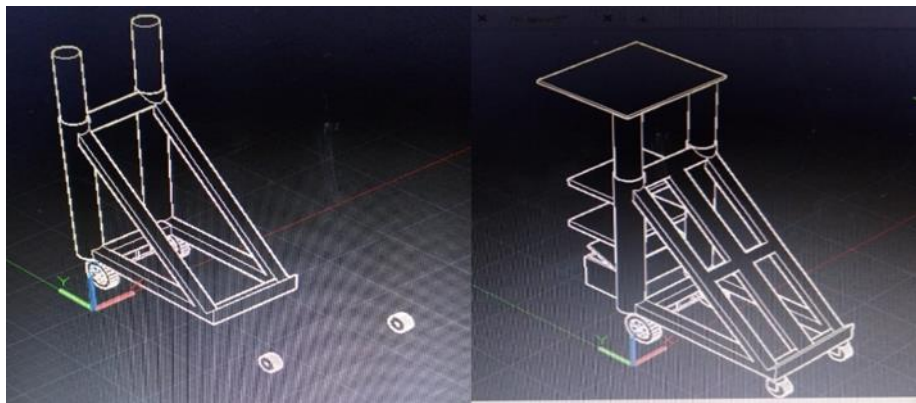
5.2 Methodology

The development of the laboratory began with the creation of a model using different materials such as cardboard, sticks, fabric and straws, when the pieces were already with their respective measures, they were cut out, the model was painted and then joined to give it the details that would be the incorporation of tires, shelves, shade and a drawer, this is shown in figure 5.9.

Figure 5.9 Elaboration of mockup

Source: Own elaboration

In addition, the virtual design of the 3D prototype was elaborated in the AutoCAD program of what would be the laboratory as shown in Figure 5.9.

Figure 5.10 Digitized prototype

Source: Own elaboration

Once the design was finalized, the materials were quoted and compared and the construction of the laboratory began. Table 5.2 lists the materials used for the constructed laboratory, as well as the quantities required in each case. During construction the tools used were a flexometer, a magnetic square, mechanical clamps, iron presses, a hammer, a torpedo level, polisher (4" cutting and grinding discs), drill, inverter, 60/13-3/32 electrodes and wire brush. The safety equipment used for handling the tool included an electronic mask, leather gloves, a boot with a dielectric sole, a work coat, gloves and safety goggles.

Table 5.2 Material for the construction of the mobile laboratory

Material	Quantity used	Size
Sill	6 m	2" (1/4)
Angle	6 m	2" (1/8)
Quadrangular PTR	15 m	1 1/4" (14)
Circular conduit pipe	1.6 m	1"
Circular conduit pipe	1.4 m	1 1/4"
Rod	1.1 m	1/2"
Rotating rims	2	6"
Wagon wheel rims	2	8"
Carousel rims	8	1"
Brackets	4	20 cm
Shelves	2	(35x75) cm ²
Butterfly clamps	2	3/4"
Bicycle horns	1	45 cm
Gray enamel	1	1 L
Red enamel	1	1/4 L
Car sunshade	1	One size fits all

Source: Own elaboration

We began by measuring the sections of PTR, sill, angle, and circular tube that would serve both for the structure of the project and for the base where the panels would be reloaded. Once the pieces were measured and cut, they were welded together.

Figure 5.11 Taking of measurements and welding



Source: Own elaboration

To achieve a better result, the corners of the structure were polished, removing the imperfections generated by the welding and then, in the lower part of the base, two pieces of angle of 35 cm each were added, which would function as the support for the drawer, and then the pieces were joined together.

Figure 5.12 Joining the pieces



Source: Own elaboration

With the shade in place and most of the structure ready, it was painted to later add details such as shelves, drawer, tires, the angles were measured from 10° to 45° and handles were added to facilitate the transport of the laboratory.

Figure 5.13 Finished structure



Source: Own elaboration

Finally, with the structure assembled and working, several tests were carried out in which different factors such as panel ventilation, shading, angles and soils were varied in order to demonstrate the effectiveness of the panel for the transport and analysis of the VFM as shown in Figure 5.13 For these tests the equipment required was a hand-held pyranometer, infrared thermometer, solar panel multimeter, a fan, anemometer and the JAM72S10 410/MR 410 W solar panel.

The first case analyzed was to determine the partial shading effect of the module by using a tarp to shade the panel cells horizontally and then shading it vertically. In the second analysis, the albedo effect was determined by using 4 different shades of flooring around the module, transporting it to different areas of the institute. The efficiency of the module was also determined by positioning it at each tilt angle available in the laboratory. And finally, the performance of the module was analyzed with and without cooling using a fan.

Figure 5.14 Laboratory tests



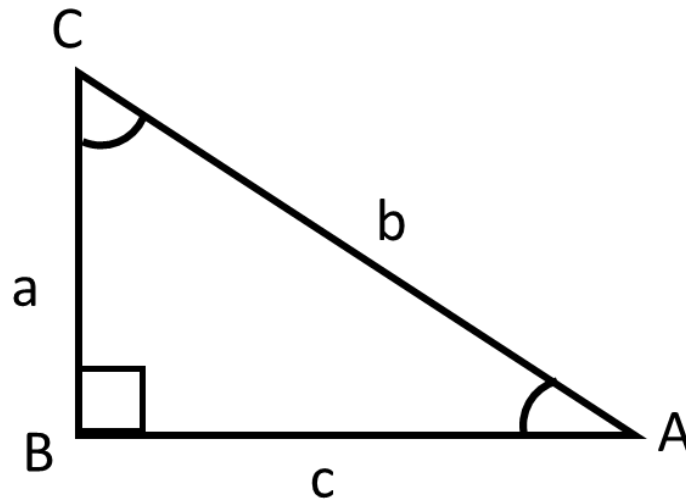
Source: Own elaboration

5.3 Results and discussion

To define the dimensions of the laboratory, it is necessary to take into account that the structure is intended to carry a 2.1m x 1m VFM surface. In addition, the height of the structure is defined considering that the panel will be adjusted from 10 to 45°.

Based on the above considerations, the variables are defined, and calculations are performed using the following trigonometric identities. Figure 5.15 shows a right triangle representing the silhouette of the mobile laboratory, where the hypotenuse (b) represents the length required to vertically lay the module and A is the angle of inclination to be given to the module.

Figure 5.14 Right triangle with defined angles and legs.



$$\sin = \frac{co}{h}, \quad co = a, \quad h = b \quad (3)$$

$$\cos = \frac{ca}{h}, \quad ca = c, \quad h = b \quad (4)$$

$$\tan = \frac{co}{ca}, \quad co = a, \quad ca = c \quad (5)$$

The height and length required for the structure when having an angle of inclination of 45° is calculated below, where $\sphericalangle A = 45^\circ$, $b = 2.1\text{m}$, $co = \text{height}$ and $ca = \text{length}$.

$$\sin\theta = \frac{a}{b} \therefore a = \sin\theta * b \quad (6)$$

$$co = \text{sen}(45^\circ) * 2 = 1.48m \quad (7)$$

$$\cos\theta = \frac{c}{b} \therefore c = \cos\theta * b \quad (8)$$

$$ca = \cos(45^\circ) * 2.1m = 1.48m \quad (9)$$

To find the distance to lengthen the base of the structure now the calculations are performed with the minimum angle of inclination to which the module will reach, i.e. 10° , where $\sphericalangle A=10^\circ$, $b=2.1m$, co = height and ca = length.

$$\text{sen}\theta = \frac{a}{b} \therefore a = \text{sen}\theta * b \quad (10)$$

$$co = \text{sen}(10^\circ) * 2.1m = 0.36m \quad (11)$$

$$\cos\theta = \frac{c}{b} \therefore c = \cos\theta * b \quad (12)$$

$$ca = \cos(45^\circ) * 2 = 2.06m \quad (13)$$

We have that the length of the base extends from 1.48 m to 2.06 m, therefore, the minimum length of the span protruding from the base to reach 2.06m is,

$$1.06 - 1.48 = 0.58 m$$

The graduation that the laboratory will have to adjust the angle of inclination of the module will go from 10° to 45° in intervals of 5° . Table 5.1 shows the data of the height to be marked on the structure according to the desired angle.

Table 5.1 Gradation of the structure.

Angle (°)	Height (m)
45	1.48
40	1.35
35	1.20
30	1.05
25	0.89
20	0.72
15	0.54
10	0.36

Source: Own elaboration

Once the dimensions of the laboratory have been obtained, the costs of the materials necessary for its construction are shown in Table 5.1.

Table 5.2 Materials and costs for the construction of the laboratory

Material	Length	Caliber	Cost
Sill	6 m	2" (1/4)	\$547.72
Angle	6 m	2" (1/8)	\$532.90
Quadrangular PTR	15 m	1 1/4" (14)	\$988.68
Rims	-	-	\$1900.00
Paint	-	-	\$240.00
Total			\$4609.3

Source: Own elaboration

C. Experimentation using the portable laboratory

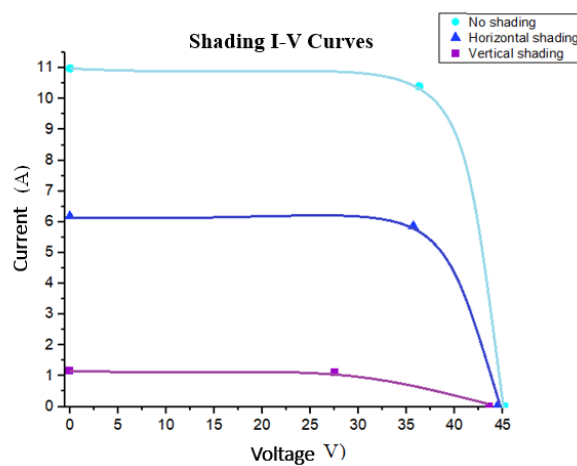
To test the feasibility of using the portable laboratory, the 410W JaSolar module was subjected to different tests. Table 5.3 shows the data obtained from the first form of experimentation, where the electrical parameters of the module were measured by directly receiving the irradiance, partially shading it horizontally and partially shading it vertically. Figure 5.16 shows the I-V curves generated according to each situation, while Figure 5.17 shows the efficiencies obtained in each case.

Table 3.3 Electrical parameters of the shaded panel

Parameters	Horizontal shading	Vertical shading	No shading
Voc [V]	44.4	43.6	45.3
Isc [A]	6.18	1.16	10.98
Pmax [W]	209	30.2	378
Vmp [V]	35.7	27.5	36.3
Imp [A] Imp [A]	5.86	1.10	10.4
Efficiency [%] Efficiency [%] Incident radiation [W/m ²	8.65	1.24	15.60
Incident radiation [W/m ² Incident radiation [W/m ²	1208	1217.2	1211.2
Cell temperature [°C] Cell temperature [°C	43.8	48.3	45.6
Ambient temperature [°C]	24	24	24

Source: Own elaboration

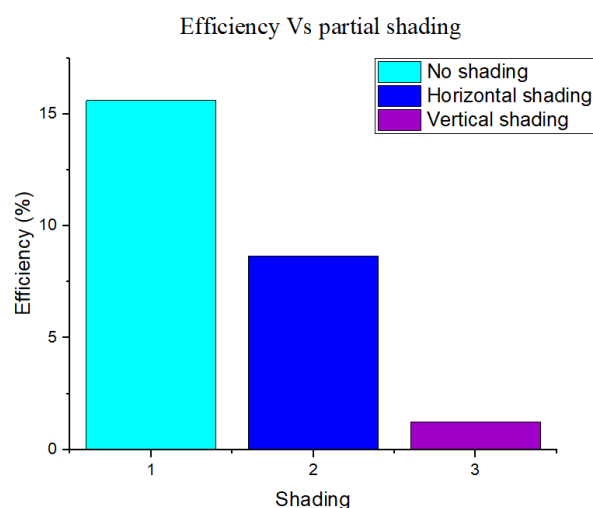
Figure 5.15 Comparison between the shaded I-V curves and the real curve



Source: Own elaboration in OriginLab

Fig. 5.15 Comparison between the shading I-V curves and the real curve.

Figure 5.16 Efficiency of the module affected by partial shading



Source: Own elaboration in OriginLab

The behavior of the shading curves with respect to the behavior of the curve without shading is notorious. The effect of vertical shading affects in a greater way the maximum power obtained since the interconnection of the cells is more affected in this way, where the continuity of the connection of several rows of cells is intervened, while the horizontal shading affects only a part of the interconnection of the cells. Also, it can be seen that the module efficiency decreases greatly with the two types of shading, being reduced by up to 1.24% in the case of vertical shading and by 8.65% in the case of horizontal shading. For this reason, photovoltaic installations should be located in areas free of objects that could cause these efficiency drops.

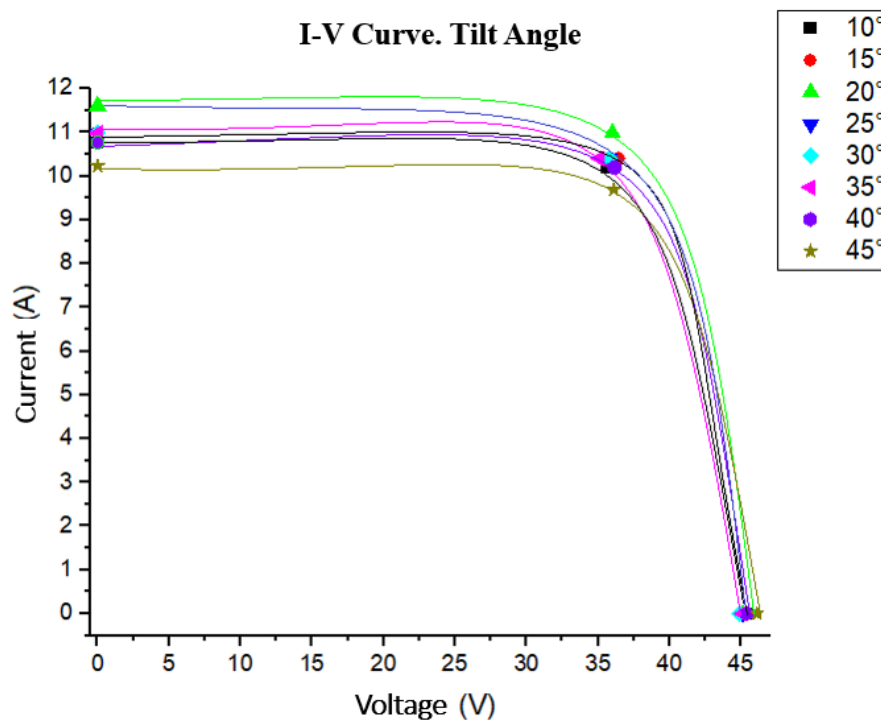
Table 3.4 lists the electrical parameters of the module at different tilt angles. For this test, the portable laboratory was used to simulate the installation of the module from 10 to 45° tilt, orienting the module to the south. Figure 3.4 shows the I-V curves obtained from the measurement at each angle at which the module was placed, which varied by 5° between each measurement. The efficiency of the module with respect to each inclination is shown in Figure 3.5.

Table 5.4 Electrical parameters of the panel installed at different inclinations

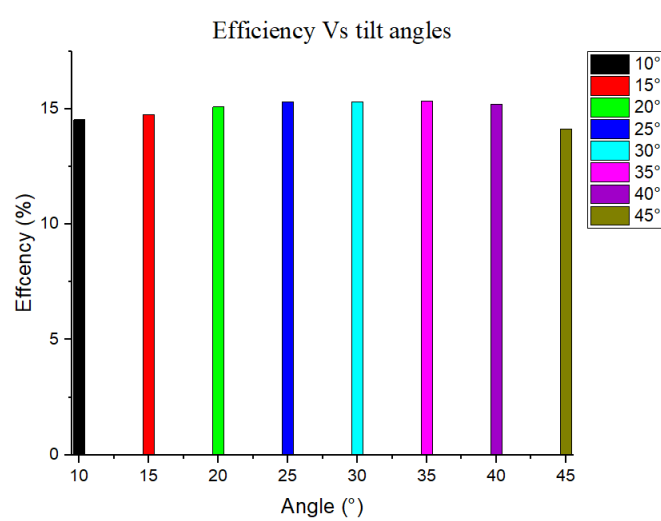
Parameters	10°	15°	20°	25°	30°	35°	40°	45°
Voc [V]	45.5	45.4	45.1	45.1	44.9	45.1	45.4	46.1
Isc [A]	10.77	10.98	11.61	10.98	10.98	10.98	10.77	10.23
Pmax [W]	382	380	390	375	373	367	370	349
Vmp [V]	35.6	36.4	35.2	36	35.8	35.1	36.1	36.1
Imp [A] Imp [A]	10.2	10.4	11	10.4	10.4	10.4	10.2	9.69
Efficiency [%]	14.53	14.75	15.08	15.31	15.31	15.34	15.21	14.12
Irradiance [W/m ²]	1317.6	1288	1292.7	1224	1217.6	1195.8	1215.6	1235
Cell temperature [°C]	45.1	43.6	48.1	51.4	51.2	47.4	45.8	42.5
Ambient temperature [°C]	24	24	24	24	24	24	24	24

Source: Own elaboration

Figure 5.17 I-V curves generated by the module at different tilt angles



Source: Own elaboration in OriginLab

Figure 5.18 Efficiency of the module affected by different tilt angles

Source: Own elaboration in OriginLab

As ventilation is applied to the module, the cell temperature decreases and the open circuit voltage increases or is maintained even though the irradiance decreases. In Figure 3.9, it is shown that the module becomes more efficient using cooling. The relationship between cell temperature and open circuit voltage is inversely proportional, the lower the cell temperature the higher the voltage and vice versa.

5.4 Conclusions

In conclusion, the laboratory meets the desired characteristics, facilitates the transport of the module safely, as well as work tools since the laboratory has a tool drawer, in terms of mobility has two types of tires, the laboratory also has a removable shade, tool drawer has a dimension of (64x41x30)(cm³) 3and is recessed, rear tires that are fixed and the front tires that are swivel tires to take it towards the desired direction and removable shade that can overhang up to 50 cm high.

The lab also helps make measurements much more efficient speaking of the time in which they can be made, the mobile lab has a tilt from 10° to 45° degrees with 5° degree intervals, this was graduated in this way to facilitate tilt adjustment.

It was observed that shading significantly affects peak power and module efficiency, with vertical shading being the most detrimental. The optimum tilt angle for the module was determined to be between 25° and 35°, while surfaces with higher albedo coefficient, such as green grass and gray pavement, resulted in higher efficiency. It was also shown that cooling by means of a fan increases the efficiency of the module.

These results demonstrate the importance of considering factors such as shading, tilt, and environmental conditions when designing and installing photovoltaic systems, in order to maximize energy generation and optimize performance.

5.5 References

1. Sukhatme, S. P., & Nayak, J. K. (2009). Solar energy: Principles of thermal collection and storage. ResearchGate.https://www.researchgate.net/publication/230898422_Solar_Energy_Principles_of_Thermal_Collection_and_Storage. Accessed 03 May 2023.
2. Duffie, J. A., & Beckman, W. A. (2013). Solar Engineering of Thermal Processes. pdfcoffee.com. <https://pdfcoffee.com/solar-engineering-of-thermal-processes-pdf-free.html>. Accessed 04 May 2023.

3. Goswami, D. Y. (2015). *Principles of Solar Engineering (Third Edition)*. CRC Press, Taylor et Francis Group. <https://www.advan-kt.com/principlesofsolarengi.pdf>. Accessed 05 May 2023.
4. Selmi, T., Masmoudi, A., & Gastli, A. (2012). MATLAB/simulink based modelling of solar photovoltaic cell - researchgate. ResearchGate. https://www.researchgate.net/publication/258913169_MATLABSimulink_Based_Modelling_of_Solar_Photovoltaic_Cell. Accessed 05 May 2023.
5. Liang Tsai, H., Siang, C., & Jie Su, Y.-Y.-J. S. (2008). Development of generalized photovoltaic model using. Researchgate. https://www.researchgate.net/publication/44262416_Development_of_generalized_photovoltaic_model_using_MATLABSIMULINK. Accessed 06 May 2023.
6. Cepeda Moya, J. S. (2017). Aspectos que afectan la eficiencia en los paneles fotovoltaicos y sus potenciales soluciones. Retrieved from <http://hdl.handle.net/11634/4196>. Accessed 07 May 2023.
- 1) 7. Robles Algarín, C. A. (2019a). Sistemas híbridos: una estrategia para mejorar la eficiencia en los paneles solares. <http://hdl.handle.net/20.500.12494/9302>. Accessed 10 May 2023.
7. Cushicóndor Collaguazo, S. (2019, April 15). Estimación de irradiancia solar basada en modelos matemáticos y medición de variables eléctricas de paneles fotovoltaicos. Escuela Politécnica Nacional. <http://bibdigital.epn.edu.ec/handle/15000/2017>. Accessed 10 May 2023.
8. Arbona, J. (2022, June 20). ¿Cómo poner e inclinar mis placas solares? orientación en México. <https://tarifasdeluz.mx/autoconsumo/instalacion/inclinacion-paneles-solares>. Accessed 11 May 2023.
9. Benito Maria, M. (2022). Estudio de la inclinación óptima de paneles solares bifaciales monocristalinos de silicio. Universidad de Valladolid. <https://uvadoc.uva.es/handle/10324/54254>. Accessed 11 May 2023.
10. Ortiz, J. D. (2013). Viabilidad técnico-económica de un sistema fotovoltaico de pequeña escala. VirtualPro. <https://www.virtualpro.co/biblioteca/viabilidad-tecnico-economica-de-un-sistema-fotovoltaico-de-pequena-escala>. Accessed 12 May 2023.

Evaluation of obtaining biohydrogen by different fermentation methods

Evaluación de la obtención de biohidrógeno por diferentes métodos de fermentación

MURGUIA-FIERRO, Salma Verónica†, LANDEROS-QUIÑONES, Carlos, REYES-CABRERA, Estefanía Guadalupe and PEREZ-GARCIA Laura Andrea*

TecNM/ Instituto Tecnológico de La Laguna, Laboratorio de Energías Renovables, México.

ID 1st Author: *Salma Verónica, Murguia-Fierro* / **ORC ID:** 0009-0001-5331-9125, **CVU CONAHCYT ID:** 1165081

ID 1st Co-author: *Carlos, Landeros-Quiñones* / **ORC ID:** 0009-0005-1289-0754, **CVU CONAHCYT ID:** 1288151

ID 2nd Co-author: *Estefania Guadalupe, Reyes-Cabrera* / **ORC ID:** 0009-0005-4925-7397, **CVU CONAHCYT ID:** 1288239

ID 3rd Co-author: *Laura Andrea, Perez-Garcia* / **ORC ID:** 0000-0002-5880-6192, **CVU CONAHCYT ID:** 887623

DOI: 10.35429/P.2023.1.61.70

S. Murguia, C. Landeros, E. Reyes and L. Pérez

*maria_francisco@micorreo.upp.edu.mx

Á. Marroquín, L. Castillo, J. Olivares and A. Álvarez (AA. VV.). Young Researchers. Engineering Applications - Proceedings-©ECORFAN-México, Queretaro, 2023.

Abstract

There are a lot of projects around the methods of obtaining renewable fuels that are less harmful to the environment. In that sea of investigations, one of the less explored and with greater potential to become a principal biofuel is biohydrogen production through fermentations. However, biohydrogen technologies production has limitations such as low productivity, therefore are not profitable yet. Through this project, the search for the evaluation of practice to attain biohydrogen to determine how feasible the development of said technology, as well as the efficiency as a process is the main goal. In this project, development of multiple fermentations, analysis of growth curves in different growth mediums such as nutrient agar, BBM and TAP mediums in addition with microalgae *Chlamydomonas*, were made.

Biohydrogen, Investigation, Fermentation; Microalgae *Chlamydomonas*

6 Introduction

The project called Evaluation of Obtaining Biohydrogen by Different Fermentation Methods was developed with the objective of analyzing the current methods of biohydrogen production by different fermentations and to develop a system that operates optimally and then compare with different fermentation methodologies. In addition, the project aims to give a clearer understanding of the processes of obtaining hydrogen and the different factors that affect its production.

In previous works, the analysis of the evaluation of production of biohydrogen depends mainly on different mediums of cultivation and the use of different microorganisms.

Throughout the project, analyses of bacterial samples in different cultivation mediums were performed. These analyses comprise the growth and count of each bacterial group in different cultivation medium, analysis of the type of fermentation and biohydrogen production. First, a group of bacteria was selected; i) *Escherichia coli*, ii) *Enterobacter* sp. and iii) *Citrobacter freundii*, and two commercial cultivation medium; a) nutrient broth and b) trypticasein soy broth. The analysis period comprised 96 hours in which the samples were incubated in 250ml flasks (Pyrex) with a working volume of 150ml inside an incubator (Gutstark) at 37°C. Spectrophotometer (jf721) measurements were performed at 600 nm wavelength every 2 hours for 96 hours. Afterwards, fermentation and growth of the bacteriological strains was carried out in a new medium: Microalgae. This medium adds microalgae of the *Chlamydomonas* type in nutrient broth, keeping them under constant agitation.

The main reason for the project is to advance biofuel technology, focused on the production of biohydrogen by fermentative means, so that it will be possible to contribute to current research with the data obtained. At present, there is a limited database on the use of bacteria with microalgae to create consortium-type systems for biohydrogen production, which is why it was decided to perform an analysis of this type of systems and to be able to complement future research focused on this topic.

It was hypothesized that there would be an exponential growth indicated in the growth curves, as well as the obtaining of biohydrogen at the end of fermentation.

6.1 Methodology

We began with the selection of bacteria as biohydrogen generation medium in our system, which were three: i) *E. coli*, ii) *Enterobacter* sp. and iii) *C. freundii*. These bacteria were selected due to their characteristic that within their metabolism they synthesize biohydrogen. Each strain was isolated using the radial quadrant streak seeding technique. The strains were then inoculated in nutrient broth and trypticasein soy broth (STC) and subjected to fermentation in an incubator at 37°C for 96 hours. Subsequently, spectrophotometer measurements were performed at a wavelength of 600 nm in absorbance mode every two hours during the 96 hours. The data obtained from the spectrophotometer were used to plot the growth kinetics of each of the bacteria.

To obtain and store biohydrogen, flasks were used for each of the cultivation mediums. For biogas storage, a balloon was used as a container for the gasses produced, as well as syringes.

When the data recording was complete, a consortium was made between each bacterium, in order to analyze their behavior and joint growth, using the same parameters.

After performing the analysis with the nutritive cultivation medium, the same steps were repeated, but the cultivation medium was changed to microalgae, which requires a different treatment during the growth stage than the one already used.

In their case, it was kept in agitation for the first 24 hours and then measurements were taken at a wavelength of 750 nm every 2 hours for 3 days. In between, the samples were shaken again.

The method for analyzing gas generation was the same as for the previous medium: by volumetric visualization in balloons. In the case of microalgae, the samples were in *Chlamydomona* algae medium with BBM medium and TAP medium along with bacteria. The ratio of microalgae to medium was 1/10, in 100 mL total cultivation medium. A constant pH of 6 was maintained in all cultivation mediums at 29°C (room temperature).

These processes were repeated 3 times each to obtain more accurate results and to be able to verify in case something went wrong.

At the beginning, since the necessary equipment was not available to perform the measurements in the renewable energy laboratory, the chemistry laboratory had to be used every two hours, with the permission of the laboratory manager.

Once the spectrophotometer and incubator were obtained, these trips were avoided.

All the cultivation mediums were made with materials found in the renewable energy laboratory, except for the algae, which were already in an active cultivation medium. From this medium only 10 mL was removed per cultivation medium to be made.

The bacteria were obtained from the renewable energy laboratory, which were already being used by the renewable energy team.

The hours of measurements began at 7 AM in order to conclude at 7 PM (opening and closing time of the Tecnológico de La Laguna) in this way, it was possible to obtain a 24-hour curve by making two measurements starting at different time periods.

Consisting of a grill to sterilize the cultivation medium, the flasks used and lighters for streaking.

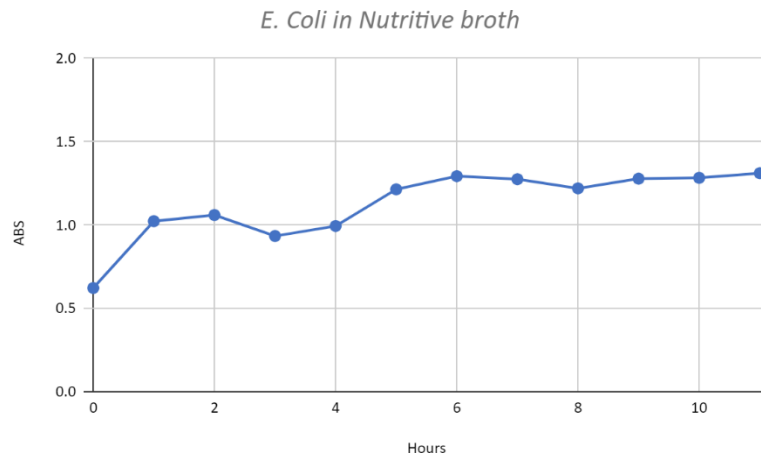
The measurements were performed in groups of 6 samples, 3 for each cultivation medium.

Stirring is a necessity for proper growth of microalgae.

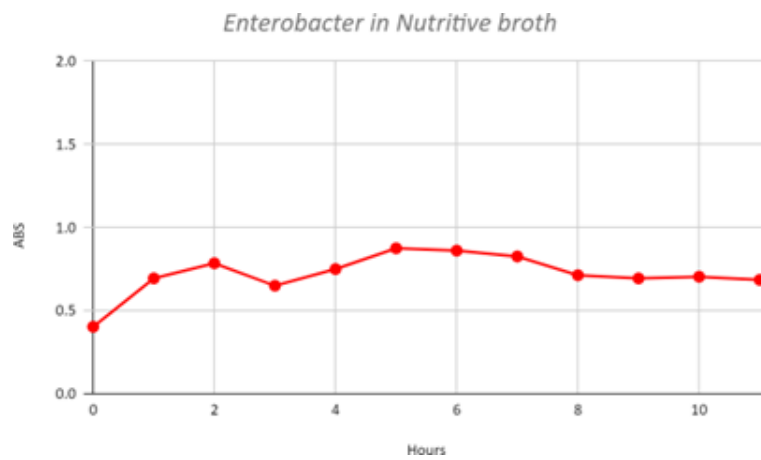
6.2 Results obtained

For the measurement of the growth curves, the bacterial strains were reactivated in the medium indicated below. Measurements were taken with a spectrophotometer at different wavelengths (600 for nutrient broth and trypticasein soy, 750 for microalgae in BBM and TAP) in two-hour periods for three days in order to analyze their growth.

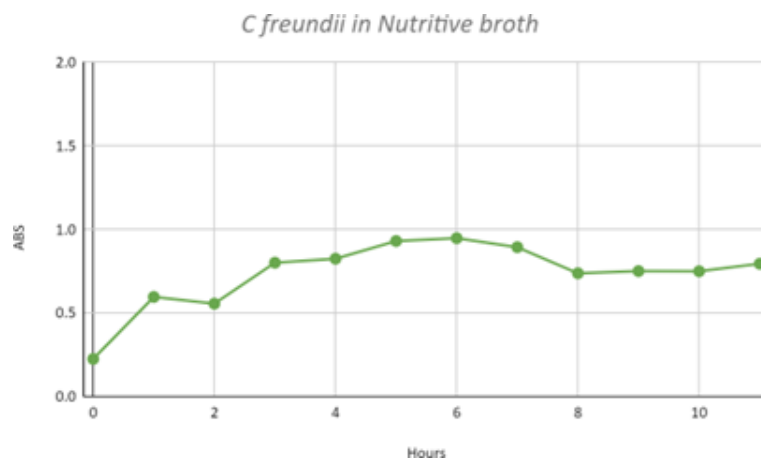
The growth graphs obtained from the nutrient and stc cultivation medium are shown below:

Graphic 6.1 *E. coli* growth curve in nutritive broth

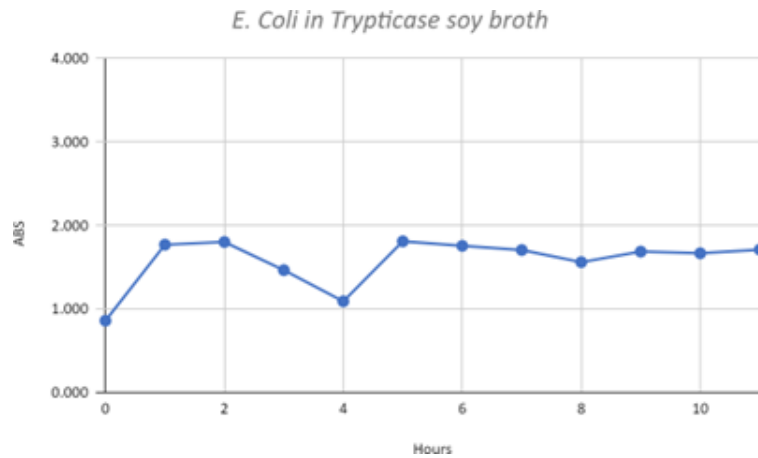
This graphic depicts the growth curve of *E. coli* bacteria in a nutrient broth medium specified for bacterial growth and other microorganisms that can be worked with. As can be seen, the bacteria are in a period of growth after 12 hours of incubation, which is beneficial for the analysis of growth in this and other mediums. In this way, we can determine whether or not the medium is suitable for the bacteria, which is our main source in this process.

Graphic 6.2 *Enterobacter* growth curve in nutrient cultivation medium

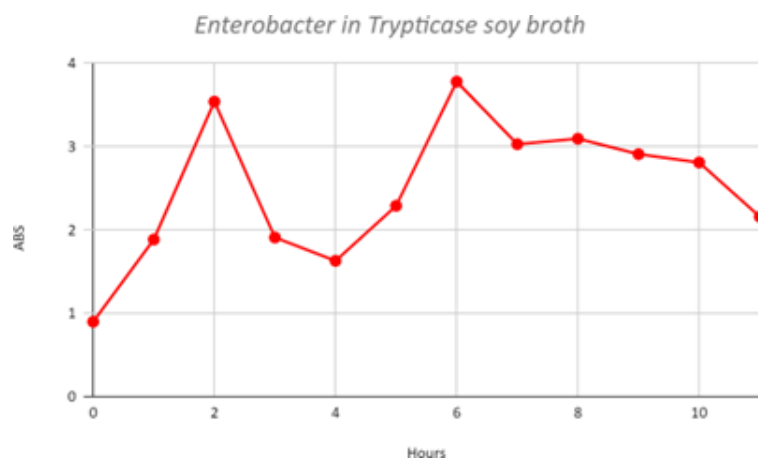
Graph depicting the growth of *Enterobacter* bacteria in the nutrient broth medium in the indicated period.

Graphic 6.3 *C. freundii* growth curve in nutrient cultivation medium

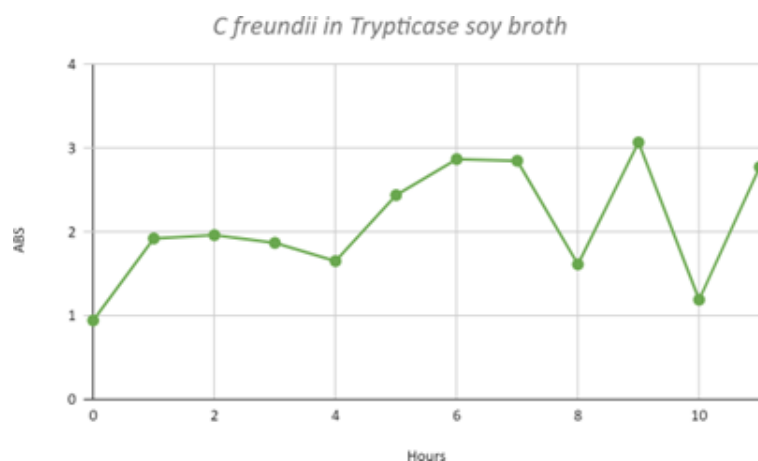
Graphic depicting the growth of *C. freundii* bacteria in the nutrient broth medium in the indicated period.

Graphic 6.4 *E. coli* growth curve in STC cultivation medium

Graphic depicting the growth of *E. coli* bacteria in trypticase soy broth medium, a nutrient alternative, but similar in function to nutrient broth.

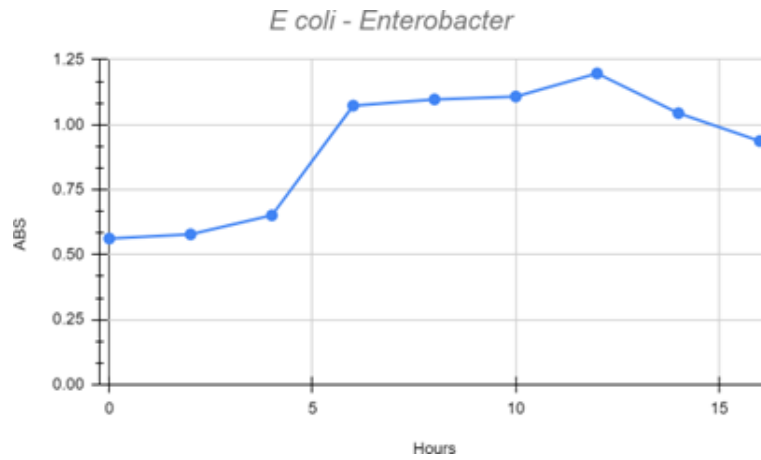
Graphic 6.5 Growth curve of *Enterobacter* in STC cultivation medium

Graphic showing the growth of *Enterobacter* bacteria in trypticase soy broth medium at the indicated time.

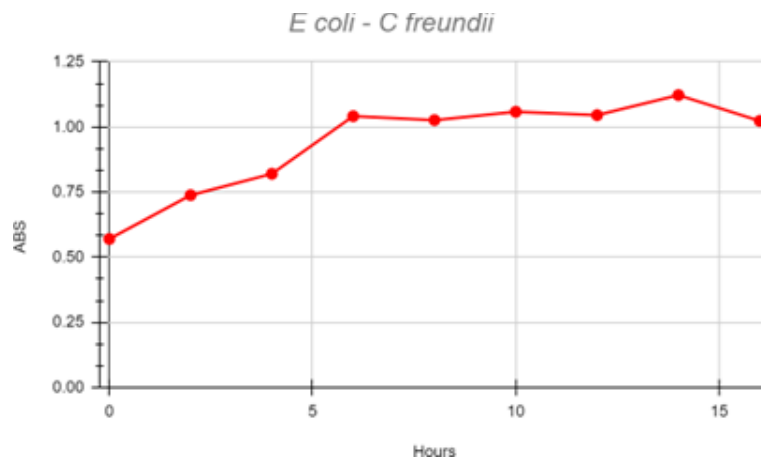
Graphic 6.6 Growth curve of *C. freundii* in STC cultivation medium

Graphic showing the growth of *C. freundii* bacteria in the trypticase soy broth medium at the indicated time.

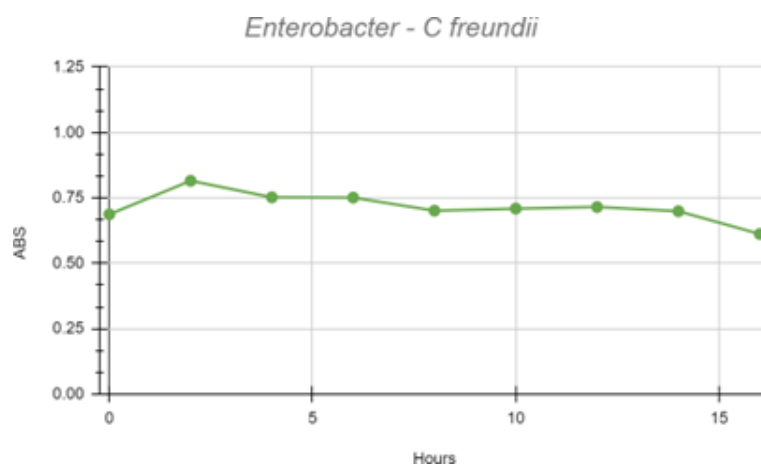
The growth curve of the bacteria in nutrient cultivation medium, but in the form of a consortium, is presented below:

Graphic 6.7 Growth curve of *E. coli* and *Enterobacter* in nutrient cultivation medium

For these curves, it was decided to make consortia between the available bacteria in order to induce a state of stress that would promote their development and, thus, the production of biohydrogen.

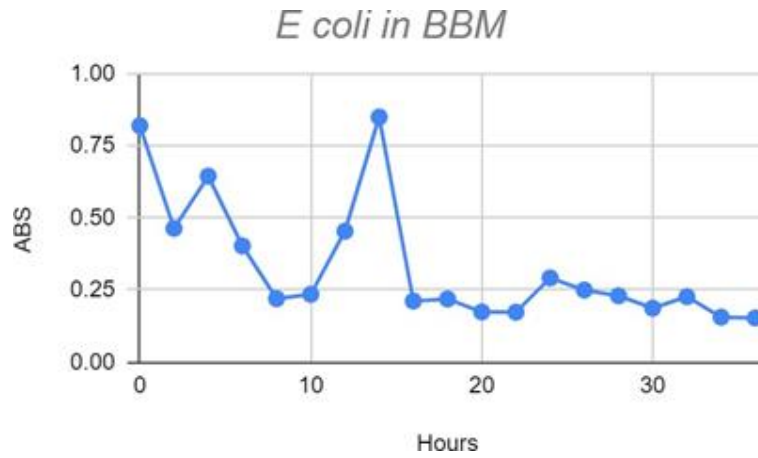
Graphic 6.8 Growth curve of *E. coli* and *C. freundii* in nutrient cultivation medium

Graphic showing the growth of *E. coli* and *C. freundii* bacteria in consortium, in nutrient broth medium, in the indicated time.

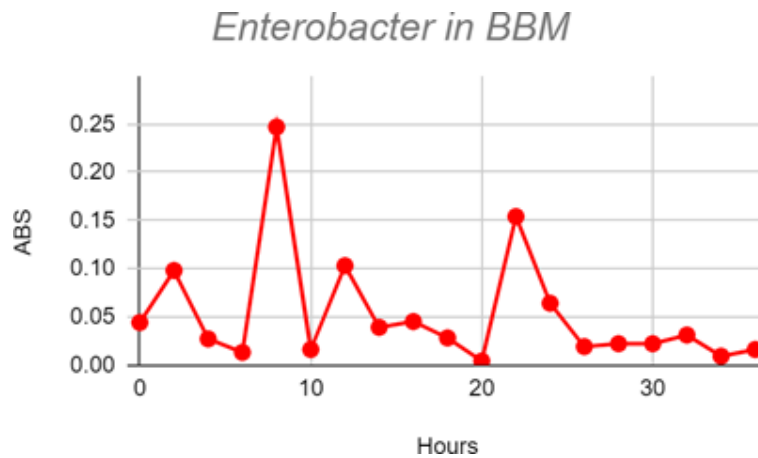
Graphic 6.9 Growth curve of *Enterobacter* and *C. freundii* in nutrient cultivation medium

Graphic depicting the growth of *Enterobacter* and *C. freundii* bacteria in consortium, in nutrient broth medium, in the indicated time.

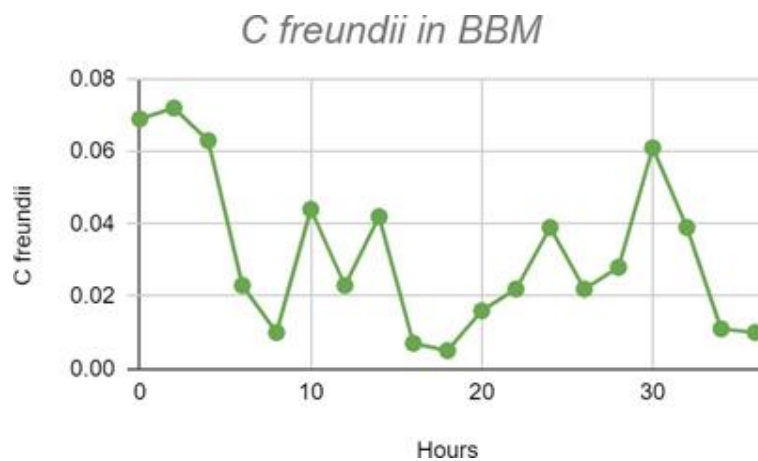
The growth curves of the bacteria in consortium with the microalgae in BBM medium are presented below:

Graphic 6.10 Growth curve of *E. coli* in *Chlamydomonas* BBM cultivation medium

Graphic showing the consortium between *E. coli* and the microalgae *Chlamydomonas* in BBM medium, an ideal medium for the development of microalgae. From these graphs, the analysis of the theory of coexistence between bacteria and microalgae for their growth and development of biohydrogen was proposed.

Graphic 6.11 Growth curve of *Enterobacter* in *Chlamydomonas* BBM cultivation medium

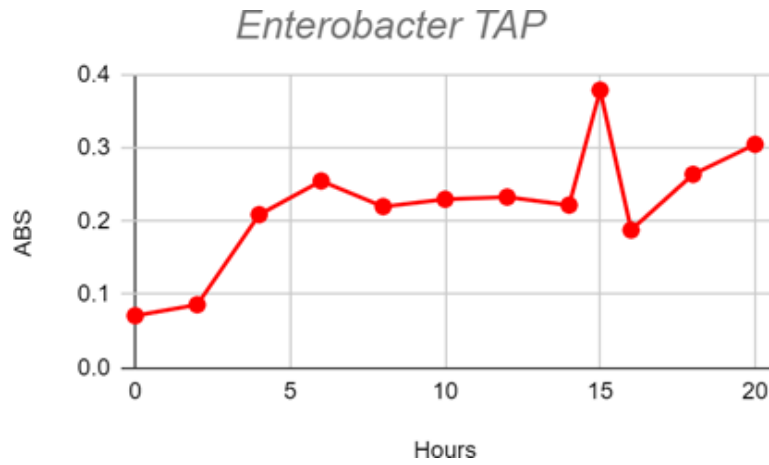
Graphic depicting the consortium between *Enterobacter* and the microalgae *Chlamydomonas* in BBM medium, at the indicated time.

Graphic 6.12 Growth curve of *C. freundii* in *Chlamydomonas* BBM cultivation medium

Graphic showing the consortium between *C. freundii* and the microalgae *Chlamydomonas* in BBM medium, at the indicated time.

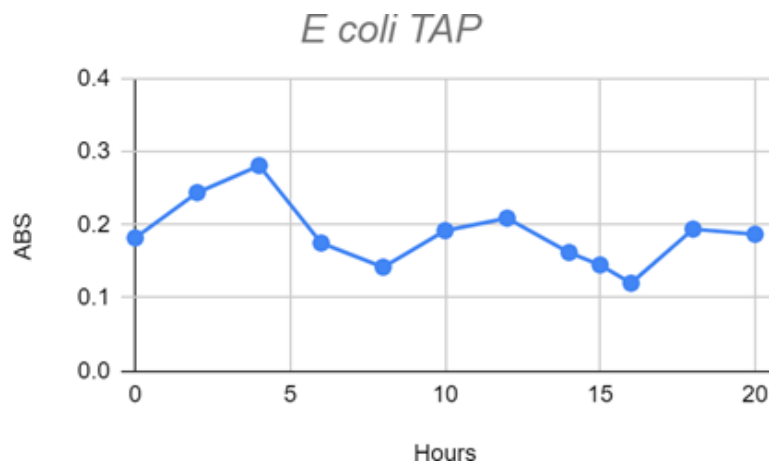
Finally, growth curve of the bacteria on *Chlamydomonas* in TAP medium:

Graphic 6.13 *E. coli* growth curve in *Chlamydomonas* TAP cultivation medium



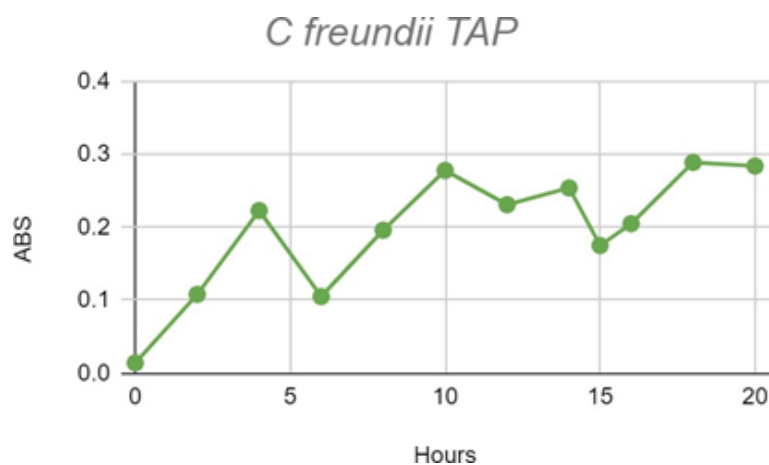
For this curve, the growth of bacteria in consortium with *Chlamydomonas* was analyzed, but in a different cultivation medium than BBM, TAP medium. The difference between these two mediums is the nutrients inside.

Graphic 6.14 *Enterobacter* growth curve in *Chlamydomonas* TAP cultivation medium



Graphic depicting the consortium between *Enterobacter* and the microalgae *Chlamydomona* in TAP medium, at the indicated time.

Graphic 6.15 Growth curve of *C. freundii* in *Chlamydomonas* TAP cultivation medium



Graphic showing the consortium between *C. freundii* and the microalgae *Chlamydomona* in BBM medium, at the indicated time.

As can be seen, the growth of the bacteria is highly dependent on the medium in which they are found. This is due to differences between each medium, such as nutrients.

One of the major factors that could interfere with bacterial growth would be temperature. Among the nutrient medium and consortia of microorganisms, the temperature varied from 35° to 29°C. This affects the growth of bacteria and thus, the production of biohydrogen.

As for biohydrogen production, only one sample was able to effectively inflate a balloon, that being *Enterobacter* in nutrient cultivation medium. This is due to multiple reasons, one of which would be fermentation time. By having more time, fermentation is carried out properly, allowing the rest of the cultivations to perform the metabolism necessary to process the nutrients and thus release the hydrogen.

Another factor that can be determinant would be the incubation conditions of both the cultivation medium, as well as of the fluted petri dishes. A couple of times it was detected that there were temperature increases inside the incubator, this could cause the bacteria to suffocate and a higher stress to the bacteria does not always translate as something positive.

On the other hand, it is suspected that the constant movement of the samples through the Tecnológico de La Laguna may have been enough to stress the bacteria and thus affect the fragile development in cultivation.

One of the major factors with which we were competing was the time between each process, and this is a variant which can definitely be altered for greater probability of success in this type of project.

Another thing to keep in mind regarding this type of consortia is that microalgae are very aggressive with bacteria, so much so that in many water purification and treatment plants, the use of microalgae is employed to deal with these types of contaminants. Clearly there is a relationship between bacteria and microalgae for the production of biohydrogen since, theoretically, these two can share a symbiotic relationship. However, there are factors such as type of microalgae or bacteria, temperature, agitation state, exposure to illumination, fermentation period, which could make a big change in these projects and should definitely be analyzed and considered in the future.

Objectively, the analysis of the fermentations can be done correctly, it can be deduced exactly what factors affected these cultivations and if the project would be replicated, more knowledge would be available regarding this area of biofuels.

6.3 Acknowledgments

The authors would like to thank the Renewable Energy Laboratory for the financial support that made possible the development of this project.

6.4 Conclusions

All the samples showed exponential growth at some point, with the exception of the BBM medium with *Chlamydomonas*, which had the lowest growth rate. The rest showed a much higher growth of at least 2% every two hours, giving the conclusion that the bacteria did grow in the prepared medium. As for the biohydrogen production, it could be observed in the *Enterobacter* sample on nutritive agar and in the three TAP mediums with *Chlamydomona*, with an index of 60% of biogas being biohydrogen, giving positive results.

As for growth, it is quite apparent that it was much better in a medium specifically made for bacterial growth than in one in which it must compete against microalgae because of their antagonistic relationship. Also at issue is the time between each process. As already mentioned, this can be optimized by allowing cultivations and fermentations to be carried out with greater margin.

6.5 References

- Algas y bacterias forman equipo para aumentar la producción de hidrógeno. (2019, 11 septiembre). SINC. Recuperado 25 de mayo de 2023, de: <https://www.agenciasinc.es/Noticias/Algas-y-bacterias-forman-equipo-para-aumentar-la-produccion-de-hidrogeno#:~:text=La%20unión%20del%20alga%20verde,a%20la%20vez%20que%20descontaminar.>
- CK-12 Foundation. (s. f.). CK-12 Foundation. <https://flexbooks.ck12.org/cbook/ck-12-conceptos-de-ciencias-de-la-vida-grados-6-8-en-espanol/section/5.1/primary/lesson/características-de-las-bacterias/>
- Yordán, E. (2022, 24 agosto). Qué son las microalgas: características, ejemplos e importancia. *ecologiaverde.com*. <https://www.ecologiaverde.com/que-son-las-microalgas-caracteristicas-ejemplos-e-importancia-4013.html>
- Editorial Grudemi. (2022, 20 octubre). Microalgas - ¿Qué son?, características, tipos, estructura, ejemplos y más. *Enciclopedia de Biología*. <https://enciclopediadebiologia.com/microalgas>
- Iqbal, K., Saxena, A., Pande, P., Tiwari, A., Joshi, N. C., Varma, A., & Mishra, A. (2022). Microalgae-bacterial granular consortium: Striding towards sustainable production of biohydrogen coupled with wastewater treatment. *Bioresource Technology*, 354, 127203. <https://doi.org/10.1016/j.biortech.2022.127203>
- Sirohi, R., Joun, J., Lee, J. H., Yu, B. P., & Sim, S. J. (2022). Waste mitigation and resource recovery from food industry wastewater employing microalgae-bacterial consortium. *Bioresource Technology*, 352, 127129. <https://doi.org/10.1016/j.biortech.2022.127129>
- Libretexts. (2022). 17.1C: Metabolitos Primarios y Secundarios. LibreTexts Español. [https://espanol.libretexts.org/Biologia/Microbiolog%C3%ADa/Libro%3A_Microbiolog%C3%ADa_\(Sin_1%C3%ADmites\)/17%3A_Microbiolog%C3%ADa_Industrial/17.1%3A_Microbiolog%C3%ADa_Industrial/17.1C%3A_Metabolitos_Primarios_y_Secundarios](https://espanol.libretexts.org/Biologia/Microbiolog%C3%ADa/Libro%3A_Microbiolog%C3%ADa_(Sin_1%C3%ADmites)/17%3A_Microbiolog%C3%ADa_Industrial/17.1%3A_Microbiolog%C3%ADa_Industrial/17.1C%3A_Metabolitos_Primarios_y_Secundarios)
- UCC+i. (s. f.). “La combinación de algas y bacterias aumenta la producción de hidrógeno en un 60%”. <https://www.uco.es/ucci/es/noticias-gen/item/3201-la-combinacion-de-algas-y-bacterias-aumenta-la-produccion-de-hidrogeno-en-un-60#:~:text=Cuando%20el%20alga%20trabaja%20sola,ha%20sido%20el%20%C3%A1cido%20ac%C3%A9tico.>
- Microalgas y bacterias para producir biohidrógeno. (s. f.). Interempresas. <https://www.interempresas.net/Grandes-cultivos/Articulos/254570-Algas-y-bacterias-para-producir-biohidrogeno.html>
- Londoño, S. L. M., & Chaparro, T. R. (2012). Producción de biohidrógeno a partir de residuos mediante fermentación oscura: una revisión crítica (1993-2011). *Ingeniare. Revista chilena de ingeniería*, 20(3), 398-411. <https://doi.org/10.4067/s0718-33052012000300014>.

Evaluation of substrates for biopolymer processing

Evaluación de sustratos para procesamiento de biopolímeros

REYES-CABRERA, Estefanía Guadalupe†*, REYES-ESPINO, Jacqueline, MURGUIA-FIERRO, Salma Verónica and PEREZ-GARCIA, Laura Andrea

TecNM - Instituto Tecnológico de La Laguna, Laboratorio de Energías Renovables, México.

ID 1st Author: *Estefanía Guadalupe, Reyes-Cabrera* / **ORC ID:** 0009-0005-4925-7397, **CVU CONAHCYT ID:** 1288239

ID 1st Co-author: *Jacqueline, Reyes Espino* / **ORC ID:** 0009-0000-9202-4066, **CVU CONAHCYT ID:** 1288140

ID 2nd Co-author: *Salma Verónica Murguia-Fierro* / **ORC ID:** 0009-0001-5331-9125, **CVU CONAHCYT ID:** 1165081

ID 3rd Co-author: *Laura Andrea, Perez-Garcia* / **ORC ID:** 0000-0002-5880-6192 **CVU CONAHCYT ID:** 887623

DOI: 10.35429/P.2023.1.71.78

E. Reyes, J. Reyes, S. Murguia and L. Perez

Á. Marroquín, L. Castillo, J. Olivares and A. Álvarez (AA. VV.). Young Researchers. Engineering Applications - Proceedings-©ECORFAN-México, Queretaro, 2023.

Abstract

The substitution by biodegradable plastics through the implementation of lignocellulosic polymers based on lignocellulose represents a potential idea to reduce their impact and take advantage of these wastes, decreasing their cost for final disposal and the environmental damage they generate. In this project, substrates based on banana and mango peels were evaluated for *Pseudomonas* to obtain a biopolymer with the objective of determining which substrates generate a greater amount of polymers by comparing mango, banana and potato peels with known growth media. The process is composed of a mechanical pretreatment and acid hydrolysis, for the delignification of the peels, compared with the basal medium and the LMC for the culture of *Pseudomonas* at 35°C under sterile conditions, neutral PH and the addition of some elements of the basal medium, cell extraction by centrifugation and a method of extraction of the polymer based on chloroform. Obtaining that the biopolymer produced in gr/L 25.86, 19.53, 6.63, 4.55, 15, for Mango, Banana, Potato, LMC and Basal medium, having better yields than the commercial media.

Biopolymers, Lignocellulosic residues, *Pseudomonas*

7 Introduction

Plastic waste pollution is one of the main environmental problems. Technological development and industrialization generate more and more waste. An average of 8 million tons of plastic are dumped into the oceans every year, which is equivalent to emptying a garbage truck full of plastics every minute. (Plastic pollution. One of the greatest environmental challenges of the 21st century, n/d).

Biopolymers present a very promising alternative for the replacement of plastics because they are completely biodegradable and are produced from renewable carbon sources. (Carlos, 2023) They also have an important application as biocompatible materials in the biomedical and pharmaceutical area, in addition to the fact that their production does not generate dependence on oil as is the case of conventional plastics, a resource that is becoming increasingly expensive and scarce, in addition to being highly polluting (García et al., 2013).

Lignocellulosic biomass has a high potential for obtaining high value-added bioproducts, among which bioplastics stand out. Lignocellulosic materials are abundant and generally low priced, being the current challenge to produce valuable products with high selectivities and yields at economic costs. This type of biomass is considered a low-cost source of carbon. (Bioplastics and high value-added bioproducts from lignocellulosic biomass - Chemical Industry, n.d.)

The project consists of the combination of biotechnology and the use of waste rich in carbon source for the production of biopolymers, through the synthesis carried out by some bacterial genera under nutritional stress, within these bacterial genera are species of *Pseudomonas* that are capable of generating a substitute product for petroleum-derived plastics, by completely biodegradable bioplastics.

7.0.1 *Pseudomonas*

The member species of the genus *Pseudomonas* spp. belong to the phylum of Proteobacteria, of the subclass gamma, group of aerobic Gram-negative bacteria measuring 0.5 to 0.8 µm by 1.5 to 3.0 µm, are highly diverse morphologically and physiologically their motility is by a single polar flagellum, they have a great capacity for adaptability to different environments, finding from animal and plant pathogens, to soil colonizers.

Their ability to produce and accumulate pha has been highly studied in different conditions, mainly the production of medium-chain PHAs, (Carreiro 3-5) these microorganisms grow at near neutral pH and mesophilic temperatures, up to 43°C. It has been reported that many species of *Pseudomonas* grow efficiently in chemically defined media containing different aliphatic compounds (carbohydrates, fatty acids, dicarboxylic and tricarboxylic acids, alcohols) and aromatics as carbon source. (Martínez, 2008).

Among the growth media for pseudomonas is King's Agar B in a solid medium that allows obtaining bacterial colonies, the presence of magnesium sulfate in its composition provides the necessary cations for the activation of pioverdine, which gives the culture medium a fluorescent greenish-yellow color. The presence of phosphate inhibits the production of pyocyanin, a specific pigment of *Pseudomonas aeruginosa* (King B Agar | *Pseudomonas* | Bioser, n.d.).

Among the liquid media, the LMC medium is characterized by providing the necessary nutrients to achieve maximum growth of *Pseudomonas*, its composition is shown in Table 7.1. While a basa medium constitutes simple media that favor the growth of undemanding bacteria, under stress conditions, covering the minimum nutritional requirements shown in Table 7.2.

Table 7.1 LMC medium

Formula	gr / L
Mannitol (substituted by glucose)	10.00
Yeast extract	10.00
Dipotassium phosphate	00.50
Magnesium sulfate	00.10
Sodium chloride	00.20

Table 7.2 Basal medium

Formula	gr / L
Yeast extract	1.00
Peptone	5.00
Disodium hydrogen phosphate	1.00
Magnesium sulfate	0.20
Glucose	10.00

7.0.2 Lignocellulosic biomass

The lignocellulosic material is the agro-industrial product of greater abundance, it is a source of renewable raw material, by constituting a structural part in the plant kingdom, are waste a low economic valuation, and a great economic and environmental impact for its final disposal, is composed mainly of cellulose, hemicelluloses and lignin compounds that stand out for their numerous applications. (René Rafael Gallego-Domínguez, 2017)

7.0.3 Banana peel

The main by-product of the banana industrial process, is the peel which represents approximately 30% of the weight of the fruit, Banana peel is rich in dietary fiber, proteins, essential amino acids, polyunsaturated fatty acids and potassium; among the efforts to use the peel, proteins, methanol, ethanol, pectins and enzymes have been obtained. (Gómez Montaña et al., 2019)

7.0.4 Mango peel

Mango is a fruit appreciated and highly consumed around the world, and in Mexico, mango is among the 3 most consumed fruits, after banana and apple Mango peel is the residue of multiple products such as juices, pickles, sauces, preserves, jams, jellies and dehydrated products, the peel represents about 32% of the total weight of the fruit which is discarded generating pollution in the environment. (Use of mango and its byproducts in animal production, n.d.)

7.0.5 Potato skin

Potato production is the main source of income due to the diversity of varieties that can be grown. It is estimated that about a quarter of the potato waste generated during industrial processing is discarded. In addition, agro-industrial waste has a considerable starch content that can be used industrially and in biotechnological processes as a substrate. (Sánchez-Castelblanco & Heredia-Martín, 2020).

7.0.6 Pretreatment

This stage is carried out with the objective of reducing the crystallinity of the cellulose, breaking the lignin-cellulose complex, increasing the surface area of the material, minimizing the presence of substances that may hinder the subsequent stages and minimizing the loss of the original material. (Antonio & Jiménez, n/d).

7.0.7 Hydrolysis

Hydrolysis is a process that consists of breaking complex carbohydrates into simple sugars to be used as a substrate for subsequent fermentation. Cellulose is hydrolyzed into D-glucose monosaccharides, while hemicellulose is hydrolyzed into pentoses and hexoses (mannose, glucose, xylose, etc.) (Oviedo, 2017).(Oviedo, 2017)

7.0.8 Cell separation methods

The various separation techniques are based on the existing differences between different cell types based on their differences in size, density, their antibody affinity towards certain cell surface epitopes, light scattering, fluorescence emission. Centrifugation is a technique to separate cells based on their density. This method is ideal for separating cells whose densities differ by more than 0.02 g/ml and is performed by conventional centrifuges (TOPIC 2 Cell Isolation and Purification Techniques - 1st Edition This document contains - Studocu, n.d.).

7.1 Methodology to be developed

The production of PHA by lignocellulosic matter requires additional processes for the release of the carbon source for microorganisms such as *Pseudomonas*, three raw materials were selected: banana peel, mango peel and potato peel, in which the same procedure was carried out.

7.1.1 Biomass preparation

To facilitate the storage of the raw material to be used, the water particles were eliminated from the material by means of a solar dryer, in which the peels were placed with the smallest possible thickness and in defined amounts in gr, remaining there until reaching constant weight, and then they were stored in separate containers.

7.1.2 Pretreatment

A mechanical pretreatment was carried out in order to reduce the size of the particles and improve the solubilization of sugars in the hydrolysis, crushing each of the three types of husks in a food processor until pulverized and then using a strainer the larger particles were removed to achieve a uniform consistency.

7.1.3 Hydrolysis

For the delignification of the pulverized husk, an acid pretreatment was carried out using a 2.5% solution of sulfuric acid at a ratio of 1:10 with respect to the biomass solution for 40 min at 125°C.

7.1.4 Preparation of the medium

After the chemical hydrolysis, a vacuum filtration with coffee filters was performed to remove the solid remains and reduce the time of a second filtration with 40 um paper. The solid remains were discarded and the filtered solution was kept to continue with the process.

Subsequently, the pH was adjusted to 7 of each of the three solutions of the hydrolyzed banana, mango and potato peels, by means of a solution of sodium hydroxide at .5 N, and the elements for the preparation of the basal medium were added (Table 2), in which glucose was replaced by the sugar present in the hydrolyzed solutions, for later comparison, a basal medium with glucose was prepared as indicated in Table 7.2. After the addition of the chemical compounds, each of the samples was sterilized at boiling point for 15 min.

7.1.5 *Pseudomonas* culture

King B medium was prepared, these media were stored in Petri dishes and after solidification they were seeded using a streaking technique with *Pseudomonas* and allowed to grow at 35 °C until visible growth was observed.

7.1.6 Culture media

For the preinoculum, a medium known for MCL growth (Table 1) was used for 24 hours at 35°C. The previously sterilized medium was inoculated with a bacteriological loop of the sample sown in solid King B medium, taking an absorbance measurement every hour for the analysis of its growth,

It was inoculated in a ratio of 1:10, pre-inoculated the same pre-inoculum 5 different samples, the one prepared with the basal medium, the LMC solution, and the three hydrolyzed solutions with banana peel, mango, potato 35°C for 72 HOURS using an Erlenmeyer flask with Bach type bioreactor and monitoring the growth by measuring absorbance at 450 nm every 2 hours.

7.1.7 Extraction of the solute

Each sample was centrifuged at 2000 rpm for 20 min and the supernatant and solute were removed, the latter was extracted by washing with distilled water.

7.1.8 Extraction of PHA

The extracted solute was dried at 60 degrees for 24 hours for the determination of the total bacterial weight, sodium hypochlorite was added at 37 degrees for 2 hours. Subsequently, the dried samples were placed in a water bath with chloroform and the resultant after evaporation was weighed.

7.2 Results

7.2.1 Preparation of the pre-treatment biomass

Three values of non-dried husk (wet weight) and their respective dry weight were recorded, and based on the following equation, the percentage of moisture was calculated. These values were averaged by type of husk to obtain a concrete value of moisture, which was compared with the theoretical values cited in other projects.

$$\% \text{ Humidity} = \frac{\text{Weight}_{\text{initial}} - \text{Weight}_{\text{final}}}{\text{Weight}_{\text{initial}}} \times 100 \quad (1)$$

Equation 1 Percentage of moisture (Gestión de RSU Propiedades 16, n.d.).

Table 7.3 Records of initial and final weights of different shells

Cascara	Wet weight (gr)	Dry weight (gr)	% Moisture	% Average humidity
Mango 1	290.043	41.906	86%	88%
Mango 2	213.000	25.780	88%	
Mango 3	183.010	18.055	90%	
Plantain 1	146.582	31.848	78%	81%
Plantain 2	74.564	11.158	85%	
Plantain 3	228.610	44.540	81%	
Papaya 1	98.818	6.918	93%	93%
Papaya 2	56.030	3.330	94%	
Pope 3	74.080	6.600	91%	

7.2.2 Pretreatment

A nutribullet was used for this process, grinding each type of peel separately (mango, potato and banana) and storing them in plastic containers.

After grinding, the larger particles were eliminated with a strainer and then regrinded until the desired size was reached.

7.2.3 Hydrolysis

For hydrolysis, the brix degrees were recorded to identify the percentage of sugars released at the end of the process; this was done only for the media in which the sugars were not free.

7.2.4 Preparation of the medium

It was recorded that for a hydrolyzed solution of 500 ml after filtration, a variable final volume was obtained for each of the substrates, the results are shown in the following table.

7.2.5 Growth media

For the preinoculum, a known medium was used for its MCL growth for 24 hours at 35°, taking absorbance measurements every hour in order to identify which pseudomonads were still in the growth phase and shorten the latency phase. At the end of the process the Brix degrees of each solution were recorded.

7.2.6 Extraction of the solute

Each sample was centrifuged at 2000 rpm for 20 min and the supernatant and solute were removed, the latter was extracted by washing with distilled water.

Table 7.4 Records of supernatant obtained after centrifugation

SUSTRATE	SUPERNATANT PER LITER
Mango	100 ml
Banana	83 ml
Potato	30 ml
MCL	22 ml
Basal	55 ml

7.2.7 Extraction of PHA

The extracted solute was dried at 60 degrees for 24 hours for the determination of the total bacterial weight, sodium hypochlorite was added at 37 degrees for 2 hours.

Subsequently, the dried samples were placed in a water bath with chloroform and the resultant was weighed after evaporation.

Table 7.5 Grams of pha per liter as a function of substrate type

SUBSTRATE	PHA (gr) liter
Mango	25.86 gr
Banana	19.53 gr
Potato	6.63 gr
CML	4.55
Basal	15.53

7.3 Discussions

It is concluded that higher amounts of PHA were obtained from mango peel because its sugar content is higher, exceeding the amount of production of the original basal medium with glucose, it was determined that providing the minimum requirements to the microorganism allows the production of PHA, while a medium rich in nutrients (LMC), generates a lower production.

The amount of PHA produced was 25.86 gr, 19.53 gr, 6.63 gr, 4.55, 15.53 for the Mango, Banana, Potato, LMC and Basal media.

7.4 Conclusions

It is concluded that greater amounts of PHA were obtained from mango peel because its sugar content is higher, exceeding the amount of production of the original basal medium with glucose, it was determined that providing the minimum requirements to the microorganism allows the production of PHA, while a medium rich in nutrients (LMC), generates a lower production.

The amount of PHA produced was 25.86 gr, 19.53 gr, 6.63 gr, 4.55, 15.53 for the Mango, Banana, Potato, LMC and Basal media.

7.5 References

Antonio, J., & Jiménez, P. (s/f). *UNIVERSIDAD DE JAÉN FACULTAD DE CIENCIAS EXPERIMENTALES DEPARTAMENTO DE INGENIERÍA QUÍMICA, AMBIENTAL Y DE LOS MATERIALES TESIS DOCTORAL ESTUDIO DEL PRETRATAMIENTO CON AGUA CALIENTE EN FASE LÍQUIDA DE LA PAJA DE TRIGO PARA SU CONVERSIÓN BIOLÓGICA A ETANOL PRESENTADA POR.*

Bioplásticos y bioproductos de alto valor añadido a partir de biomasa lignocelulósica - Industria Química. (s/f). Recuperado el 31 de agosto de 2023, de <https://www.industriaquimica.es/articulos/20210713/bioplasticos-bioproductos-alto-valor-anadido-partir-biomasa-lignocelulosica>

Contaminación por plásticos. Uno de los mayores desafíos ambientales del siglo XXI. (s/f). Recuperado el 31 de agosto de 2023, de <https://ecodes.org/hacemos/cultura-para-la-sostenibilidad/salud-y-medioambiente/observatorio-de-salud-y-medio-ambiente/contaminacion-por-plasticos-uno-de-los-mayores-desafios-ambientales-del-siglo-xxi>

MARTINEZ, D. (2008) *EFEECTO DEL GEN fadH1 EN LA PRODUCCION DE PHA CONTENIENDO MONOMEROS INSATURADOS POR Pseudomonas putida*. (s/f). Recuperado el 31 de agosto de 2023, de <https://repository.javeriana.edu.co/bitstream/handle/10554/8224/tesis219.pdf>

García, Y. G., Carlos, J., Contreras, M., Reynoso, G., Antonio, J., & López, C. (2013). Síntesis y biodegradación de polihidroxialcanoatos: plásticos de origen microbiano. *Revista internacional de contaminación ambiental*, 29(1), 77–115. http://www.scielo.org.mx/scielo.php?script=sci_arttext&pid=S0188-49992013000100007&lng=es&nrm=iso&tlng=es

Gestión de RSU Propiedades 16. (s/f). Recuperado el 31 de agosto de 2023, de https://aulagaasociacion.files.wordpress.com/2015/03/4_propiedades_rsu.pdf

Gómez Montaña, F. J., Bolado García, V. E., Blasco López, G., Gómez Montaña, F. J., Bolado García, V. E., & Blasco López, G. (2019). Compositional and antioxidant analysis of peels from different banana varieties (*Musa spp.*) for their possible use in developing enriched flours. *Acta universitaria*, 29, 1–14. <https://doi.org/10.15174/AU.2019.2260>

King B Agar | Pseudomonas | Bioser. (s/f). Recuperado el 31 de agosto de 2023, de <https://www.bioser.com/productos/king-b-agar-260p/>

Oviedo, U. DE. (2017). “OBTENCIÓN DE BIOETANOL A PARTIR DE HIDROLIZADOS DE RESIDUOS DE FRUTA” TRABAJO FIN DE MASTER POR CELIA HERNÁNDEZ GALINDO.

René Rafael Gallego-Domínguez, R. Z.-Z. M. E. de L.-O. R. M.-R. (2017). Respuesta de la caña de azúcar ante la aplicación de una mezcla de fitoestimulantes. *ICIDCA. Sobre los Derivados de la Caña de Azúcar*, 3. <https://www.redalyc.org/pdf/2231/223158039001.pdf>

Carlos, M. C. J. (2023). *Repositorio Institucional de la Universidad San Gregorio de Portoviejo: Uso factible del bloque sintético tipo Lego para mampostería no estructural de viviendas de interés social en la ciudad de Portoviejo.* Recuperado el 31 de agosto de 2023, de <http://repositorio.sangregorio.edu.ec/handle/123456789/3004>

Sánchez-Castelblanco, E. M., & Heredia-Martín, J. P. (2020). Evaluation of potato peel wastes to produce amylases from *Bacillus amyloliquefaciens* A16. *Revista de la Academia Colombiana de Ciencias Exactas, Físicas y Naturales*, 44(172), 794–804. <https://doi.org/10.18257/RACCEFYN.1122>

TEMA 2 Técnicas DE Aislamiento Y Purificación Celular - 1ª Edición Este documento contiene - Studocu. (s/f). Recuperado el 31 de agosto de 2023, de <https://www.studocu.com/es/document/universidad-de-sevilla/biologia-celular/tema-2-tecnicas-de-aislamiento-y-purificacion-celular/21188664>

Utilización del mango y sus subproductos en producción animal. (s/f). Recuperado el 31 de agosto de 2023, de <https://nutrinews.com/utilizacion-del-mango-y-sus-subproductos-en-produccion-animal/>

Annual emissions of greenhouse gases of motor vehicles in the Academic Unit Valle de las Palmas UABC

Emisión anual de gases de efecto invernadero de vehículos motorizados en la Unidad Académica Valle de las Palmas UABC

CASTAÑÓN-BAUTISTA, María Cristina†*, CUENCA-LÓPEZ, Luis Daniel and HERNÁNDEZ-VILLANUEVA, Johana Lizeth

Universidad Autónoma de Baja California, México.

ID 1st Author: *María Cristina, Castañón-Bautista* / **ORC ID:** 0000-0001-5197-3951, **CVU CONAHCYT ID:**175473

ID 1st Co-author: *Luis Daniel, Cuenca-López* / **ORC ID:** 0009-0001-6840-6942

ID 2nd Coauthor: *Johana Lizeth, Hernández-Villanueva*

DOI: 10.35429/P.2023.1.79.88

M. Castañón, L. Cuenca and J. Hernández

* a1274750@uabc.edu.mx

Á. Marroquín, L. Castillo, J. Olivares and A. Álvarez (AA. VV.). Young Researchers. Engineering Applications - Proceedings-©ECORFAN-México, Queretaro, 2023.

Abstract

The purpose of this research is to carry out a quantify motor vehicles that enter the Valle de las Palmas Academic Unit (UA) of the Autonomous University of Baja California, calculate the GHG Levels based on CO₂ emissions and evaluate the environmental impact generated by transportation according to indicators of the Transportation category of the UI GreenMetrics 2023 Guide. A manual counting method is used to know the number and type of vehicles that travel to the UA and with based on these results, determine the emissions of GHG as well as the environmental impact generated by motor vehicles that travel to the UA. Its conclude that the type of motor vehicles that travel to the UA us heterogeneous, consisting of private cars, urban transport, and motorcycles and these generate 1884 metric tons of CO₂ per year, so with these data there is a baseline of environmental impact generated by transport that travels to the UA, existing areas of opportunity for improvement for the benefit of air quality and the health of the university community.

GHG emissions, quantify motor vehicles, Higher Education

8 Introduction

The gauging is an essential tool for the study and analysis of the vehicular flow on a given road or highway to calculate the amount of CO₂ emitted in a Higher Education Institution (HEI). In a world in constant movement, vehicular traffic traveling to a HEI is a factor that directly affects the quality of life of students, faculty and administrative staff, as well as the air quality at the site. Motorized vehicles can generate a negative impact by using fossil fuels, effects such as air pollution (Mannering & Washburn, 2020) by emitting Greenhouse Gases (GHG) (Nava Carrasco, 2023) and negatively affect human health. In this context, some authors point out that transportation is the main cause of pollution in urban areas (Rehimi, Landolsi, & Kalboussi, 2017), in Europe, for example, it accounts for 71% of CO₂ emissions (Yongseng Qian, Xuting Wei, & Li, 2023), and for Mexico it contributes 40% (Hancevic, Núñez, & Rosellón, 2023). The collection of accurate and reliable data on vehicular traffic commuting to an HEI is essential for the quantification and implementation of GHG generation reduction policies related to motor vehicle emissions, as well as the optimization of HEI community travel times and alternatives in urban or shared means of transportation.

To estimate GHG pollution, it is necessary to know the vehicular traffic at peak hours and throughout the day by means of vehicle gauging to determine their quantity, composition and emission levels (Rehimi, Landolsi, & Kalboussi, 2017) of vehicles circulating on a road in a certain period of time, which allows obtaining relevant information on the volume of CO₂ emissions in the atmosphere. The application of vehicle gauging techniques can be carried out in various ways, including direct observation, the installation of electronic devices, the use of video surveillance systems and the analysis of GPS navigation data. Each of these techniques has advantages and limitations in terms of accuracy, cost and ease of implementation (Kineo Ingeniería del Tráfico, S. L., 2023).

The objective of this research work is to perform a gauging of motorized vehicles (urban transport, private vehicles, motorcycles) entering the Academic Unit (UA) of Valle de las Palmas of the Autonomous University of Baja California (UABC) and given that this traffic obeys the supply and demand of transport, perform measurements at peak hours at a certain time of day in the month of September 2022 and March 2023. With this experimental data and according to the UI GreenMetrics 2023 guide, calculate the GHG levels based on CO₂ emissions and compliance with the indicators that correspond to the Transportation category according to UI GreenMetrics 2023 (UI GreenMetric Secretariat, 2023) in order to have a baseline of the environmental impact generated by the transportation that travels to the UA.

8.1 Theoretical framework

Motorized traffic flow is the movement or circulation of motorized vehicles such as cars, buses, motorcycles, or cargo trucks that circulate on a roadway and the knowledge about the quantity and behavior of this traffic flow or vehicular gauging (Secretaría de Comunicaciones y Transporte, 2016) in a certain period of time. There are several methodologies to carry out a vehicle gauging and its selection will depend on the purpose of the study (Monetti, Contreras, & Sevillano, 2018) among which we can mention manual and automatic methods (Secretaría de Comunicaciones y Transporte, 2016):

Manual method: on-site gauging. corresponds to vehicle counting where the data collector is located at an intersection and through previously prepared logs observes and records the vehicle count (Monetti, Contreras, & Sevillano, 2018).

Automatic method: this is performed with automatic equipment designed to continuously record vehicular traffic through sensors or detectors. These devices can transmit data in real time and counting is performed through inductive loop detectors, sensors (magnetic, microwave radar, passive infrared, laser radar, ultrasonic) and video detection (Secretaría de Comunicaciones y Transporte, 2016).

Likewise, it is important to know what are the emissions generated by motor vehicles, Shiva, et al (Shiva Nagendra, Jaikumar, & Sivanandan, 2017) refer that the key pollutants from vehicle exhaust are nitrogen oxides (NO_x), carbon monoxide (CO), hydrocarbons (HC), particulate matter (PM) and carbon dioxide (CO₂). The latter is generated by the combustion of fossil fuels such as gasoline and diesel and in 2021 the transportation sector contributed 29% of GHG emissions in the United States (Environmental Protection Agency, 2023).

On the other hand, research on environmental impact generated by transportation in the context of HEIs refers mainly to the implementation of strategies to reduce the generation of GHG emissions. According to the sustainability report of San Diego State University, policies are implemented such as reducing the percentage of employees and students who travel in single occupancy vehicles, as well as by the year 2025 the purchases of university vehicles should represent at least 50% (San Diego State University, 2021). Another example, is San Jose State University, where their goal is to promote the use of bicycles, urban transportation and carpooling with a 2018 impact on GHG reduction of 28, 000 Tons (San Jose State University, 2020).

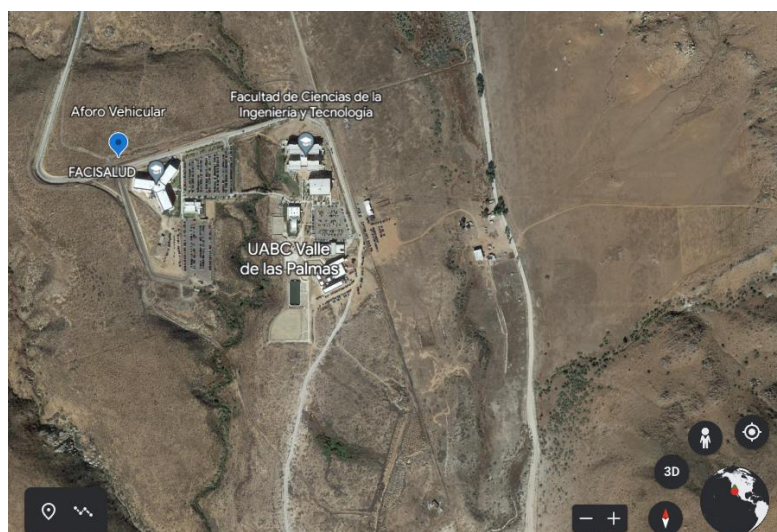
The lack of knowledge of the amount of GHG emitted in the IES, may create some uncertainty for not knowing the environmental impact that this has towards people and the natural environment, this due to the daily displacement of the university community to this area. This research is based on the results of an in situ vehicular gauging and based on the results, calculate the GHG emissions.

8.2 Methodology

8.2.1 Study area

The study site is the UA Valle de las Palmas of the UABC, located in the city of Tijuana, Baja California at the geographical coordinates 32°43'502" and 116°67'506" in an area of 50 hectares (Figure 8.1). This is an applied, descriptive and documentary research presented in three stages: vehicular gauging, GHG emissions calculation and evaluation of the environmental impact generated by transportation in the UA.

Figure 8.1 Study site: Valle de las Palmas UA



Source: (Google Earth, 2022)

8.2.2 Vehicle gauging

In order to know the number and type of motorized vehicles entering the UA, two vehicle counts are performed according to the manual method (Monetti, Contreras, & Sevillano, 2018): In September 2022, a pilot vehicle count was conducted in the UA and at peak hours, to anticipate the challenges that could be encountered when executing the definitive gauging and thus adhere to the UI GreenMetrics Guideline 2022 (UI GreenMetric Secretariat, 2022). Again in March 2023, on-site vehicle gauging is performed at the UA, where the motor vehicle count is observed and recorded in a logbook during peak hours. See annex BITACORA.

8.2.3 Calculation of GHG emissions

To calculate the GHG emissions generated by motor vehicles, the Carbon Footprint emission factor (Carbon Footprint Ltd, 2023) is used as a basis and in accordance with the UI GreenMetric Guideline 2023 (UI GreenMetric Secretariat, 2023), considering the number of vehicles entering the AU and also the distance in kilometers that a vehicle travels within the AU and considering the days worked per year in the AU to obtain the annual emissions in metric tons and generated by transportation.

8.2.4 Environmental impact generated by transportation in the AU

To evaluate the environmental impact of the AU and in accordance with the UI GreenMetric Guideline (UI GreenMetric Secretariat, 2023) in the transportation category, a self-assessment is made to the AU considering the following indicators:

- Number of vehicles used and managed.
- Number of vehicles entering daily.
- Number of motorcycles entering daily.
- Ratio of total motorized vehicles divided by the total population.
- Shuttle service within the UA.
- Number of shuttles operated by the UA.
- Average number of passengers per shuttle.
- Total trips by internal transportation services.
- Zero Emission Motor Vehicle (ZEV) Policy.
- Average daily number of ZEV motorized vehicles.
- The ratio of ZEV zero emission motorized vehicles divided by the total population of the UA.
- Total parking area (m²).
- Ratio of parking area to total area.
- Transportation program to design or limit parking area over the past three years.
- Number of transportation initiatives to reduce motor vehicle ingress.
- Policy to reduce motor vehicle travel.
- Policies for pedestrian walkways.
- Daily motor vehicle travel distance within the UA.

8.3 Results

8.3.1 Vehicle capacity. September 2022

Tables 8.1, 8.2 and 8.3 show the results of the count in the month of September conducted between 8:00 and 9:00 a.m., which show that motor vehicles entering the UA are mainly private vehicles (PV), followed by urban transport vehicles (UTV) sedan type (ST) and in smaller quantities urban buses (UB), minivans with a capacity of 17 passengers (P) and motorcycles (M).

Table 8.1 Vehicle capacity on September 19

Time	PV	AU	UTV	MV	M
8:00	155	1	4	-	-
8:15	137	-	5	-	-
8:30	130		2	1	3
8:45	54	1	3	-	-
9:00	65	-	-	-	2
Total	541	2	14	1	5

Table 8.2 Vehicle capacity on September 21

Time	PV	AU	UTV	MV	M
8:00	125	2	5	1	3
8:15	165	-	3	-	-
8:30	123	-	1	-	5
8:45	96	1	2	-	-
9:00	47	-	-	-	3
Total	556	3	11	1	11

Table 8.3 Vehicle capacity on September 23

Time	PV	AU	UTV	MV	M
8:00	110	1	6	1	2
8:15	95	-	3	-	3
8:30	59	-	1	-	1
8:45	32	1	2	-	-
9:00	27	-	-	-	1
Total	323	1	12	1	7

In the gauging carried out in September 2022, it is observed that the motorized vehicle fleet entering the UA is heterogeneous, composed mainly of private vehicles (Table 8.4).

Table 8.4 Total motorized vehicles

PV	AU	UTV	MV	M
1,420	6	37	3	23

Vehicle capacity. March 2022

Tables 8.5, 8.6 and 8.7 show the results of the count in the month of March, carried out between 8:00 and 9:00 a.m., which show that the motorized vehicles entering the AU are mainly PV, followed by UTV and, to a lesser extent, AU and M.

Table 8.5 Vehicle capacity on March 13

Time	PV	AU	UTV	MV	M
8:00	100	5	2	8	1
8:15	120	-	2	3	-
8:30	128	-	5	-	-
8:45	40	1	6	-	-
9:00	37	1	4	-	-
Total	425	7	19	11	1

Table 8.6 Vehicle capacity on March 15

Time	PV	AU	UTV	MV	M
8:00	211	3	4	2	3
8:15	135	-	6	-	1
8:30	115	-	2	2	-
8:45	40	1	4	-	-
9:00	37	1	-	-	-
Total	425	5	16	4	4

Table 8.7 Vehicle capacity on March 17

Time	PV	AU	UTV	MV	M
8:00	159	1	6	-	-
8:15	133	-	7	-	1
8:30	159	-	2	2	-
8:45	64	1	3	-	-
9:00	32	-	-	-	-
Total	547	2	18	2	1

In the gauging carried out in March 2023, it was observed that the motorized vehicle fleet entering the UA is heterogeneous, composed mainly of private vehicles (Table 8.8).

Table 8.8 Total motorized vehicles

PV	AU	UTV	MV	M
1,597	14	53	17	6

In Table 8.9, a comparison is made of the gauging carried out and as can be seen, the vehicle fleet is heterogeneous, increasing in 2023 for all vehicles, except for motorcycles.

Table 8.9 Comparison of vehicle capacity between 2022 and 2023

Year	PV	AU	UTV	MV	M
2022	1,420	6	37	3	23
2023	1,567	14	53	17	3

8.3.2 Calculation of GHG emissions

To calculate the GHG emissions generated by motor vehicles, the emission factor of the Carbon Footprint (Carbon Footprint Ltd, 2023) is used as a basis and in accordance with the UI GreenMetric Guideline 2023 (UI GreenMetric Secretariat, 2023), obtaining the following results:

a) Transport emissions per year:

Description:

According to the 2023 school term of UABC there are 205 working days in the year.

0.01 is the coefficient to calculate the metric tons generated by vehicular transportation per km (UI GreenMetric Secretariat, 2023).

$$= \left(\frac{(\text{No. transport entry})(\text{Round the day})(\text{Distance})(\text{Days of work})}{100} \right) (0.01) \quad (1)$$

Equation (1)

Result:

$$= \left(\frac{(84)(8)(2.9481 \text{ km})(205)}{100} \right) (0.01)$$

= 40.6130 *metric tons*

b) Automobile emissions per year:

Description:

205 are the working days in the year. 0.02 is the coefficient to calculate metric tons of automobiles per km (UI GreenMetric Secretariat, 2023).

$$= \left(\frac{(\text{No. of cars entering})(2)(\text{Distance})(\text{Days of work})}{100} \right) (0.02) \quad (2)$$

Equation (2)

Result:

$$= \left(\frac{(1567)(2)(2.9481 \text{ km})(205)}{100} \right) (0.02)$$

= 378.8221 *metric tons*

c) Emissions generated by motorcycles per year:

Description:

205 are the working days in the year.

0.01 is the coefficient to calculate the metric tons of motorcycles per km (UI GreenMetric Secretariat, 2023).

$$\left(\frac{(\text{No. of motorcycles entering})(2)(\text{Distance})(\text{Days of work})}{100} \right) (0.01) \quad (3)$$

Equation (3)

Result:

$$\left(\frac{(6)(2)(2.9481)(205)}{100} \right) (0.01)$$

= 0.7252 *metric tons*

d) Annual emissions generated by transportation in metric tons:

Formula:

Electricity use per year + transportation + automobiles + motorcycles

Result:

= 1495.0871 + 13.776 + 378.8221 + 0.7252

= 1888.4104 *metric tons per year*

8.3.3 Environmental impact generated by transportation in the AU.

The environmental impact of the AU was evaluated according to the criteria and indicators of the UI GreenMetric Guideline (UI GreenMetric Secretariat, 2023) in the transportation category, obtaining the results shown in Table 8.10.

Table 8.10 Results obtained from the self-assessment in the transportation category

Criteria and indicators for the transportation category		Results
5.1.	Number of motor vehicles managed	There is only a record of three vehicles used by the Institution for students' field practices.
5.2.	Number of motorized vehicles managed daily	Through the data recorded during the vehicle registration, we obtained an average of 522 motorized vehicles per day.
5.3.	Number of motorcycles entering the UA daily	On average, at least one motorcycle enters each day.
5.4.	The ratio of total motorized vehicles divided by the total population in the UA.	The ratio corresponds to the sum of the 3 previous points divided by the population of the UA in general, which is about 5947, obtaining as a result 0.0884, and corresponds to Level 4.
5.5.	Shuttle service within the AU	Not applicable
5.6.	Number of shuttles operated at your university	Not applicable
5.7.	Average ridership of each shuttle	Not applicable Not applicable
5.8.	Total trips per shuttle service each day	Not applicable Not applicable
5.9.	Zero Emission Vehicle (ZEV) Policy	In this weighting the University is in Level 1, which means that it does not have zero-emission vehicles available. To date, there is no record of a policy that promotes the use of zero-emission vehicles.
5.10.	Average number of ZEV vehicles per day	There is a record of two ZEVs for private use.
5.11.	The ratio of ZEV zero-emission motor vehicles divided by the total population of the UA.	The AU has a record of only two ZEV vehicles, which divided by the general population of 5947, gives us a result of 0.0003, placing us in Level 1 in the GreenMetrics 2023 weighting table, corresponding to the section.
5.12.	Total parking area (m ²)	It has a surface area of 32,702m ² (Google Earth, 2022).
5.13.	Ratio of parking area to total area of the AU	The total parking area is 32,702m ² between the total area of the AU is 60,471m ² multiplied by 100%, giving us a total of 54.07%.
5.14.	Transportation program designed to limit or decrease parking area on campus, during the last 3 years.	No records are available
5.15.	Number of transportation initiatives to reduce motorized vehicles.	There is no official initiative at the UA; however, unofficial carpooling is present, but the scale is unknown.
5.16.	Policies for pedestrian walkways	The UA has pedestrian paths, designed for the safety and comfort of pedestrians.
5.17.	Approximate daily travel distance of a motorized vehicle (in Kilometers)	Within the AU, a motor vehicle travels approximately 2.5 km from the entrance to the farthest parking lot.

Source of reference: (UI GreenMetric Secretariat, 2023)

8.4 Acknowledgements

We thank the Faculty of Engineering Sciences of the Autonomous University of Baja California for the grant received during the 2023 school period and for the facilities for the management and obtaining of information to carry out this research project.

8.5 Conclusion

Through the vehicular gauging carried out we can observe the changes occurred in relation to the composition of the transportation in which the university community travels to the UA, composed mainly of private vehicles and urban bus, in lesser quantity the use of motorcycles. Also, in the 2023 gauging, an increase in the vehicle fleet accessing the UA was observed. Therefore, an opportunity for improvement will be to offer urban transportation alternatives that reduce travel time and vehicle use per occupant.

GHG emissions due to the displacement of motorized vehicles that travel to the UA is 1884 metric tons per year, which are the baseline to offer the university community alternatives in the use of transportation that contribute to the reduction of GHG emissions.

Based on the self-assessment in the transportation category, there are opportunities in terms of urban transportation, the implementation of policies that raise awareness of the use of zero-emission vehicles, as well as incentives for the use of carpooling and thus reduce the area allocated for parking.

This study aims to be a reference and generate knowledge from which measures can be proposed to reduce exposure to polluting gases and avoid health risks to the university community, as well as the development of mitigation strategies and mitigation of GHG emissions emitted into the atmosphere.

8.6 References

Carbon Footprint Ltd. (2023). *Carbon Footprint*. Recuperado el 08 de Julio de 2023, de Carbon Footprint: <https://www.carbonfootprint.com/>

Environmental Protection Agency. (13 de Junio de 2023). *United States Environmental Protection Agency*. Recuperado el 06 de Julio de 2023, de United States Environmental Protection Agency: <https://www.epa.gov/>

Google Earth. (Julio de 2022). *Google Earth*. Recuperado el 08 de Julio de 2023, de Google Earth: <https://earth.google.com/web>

Hancevic, P. I., Núñez, H. M., & Rosellón, J. (2023). *Documento de trabajo sobre el sector energético en América Latina y el Caribe*. (D. B. America, Ed.) Obtenido de Documento de trabajo sobre el sector energético en América Latina y el Caribe: <https://scioteca.caf.com/handle/123456789/2032>

Kineo Ingeniería del Tráfico, S. L. (04 de Julio de 2023). *Kineo Ingeniería de Gestión del Tráfico*. Recuperado el 04 de Julio de 2023, de Kineo Ingeniería de Gestión del Tráfico: <https://www.interempresas.net/Medicion/FeriaVirtual/Producto-Aforo-y-clasificacion-vehicular-71058.html>

Mannering, F. L., & Washburn, S. S. (2020). Introduction to Highway Engineering and Traffic Analysis. En M. F. L., & S. S. Washburn, *Principles of Highway Engineering and Traffic Analysis, 7th Edition* (págs. 1-10). Hoboken, NJ, United States: John Wiley & Sons. Recuperado el 04 de Julio de 2023, de <https://www.wiley.com/en-us/Principles+of+Highway+Engineering+and+Traffic+Analysis,+7th+Edition-p-9781119493969#download-product-flyer>

Monetti, J., Contreras, M., & Sevillano, G. (2018). Propuesta de recolección de datos para aforo vehicular. En R. d. Informática (Ed.), *XX Workshop de Investigadores en Ciencias de la Computación (WICC 2018, Universidad Nacional del Nordeste)*. (págs. 838-842). Corrientes: Facultad de Ciencias Exactas y Naturales y Agrimensura. Recuperado el 06 de Julio de 2023, de <http://sedici.unlp.edu.ar/handle/10915/67063>

Nava Carrasco, G. M. (21 de Marzo de 2023). Análisis de las emisiones atmosféricas y combustión incompleta de los vehículos automotores del distrito de Hualmay 2021. Perú, Perú. Recuperado el 04 de Julio de 2023, de <http://hdl.handle.net/20.500.14067/7544>

Rehimi, F., Landolsi, J., & Kalboussi, A. (2017). Urban traffic and induced air quality modeling and simulation: Methodology and illustrative example. *Urban Climate*, 21, 154-172. doi:<https://doi.org/10.1016/j.uclim.2017.06.002>

San Diego State University. (2021). *UC San Diego 2021 Sustainability Report*. Recuperado el 2023, de UC San Diego 2021 Sustainability Report: <https://sustainability.ucsd.edu/about/reports/2021.html>

San Jose State University. (2020). *San Jose State University*. Recuperado el 07 de Julio de 2023, de San Jose State University: <https://www.sjsu.edu/sustainability/>

Secretaría de Comunicaciones y Transporte. (2016). *Secretaría de Comunicaciones y Transporte*. (S. d. Transporte, Ed.) Recuperado el 06 de Julio de 2023, de Secretaría de Comunicaciones y Transporte.

Shiva Nagendra, S. M., Jaikumar, R., & Sivanandan, R. (2017). Modal analysis of real-time, real world vehicular exhaust emissions under heterogeneous traffic conditions. *Transportation Research Part D*, 54, 397-409. doi:<http://dx.doi.org/10.1016/j.trd.2017.06.015>

UI GreenMetric Secretariat. (2022). *UI GreenMetric Secretariat*. Recuperado el 07 de Julio de 2023, de UI GreenMetric Secretariat: <https://greenmetric.ui.ac.id/>

UI GreenMetric Secretariat. (2023). *UI GreenMetric World University Rankings 2023*. (I. L. (ILRC), Ed.) Recuperado el 06 de Julio de 2023, de UI GreenMetric World University Rankings 2023: <http://www.greenmetric.ui.ac.id/>

Yongseng Qian, J. Z., Xuting Wei, J. Z., & Li, H. (March de 15 de 2023). Hybrid characteristics of heterogeneous traffic flow mixed with electric vehicles considering the amplitude of acceleration and deceleration. *Physica A: Statistical Mechanics and its Applications*, 614, 1-14. doi:<https://doi.org/10.1016/j.physa.2023.128556>

Comparison of gasoline, hybrid and electric vehicles

Comparación de automóviles a gasolina, híbrido y eléctrico

GARCÍA-CONTRERAS, Cecilia Pamela, ONTIVEROS-SÁNCHEZ, Kenneth Arturo, MADRID-CAMACHO, Erick Ernesto and ALVAREZ-MACÍAS, Carlos*

Instituto Tecnológico Nacional de México, Instituto Tecnológico de la Laguna. México.

ID 1st Autor: *Cecilia Pamela, García-Contreras* / **ORC ID:** 0000-0003-3056-0896, **CVU CONAHCYT ID:** 1271712

ID 1st Co-author: *Kenneth Arturo, Ontiveros-Sánchez* / **ORC ID:** 0009-0004-1105-7958

ID 2nd Co-author: *Erick Ernesto, Madrid-Camacho* / **ORC ID:** 0009-0000-9548-6864

ID 3rd Co-author: *Carlos, Alvarez-Macías* / **ORC ID:** 0000-000 2-2263-0316, **CVU CONAHCYT ID:** 165872

DOI: 10.35429/P.2023.1.89.106

C. García, K. Ontiveros, E. Madrid and C. Álvarez

* calvarezm@correo.itlalaguna.edu.mx

Á. Marroquín, L. Castillo, J. Olivares and A. Álvarez (AA. VV.). Young Researchers. Engineering Applications - Proceedings-©ECORFAN-México, Queretaro, 2023.

Abstract

It is well known that hybrid and electric cars have been proposed and considered as the available alternative to gasoline vehicle, to try and reduce the consumption of fossil fuels to meet global environmental objectives. Therefore, the average user should have an analytical comparison to determine if the available alternatives are useful to them and their particular situation. As such, this project aims to provide a purchasing recommendation to the average user based off their needs while highlighting the strengths and weaknesses of the three types of automobiles available: gasoline, hybrid and electric. To complete this comparison, the best-selling cars in Mexico of each available category, with similar measurements and passenger capacity, were selected. Subsequently, it was decided that a journey of over 1000 km across the country would be the best comparison, deciding on the travel route to start from Torreón, Coahuila to Puebla, Puebla. After calculating the total energy needed for each vehicle to complete the same route, the stops needed to recharge and complete the route, as well as the time needed, it was concluded that compared to the gasoline car, the hybrid is an option with similar performance on long trips, while the electric car is not recommended for long trips like the one analyzed in this report.

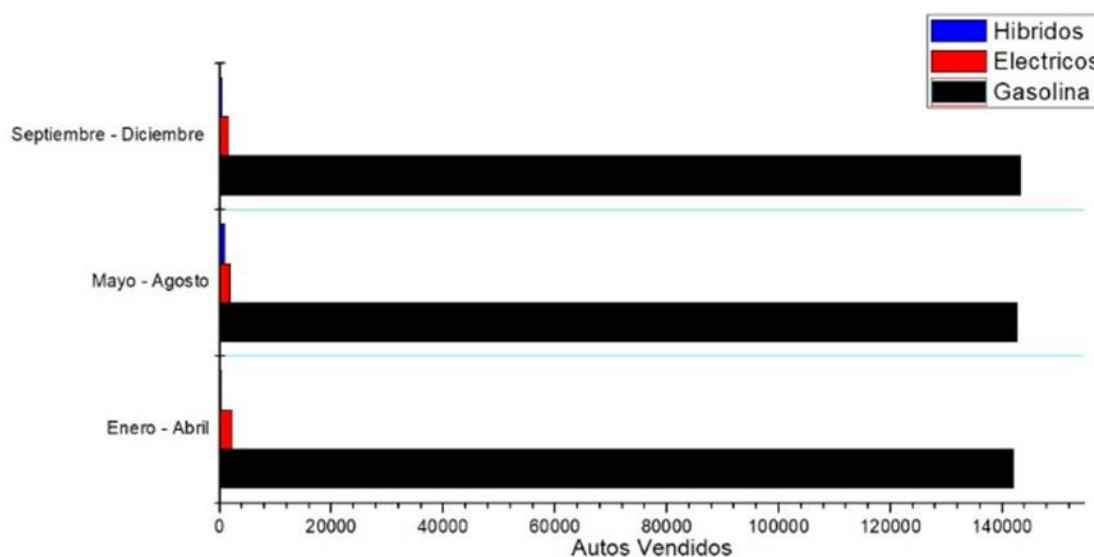
Car comparison, Comparative analysis, Mobility alternatives, Electric vehicles, Hybrid vehicles

9 Introduction

In the current context, the challenges that society faces with climate change and the need to reduce greenhouse gas emissions are of common interest. It is also well known that light-duty automobiles are one of the main environmental pollutants. In Mexico alone, private automobiles generate 18% of CO₂ emissions, the main gas that causes the greenhouse effect (IMCO, Instituto Mexicano para la Competitividad A.C., 2022). Due to this, more sustainable transportation alternatives have emerged in recent years, such as hybrid and electric vehicles, which seek to reduce gasoline consumption and promote the adoption of more environmentally friendly technologies. However, despite their availability in the market for years, in 2022, more than 1.1 million units of light vehicles were sold in Mexico, 98% of which were gasoline-powered, while only 1% were hybrid and 1% electric cars (Statista Research Department, 2023).

Figure 9.1 below shows a graph representing the number of cars sold in 2022. It should be noted that the number of electric and hybrid cars sold was minimal compared to gasoline cars.

Figure 9.1 Number of light-duty cars sold in Mexico, 2022



Source of Consultation: (Statista Research Department, 2023)

The automotive market in Mexico shows a dominant position of gasoline vehicles, due to their recognition and demand by consumers, as they adapt to diverse needs. However, the growing concern to reduce fossil fuel consumption has given rise to two new categories in the personal transportation market: electric and hybrid cars. These options provide an alternative to reduce dependence on fossil fuels, especially if the electric part comes from renewable energy sources.

Despite this, it is evident that most Mexicans are not sufficiently informed or interested in learning about the new technologies available in the automotive sector. However, Mexico has committed to reduce CO₂ emissions, setting the goal of a 25% decrease by 2030, according to the General Law on Climate Change (Secretaría de Medio Ambiente y Recursos Naturales, 2015). To achieve these goals within the proposed timeframe, it will be necessary to change the purchasing trend over the next decade. This is difficult to achieve if average consumers lack interest and knowledge about the benefits and opportunities offered by new technologies compared to traditional vehicles.

This study explores and compares gasoline, electric and hybrid vehicle technologies in order to provide a comprehensive and objective assessment for consumers. The relevance of this topic lies in its ability to address current environmental and energy challenges in the transportation sector. The added value of this study lies in its comparative and comprehensive approach, providing a solid basis for informed decision making. Each type of vehicle has unique characteristics, from internal combustion engines in gasoline vehicles to electric systems in electric and hybrid vehicles. The problem it seeks to address is the lack of clear information for consumers when choosing between these technologies, with the central assumption that a detailed analysis will enable more conscious decisions and contribute to pollution reduction.

The chapter is structured to understand the mathematical calculations made to complete this study, presenting the equations used, with their components and meanings. The following parts of the chapter are to understand the performance of the different types of cars, in order to compare them.

9.1.1 Energy

Energy is the capacity of bodies to do work and produce changes in themselves or in other bodies (Secretaría de Energía de la República de Argentina, 2003). That is, the concept of energy is defined as the ability to make things work, having different ways to affect a body, we have different equations that help us to calculate certain parts that make up the total energy required to complete the desired work. As well as they are divided into different types of energy such as:

9.1.1.1 Kinetic energy

Kinetic energy is the energy associated with bodies in motion, depending on the mass and velocity of the body. The way to calculate it is presented in Equation 1.

$$E_K = \frac{1}{2}mV^2 \quad (1)$$

In this equation we have the following variables to consider:

- The mass of the car and passengers, measured in kilograms.
- The speed at which the car moves, measured in meters per second.

9.1.1.2 Potential Energy

Potential energy is the capacity of bodies to do work W , depending on their configuration in a system of bodies exerting forces on each other. It can be thought of as the energy stored in a system, or as a measure of the work that a system can deliver (W. Sears, W. Zemansky, & Young, 2009). The way to calculate it is presented in Equation 2:

$$E_U = mgh \quad (2)$$

In this equation we have the following variables to consider:

- The difference in altitudes between each state, divided into each segment of the path, measured in meters.
- The total mass of each vehicle and passengers, measured in kilograms.
- The gravity constant, measured in meters over second squared.

9.1.1.3 Drag energy

Drag energy comes from the multiplication of the friction force or frictional force (created by the resistance offered by a fluid when an object moves through it) and the distance traveled (Gencel, 2012). The way to calculate it is presented in Equation 3:

$$E_F = F \times d = \frac{1}{2} \times \sigma \times A \times v^2 \times \rho \times d \quad (3)$$

In this equation we have the following variables to consider:

- The drag force considers:
 - The drag coefficient of the cars, taking an average 0.27 for the three vehicles.
 - The cross-sectional area of each car, measured in meters squared.
 - The velocity at which each vehicle is traveling, squared, resulting in m^2/s^2 .
 - The density of the air, a constant of 1,225 kg/m^3 , since this is the medium in which the trip is made.
- The distance traveled, measured in meters.

9.1.1.4 Friction energy

Finally, the friction energy of the tires with the pavement was considered, which, like the drag energy, is obtained from the multiplication of a force (the friction force, created between two surfaces in contact, opposing sliding) and the distance traveled (W. Sears, W. Zemansky, & Young, 2009). The way to calculate it is presented in Equation 4.

$$E_F = F \times d = \mu \times N \times d = \mu \times mg \times d \quad (4)$$

In this equation we have the following variables to consider:

- The frictional force is calculated from:
 - The coefficient of friction between the two surfaces to be considered. A coefficient of 0.12 is taken due to the composition of the tires and regular concrete (AVSLD International, 2013).
 - The normal force, being the force exerted by a surface when a body rests on it. In the case to be considered of a horizontal car, the normal is replaced by the weight of the car; that is, the mass (in kilograms) times the gravity (meters over second squared).
- Similar to the previous equation, the distance traveled, measured in meters.

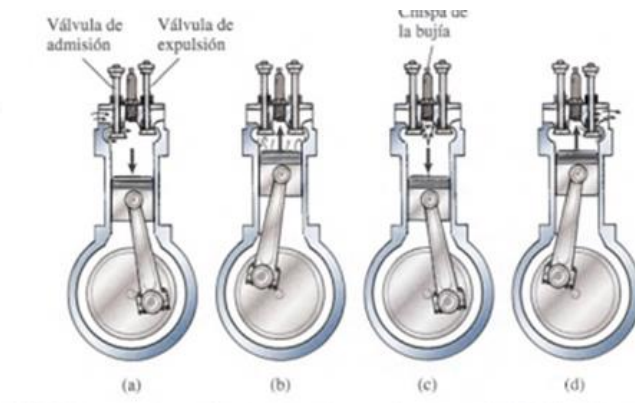
Finally, a single equation is observed as a summation of all the previous ones. The total energy of a body in motion is given in Equation 5:

$$E_T = E_K + E_U + E_R + E_F \quad (5)$$

9.1.2 Gasoline car

The gasoline car, the most common model and known to the average user, runs on an engine that has gasoline as fuel and this goes through the Otto cycle. The gasoline engine is also known as a four-stroke engine, shown in Figure 9.2 (Tippens, 2001).

Figure 9.2 The four-stroke gasoline engine (a) Intake stroke (b) Compression stroke (c) Working stroke (d) Exhaust stroke



Source: (Tippens, 2001)

- Intake stroke: where the engine's four-stroke process starts.
- Compression stroke: the mixture enters through the intake valve, which closes during the compression stroke.
- Working stroke: the piston moves up causing a pressure rise, before it reaches the top, the mixture ignites, which causes a change in temperature and pressure in the working stroke.
- Ejection stroke: The products resulting from combustion are expelled from the engine and released into the environment. Among these products is, to a large extent, CO₂.

In summary, it can be said that the gasoline engine works from a spark that ignites the mixture of gasoline and air. This engine has an efficiency of 25%, compared to the diesel or gas oil engine which has an efficiency between 40% and 45%, due to the fact that the larger and more refined the engine, the better its performance (Tippens, 2001). Table 9.1 shows the comparison between the energy yield of a gasoline engine and a diesel engine.

Table 9.1 Comparison between gasoline and diesel

Fuel	Energy per liter	
Gasoline	32,18 MJ/l	8.94 kWh
Diesel	35,86 MJ/l	9.96 kWh

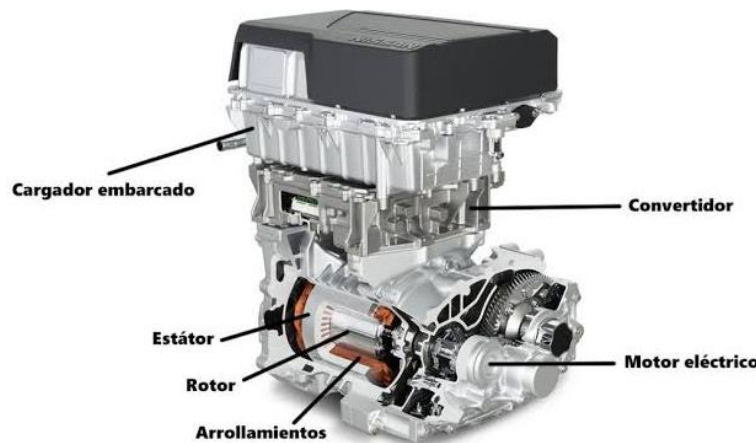
Source: (Tippens, 2001)

According to Pemex figures, between January and May 2022, an average of 1 million 19 thousand barrels of fuels were consumed daily, of which 81.95 are magna gasoline, while the other 18.1% is premium gasoline. It was also reported that during said year fuel sales grew 39.3% at annual rate in the month of June. (Usla, 2022) The increase in gasoline consumption has caused, as a direct consequence, the production of more greenhouse gases, especially in large cities with millions of cars in use per day. There have been initiatives to reduce this consumption and pollution, which in addition to affecting the atmosphere, can affect human health; a national example is the "Hoy no circula" program, applied in Mexico City (the 16 municipalities) and in 18 municipalities of the State of Mexico. Such program consists of restricting the use of polluting cars certain days of the week, having a penalty or fine in case of disregarding the program (Comisión Ambiental de la Megalópolis, 2018). However, these same measures have boosted the alternatives that car manufacturers have designed: electric and hybrid cars, which are exempt from the program and can circulate any day of the week without any penalty (Baysan Quality Blog, 2019).

9.1.3 Electric cars

Electric cars, as their name suggests, are vehicles that run on electric energy, propelled only by a lithium electric motor. This type of motor eliminates the need for a fossil fuel for its operation, since they are powered by the electric energy stored in the battery. These batteries can be made of different materials and with different capacities, but they are all recharged by plugging the vehicle into the mains with an estimated full charge time of 6 to 8 hours or quick charges of 15 to 42 minutes, depending on the model, or by taking advantage of the braking energy. The regenerative braking system allows them to harness energy causing more energy efficiency (Díez González, 2019). Figure 9.3 shows the electric motor and its components.

Figure 9.3 Components of an electric motor



Source: (Díez González, 2019)

The energy efficiency of this type of motors is almost 75% compared to 25% of the rest of traditional vehicles, due to a decrease in energy loss and use during braking, which contributes to greater savings, in addition to eliminating the emission of polluting gases (Díez González, 2019).

Electric vehicles commonly use permanent magnet synchronous motors, which allow them to achieve efficient mobility. These motors work by transforming electrical energy into mechanical energy through electromagnetic rotation. The field excitation in synchronous motors comes from a small generator or other DC source. In this type of motor, the interaction between two magnets, which attract or repel depending on the alignment of their poles, generates a forward or backward displacement. (Bonfiglioli Riduttr Industrial, 2019).

As for permanent magnet electric motors, they typically use ferrite magnets attached to the rotor, resulting in energy efficiency and power density approximately 25% higher than conventional induction motors. When high-capacity neodymium magnets are used, performance can be increased by 50% to 100% compared to induction motors.

Permanent magnet synchronous motors rotate in synchrony with the power frequency and can generate any torque up to the motor's maximum. These motors, being permanently excited, respond optimally to load variations. A synchronous motor consists of a stator, which is a hollow, fixed cylinder responsible for transmitting motion to the rotor by generating a rotating magnetic field. The stator acts as a magnet whose polarity constantly changes to allow displacement. The synchronous speed, which corresponds to the speed of the rotating magnetic field, is a fundamental factor in its operation. On the other hand, the rotor is a cylinder that rotates inside the stator and is connected to the gears that drive the vehicle. The alignment of the rotor and stator poles causes the motor to stop. To keep the rotor in the stator in motion, the polarity of the rotor magnets is reversed by means of coils connected to a rotating collector. This configuration ensures that the magnetisms between the stator and rotor never align, thus allowing the rotor to continue spinning (Bonfiglioli Riduttr Industrial, 2019).

Fast charging of electric car batteries has been a significant challenge compared to the time required to fill a tank of gasoline in an internal combustion vehicle. However, significant advances in charging technology and networks have been made to improve the speed of charging electric vehicles. Fast charging, which takes place at high-powered charging stations, can charge an electric vehicle in a much shorter time, typically 30 minutes to an hour. On the other hand, this process can increase the temperature of the battery due to the intense energy flow, which can have a negative impact on long-term durability and accelerate battery degradation.

To address these challenges, automakers and charging companies are implementing measures to regulate battery temperature during fast charging and optimize thermal management systems. More advanced battery technologies are also being developed that can better withstand fast charging without compromising performance and lifetime.

In summary, fast charging offers shorter charging times for electric vehicles, but can affect battery life due to temperature rise. Efforts are underway to mitigate these effects through temperature regulation and the development of more advanced battery technologies (Stone, 2021).

9.1.4 Hybrid automobile

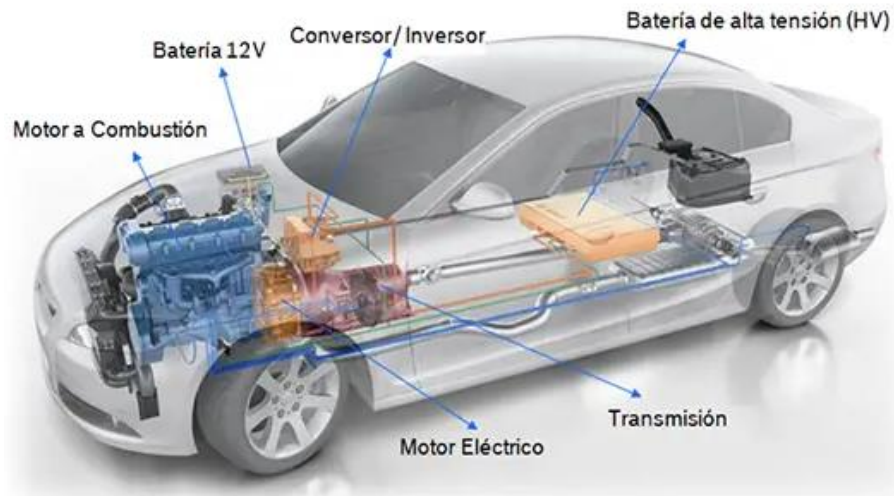
A hybrid vehicle combines an internal combustion engine with one or more electric motors to generate the necessary energy to propel the vehicle. The operation of a hybrid vehicle is integrated with a system known as "start-stop", which is responsible for turning the internal combustion engine on and off as needed.

The hybrid vehicle operates in different speed ranges for both engines: on short trips and at low speeds, the electric motor is the only one in operation, while on long trips and at high speeds, both engines work together.

An outstanding feature of the hybrid vehicle is the regenerative braking, which allows the battery of the electric motor to be recharged each time the vehicle is braked. This results in fuel savings of approximately 50% compared to a vehicle equipped only with an internal combustion engine. Unlike electric vehicles, hybrids do not need to be plugged in, as the internal combustion engine and regenerative braking allow efficient performance of the electric motor, which helps to significantly reduce gasoline consumption in urban environments.

The savings in pollutant emissions can reach up to 80% (Alfaro, 2022). The efficiency of these cars is higher on short trips in the city, where only the electric motor is used, resulting in lower fuel consumption (Antonio, 2022).

The internal combustion engine (ICE) of a hybrid vehicle is similar to that found in conventional vehicles and can be gasoline or diesel. The ICE is primarily used to charge the vehicle's battery and provide additional power when needed. During operation, the ICE can directly drive the wheels or recharge the battery. On the other hand, the hybrid vehicle's electric motor is powered by electricity stored in a battery. This electric power drives the vehicle at low speeds or acts as a backup to the ICE in situations of high power demand. In addition, the electric motor also acts as a generator by converting the vehicle's kinetic energy into electricity during braking or deceleration, through a process known as regenerative braking. The main components of this motor are shown in Figure 9.4.

Figure 9.4 Components of a hybrid car

Source: (Rodríguez, 2023)

The hybrid car uses the electric motor up to 60 km/h, if more power is needed the system activates the combustion engine, which is more effective at higher speeds.

The system of these cars detects when it is necessary to use an engine. While the gasoline engine is being used and the car is braking, at the moment of braking some energy is recovered from the electric motor, making its autonomy effective. (Toyota, 2021).

In this work, a comprehensive comparison of the best-selling cars of the three types of automobiles: gasoline, hybrid and electric, is made in order to provide the average consumer with a purchase recommendation based on individual needs. Through a detailed analysis and calculation of costs and travel times, the strengths and weaknesses of each option will be highlighted, thus providing a clear and complete view of the alternatives available in today's market.

9.2 Methodology to be developed

In this study, public information on sales in Mexico was used to determine consumer preferences in the last year with respect to the three types of vehicles available in the market: gasoline, electric and hybrid.

A comparative table between the cars investigated is presented in Table 9.2 below, with the data provided through each car's manual.

Table 9.2 Comparative table of cars

	Electric JAC e10X	Hybrid Toyota Prius	Gasoline Nissan Versa
Performance.	Batteries and motor (electrical to mechanical power)	Electricity, fuel (electrical and chemical to mechanical energy)	Fuel, (chemical to mechanical energy)
Efficiency.	75%	11%	25%
Weight (kg).	1555	1380	1104
Frontal area (m ²).	2.49	2.5	2.55
Estimated life time.	180000 km.	200.000 km.	250.000 km.

Source: (JAC, 2022), (Toyota, 2022), (Nissan, 2023)

Subsequently, a route of between 700 to 1500 km was selected, with an average duration of less than 24 hours, which stays within Mexico and presents different topographic conditions, such as ascents and descents. The route starts in Torreón, Coahuila, and with the help of the Google Maps tool (Google Maps, 2023) the best route for this trip was defined, as well as the sections to be analyzed and the average time of these sections for analysis. Data was collected on the differences in altitude on each section, as well as the average time and speed of travelers on each section, presented in Table 9.3.

Table 9.3 Path divided by the different altitudes, distance, time and average speed from each state to another

Section	Altitude difference (m)	Kilometers (km)	Total, Kilometers (km)	Hours	Speed (km/h)*	Speed (m/s)*
Coahuila to Durango	771	8	8	0.18	45	12.50
Durango to Zacatecas	545	174	182	1.82	95.4	26.50
Zacatecas to Aguascalientes	-555	268	450	2.96	90.4	25.11
Aguascalientes to Jalisco	530	101	551	1.12	90.4	25.11
Jalisco to Guanajuato	-690	80	631	0.88	90.4	25.11
Guanajuato to Querétaro	225	172	803	1.74	98.94	27.48
Querétaro to Tlaxcala	419	229	1032	2.31	98.94	27.48
Tlaxcala to Puebla	-104	84	1116	1.44	58.14	16.15

*With the approximate time to travel the distance given by Google Maps (Google Maps, 2023) and the measurement of this distance, the average speed of each journey could be calculated. Then a simple conversion from km/h to m/s was made.

Source: (Wikipedia, n.d.)

As a next step, it will be calculated how many stops will be made for gasoline and/or electric charging, using the performance information that the manufacturers of each vehicle have publicly available. To do this, first calculate the energy required for each car in each already defined trip; this with the help of Equation 5, of the total energy of a moving vehicle. It is important to keep the units homogeneous in order to obtain correct results. Equation 6 shows the units required to solve Equation 5.

$$E_T = \frac{kg \cdot (m/s)^2}{2} + (kg \cdot [m/s^2] \cdot m) + \frac{m^2 \cdot (m/s)^2 \cdot (kg/m^3) \cdot m}{2} + (kg \cdot [m/s^2] \cdot m) \quad (6)$$

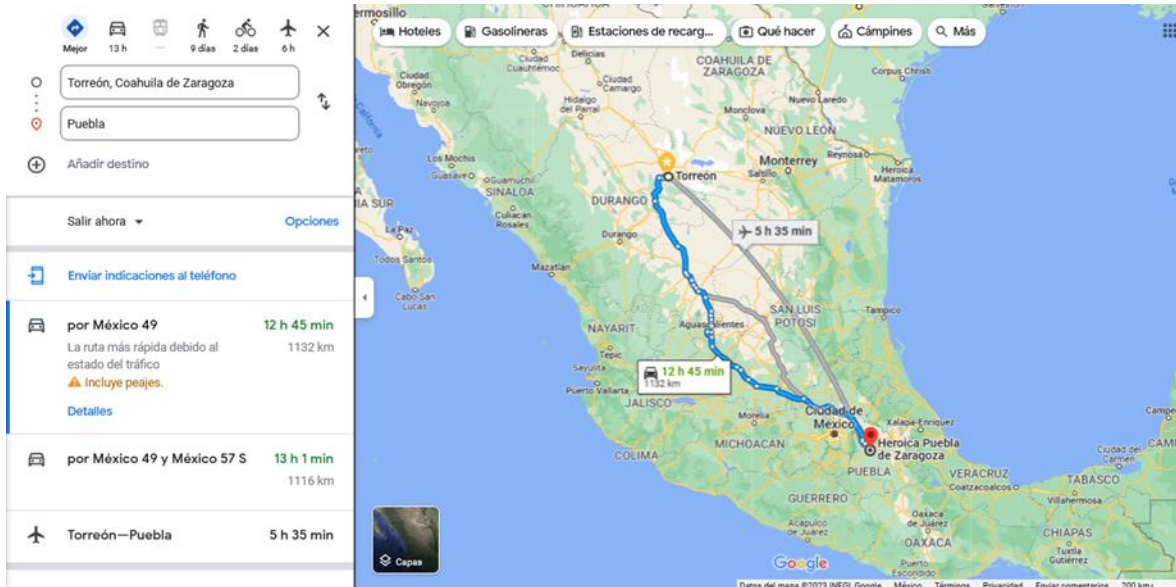
Once the amount of energy required for each section was obtained, it was evaluated whether each car was able to cover that energy with its performance and the energy available at the beginning of the section. In case a car was not able to cover the whole stretch, a stop was considered before reaching the minimum load level established. On the other hand, if the car was able to cover the required energy with the energy available at the beginning of the stretch, the amount of energy remaining in the car after the run was calculated, discounting the liters of gasoline or the percentage of battery used. In addition, the time required for each section and stop was estimated and added to the departure time of the three cars. However, in the event that the stops accumulated to a travel time of more than 20 hours at a time, a second calculation was considered, taking into account stops to sleep in a hotel, with average lodging costs at the point where the stop was made.

Finally, with the total number of stops necessary for the three cars to complete the same trip and the estimated time of arrival of each one, the costs associated with each car to complete the trip were calculated.

9.3 Results

This study compares the Nissan Versa (gasoline model), Toyota Prius (hybrid model) and JAC E10X (electric model) for the same route starting from Torreón, Coahuila to Puebla, Puebla. The approximate time taken by the Google Maps tool for this route is 12 hours and 45 minutes, for a total of 1116 km. Figure 9.5 shows a screenshot to demonstrate what the Google Maps tool shows when requesting a route from Torreón, Coahuila to Puebla, Puebla.

Figure 9.5 Screenshot, Torreon to Puebla Route



Source: (Google Maps, 2023)

To calculate the energy required of each car in each section of the route, in equations 1, 2 and 4 the mass of the vehicle along with the passengers must be taken into account. Noting that the capacity of the cars is 5 persons, a family of 5 persons was considered as the passengers for this trip. The average weights of a common family in Mexico (IMCO, Mexican Institute for Competitiveness, 2016) are presented in Table 9.4.

Table 9.4 Average passenger information

Passengers	Age	Average weight.
Child	2 years old	12 kg
Child	12 years old	41.5 kg
Youth	16 years old	58 kg
Adult	45 years old	71 kg
		Total: 253.5kg

Source: (IMCO, Mexican Institute for Competitiveness, 2016)

While Table 9.5 shows the additional data, necessary for the energy calculations presented in Equations 1, 2, 3 and 4.

Table 9.4 Required data

	Name	Dates
General	Gravity (m/s^2)	9.81
	Air density (kg/m^3)	1.225
	Drag coefficient (cars)	0.27
	Coefficient of friction (cars)	0.12
	Gasoline Efficiency (kWh/liter)	9
Total Yield (kWh)	Electric	31.4
	Hybrid	387
	Gasoline*	369
Weight (kg)	Passenger	253.5
	Electric	1555
	Hybrid	1380
	Gasoline	1104

*The kWh performance of the hybrid and gasoline model cars was obtained from the gasoline tanks that the manufacturer specifies for each car, multiplied by the energy yield per liter of gasoline (Table 1.2.2).

Source: (W. Sears, W. Zemansky, & Young, University Physics, Vol. 1., 2001), (Gencel, On "friction" in moving fluids and their solid boundary and on "lost" energy, 2012), (AVSLD International, 2013), (JAC, 2022), (Nissan, 2023), (Toyota, 2022)

The energy required for each trip was originally calculated in Joules. However, for the use of future calculations, the units of Joules were converted to kWh, taking into account the conversion of 1 Joule= 3600000 kWh. The result of this calculation for the three cars is shown in Table 9.5 The complete results (with Joules and km/kWh) can be found in Annex I).

Table 9.5 Energy required by the cars to be analyzed, according to the distance to be traveled

Section	Energy required (in kWh)		
	Gasoline	Electric	Hybrid
Coahuila to Durango	6.58	8.713	7.88
Durango to Zacatecas	93.70	119.739	109.56
Zacatecas to Aguascalientes	136.83	175.243	160.23
Aguascalientes to Jalisco	54.37	69.784	63.77
Jalisco to Guanajuato	38.99	49.838	45.60
Guanajuato to Querétaro	92.54	117.876	107.97
Querétaro to Tlaxcala	123.61	157.466	144.22
Tlaxcala to Puebla	39.52	51.735	46.98
Totals	586.14	750.39	686.2

Source: Own elaboration

Subsequently, the stops of each car along this route must be calculated. For this, two possible cases are considered:

- Case 1: The possible performance of the vehicle exceeds the energy demanded by the route, without exceeding a minimum limit of fuel/battery available. The minimums are: 10 liters of gasoline (for the internal combustion car and the hybrid) and 10% of battery (for the electric car).
- Case 2: The available energy of the vehicle is not enough to cover the energy cost of the trip. Then one or more stops must be considered to recharge the fuel or battery; as many stops as necessary to complete the stretch considered must be considered.

Based on these two cases, the initial and final liters/battery and their consumption in each section were calculated, in addition to the initial, final and consumed energy; as well as the time of the trip, considering an average time of 20 minutes for the gasoline refueling stops and approximately 42 minutes for the fast charging of the electric car. In addition, the Excel sheet divides the sub-sections of stops with initial kilometer and final kilometer, in order to know in which kilometer a charge should be made in each particular case. The complete tables, produced in Excel, will be available for review in Annex II.

Once the stops have been calculated, the geographical location of the stop made is obtained and the corresponding prices for the region are consulted to be taken into account in the cost calculation. In the case of the hybrid and internal combustion, the average price of gasoline in the different states where a stop was made was consulted. This price was then multiplied by the difference of the total tank capacity minus what was left in the tank at that stop, in order to obtain a car as full as possible for the next stop. Tables 9.6 and 9.7 below show the stops for the gasoline and hybrid car, along with a summary of the calculations made.

Table 9.6 Gasoline car analysis

Kilometer	Stop	Gas		Expense
		Location	Gasoline price*	
0	0	Torreón, Coahuila	\$ 21.25	\$ 871.25
450	1	Lagos de Moreno, Jalisco	\$ 21.87	\$ 677.97
1049	2	Villa Tezontepec, Hidalgo	\$ 21.26	\$ 670.27
Total, of Stops	2		Total	\$ 1348.24
Total hours			12.63	Days on the road
Departure Time	06:00:00 a. m.	Arrival time	06:37:38 p. m.	0.53

*Gasoline prices may vary from day to day, however, for these calculations, the prices in the localities corresponding to May 15, 2023 are taken into account.

Source: (Gasolina MX, 2023)

Note that a "zero" load is taken into account for the final price, which is the initial load, made before starting the trip. This load is a full tank load (equivalent to 41 liters), in order to obtain full capacity at the beginning of the trip. It was observed that, starting with a full tank, the first load should be made at kilometer 450, which is in Lagos de Moreno Jalisco; where 31 liters of gasoline should be loaded. The second stop is at kilometer 1049, in Villa Tezontepec, Hidalgo, where a refueling of 32 liters of gasoline is done.

Additionally, it is noted that, despite having two stops, the calculated time to complete this trip is around the 12 hours and 45 minutes that the Google Maps tool predicted for this trip (Google Maps, 2023).

Table 9.7 Hybrid car analysis

Kilometer	Stop	Hybrid Location	Gasoline price	Expense
0	0	Torreón, Coahuila	\$ 21.25	\$ 913.75
551	1	Encarnación de Díaz, Jalisco	\$ 22.55	\$ 855.51
803	2	Apan, Hidalgo	\$ 21.26	\$ 701.58
Total, Stops	2		Total	\$ 1557.09
Total Hours			13.13	Days on the road
Departure Time	06:00:00 a. m.	Arrival time	07:07:58 p. m.	0.55

*Gasoline prices may vary from day to day, however, for these calculations, the prices in the locations corresponding to May 15, 2023, are taken.

Source: (Gasolina MX, 2023)

For the analysis of the hybrid car, there is a great similarity with the analysis of the gasoline car, having a total of only two stops in the whole trip. In addition, a "zero" charge is also considered in which the 43-liter tank is filled before starting the trip. At the first stop there is a refueling of 38 liters of gasoline in Encarnación de Díaz, Jalisco. At the second stop, 33 liters of gasoline are refilled in Apan, Hidalgo. Note that, from the calculation of the energy required, the hybrid vehicle needs more energy than the gasoline model. This may be due to the weight of the car, thus affecting the amount of energy required to move the car over the same distance. However, this extra effort may also be reflected in the difference in the final costs of the analysis of the gasoline car and the hybrid.

On the other hand, it was noted that the calculation for the electric car was more extensive than the previous two, resulting in a travel time much longer than a day's travel or 20 hours of driving. The trip, considering only fast charges and assuming a continuous change of driver, takes 2 nights and 3 days of travel. For this reason, it was decided to do two analyses for the electric car: 1) Electric car analysis, considering only stops for fast charging. 2) Electric car analysis, considering slow and fast charging stops.

Assuming that there is indeed a family making this trip, it is most likely that the adults will opt to stay in a hotel along the way when it gets very late (around 10 pm). In this second analysis, it was considered that at the hotel they stay overnight there are slow charging stations to charge the car to 100% overnight. However, instead of considering only the 6 hours of charging needed for the vehicle, 8 hours of sleep were considered, taking into account that the family is mostly composed of minors.

Table 9.7 shows the summary of the calculations for the electric car analysis, considering only fast charging through the project.

Table 9.7 Electric car analysis, fast charging stops

State	Electric (fast charging stops)			Total hours
	# Quick stops	Parking price	Parking Expense	
Coahuila	0	\$ 22.5	0	56.00
Durango	6	\$ 15	\$ 90	Days on the road
Zacatecas	8	\$ 20	\$ 160	2.33
Aguascalientes	3	\$ 48	\$ 144	Departure time (1st day)
Guanajuato	2	\$ 42	\$ 84	06:00:00 a. m.
Querétaro	11	\$ 30	\$ 330	Arrival Time (3rd day)
Tlaxcala	1	\$ 30	\$ 30	10:36:40 a. m.
Total, Stops	31	Total, Parking	\$ 838	
Price Home Load (0%-100%)	\$89.77	Total, Expenses	\$ 927.77	

Source: (Federal Electricity Commission, 2023)

It is noted that the electric car requires up to 32 stops for a trip of 1116 km. Average parking costs in each state were considered, assuming that a parking lot with fast charging available existed at each point that a stop was to be made. In addition, a "zero" charge was also considered for the electric car. However, to make this calculation, the highest cost per kilowatt-hour was obtained from CFE, being \$ 2.859 Mexican pesos in DAC tariff for 2023 (Comisión Federal de Electricidad, 2023). Multiplying this price by 100% of the battery, we have a price of \$ 89.77 Mexican pesos. At the end, this is added to the total cost of expenses and results in a cost of \$927.77 Mexican pesos.

Similarly, Table 9.8 shows the summary of the calculations considering that, at 10:00 pm (except for the last day), the family would look for (and find) a hotel with car charging service. The price of the hotel was added to the cost to be considered.

Table 9.8 Electric car analysis, considering only slow and fast charging stops

State	Electric (slow and fast charging stops)			Total hours
	# Quick Stops	Parking Price	Parking Expense	
Coahuila	1	\$ 20.00	\$ 20.00	68.43
Durango	8	\$ 25.00	\$ 200.00	Days on the road
Zacatecas	4	\$22.00	\$ 88.00	2.85
Aguascalientes	3	\$ 21.00	\$ 63.00	Price Freight at Home (0%-100%)
Guanajuato	3	\$ 20.00	\$ 60.00	89.77
Querétaro	11	\$ 50.00	\$ 550.00	Departure time (1st day)
Tlaxcala	2	\$ 30.00	\$ 60.00	06:00:00 a. m.
Total, Stops	32	Total, Parking	\$ 1,041.00	Arrival Time (3rd day)
Slow load stops				10:51:23 p. m.
Kilometer	Location	Hotel price	Nights in hotel	
335	Fresnillo, Zacatecas	\$1,200.00	1	Total expense
709	San Luis de la Paz, Guanajuato	\$940.00	1	\$ 3,181.00

Source: Own elaboration

From Table 9.8 it is noted that there are a large number of total stops, so listing them is meaningless. However, Table 9.8 shows the most important stops in this second analysis: the slow-load stops, or sleep stops. These stops are important, as they comprise a large part of the expenditure considered for this analysis, as it considers the rental of two rooms in hotels in the given locations for the family of 5 (considered in this trip) to sleep.

Finally, a detailed comparison is made between the 4 analyses performed. This comparison is shown in Table 9.9.

Table 9.9 Final comparison of car analysis

Car Analysis	Gasoline	Hybrid	Electric (fast-charging stops)	Electric (slow and fast charging stops)	
Full load performance (kWh)	369.00	387.00		31.40	
Total energy required (kWh)	586.14	686.21		750.39	
Travel hours	12.63	13.13	56.00	68.43	
Charging time per stop (min)		20.0	1.0	360.0	
Days on the road	0.5	0.5	2.3	2.9	
Number of stops	2.0	2.0	31.0	31 (fast)	2 (slow)
Charge at the end (liters, % battery)	26.3	11.0	38%	44%	
Total cost	\$ 1,348.24	\$ 1,557.09	\$ 838	\$ 3,181.00	
Sales value	\$ 326,900.00	\$ 448,100.00		\$ 439,000.00	

Source: (JAC, 2022), (Toyota, 2022), (Nissan, 2023).

From this last comparison we noticed that the full-load performance of the gasoline and hybrid cars are more than ten times higher than the full battery charge of the considered electric car. However, the car that requires more energy to complete the stretch is just the electric car, due to its weight. Additionally, I noted that the cheapest car (sales value) and the one that takes the least time to complete the trip is the gasoline car. While the hybrid vehicle can compete with the time it takes to complete this trip, the retail value and total expense is much higher than the gasoline car. On the other hand, the electric car, despite being the slowest to complete the proposed route, when only fast charges are considered, is the car with the least mobility expenses on the trip.

Thanks to Table 9.9, the weaknesses and strengths of each car can be clearly seen. The gasoline car and the hybrid car are almost the same, as both use fossil fuel to meet their energy demands. This results in very similar times and consumption, with travel times and costs varying only slightly. On the other hand, the electric and its two analyses stand out from the same table as being so different. It is clear from the first data to compare that the electric is at a disadvantage, because while the other two vehicles have a performance capacity of more than 300 kWh, the battery of the electric only has 31.4 kWh of energy available. Based on this, the cost and time comparison, it can be stated that:

- The electric car is not recommended for long journeys, with prominent height differences and at high speeds. However, if a car is required to complete journeys at moderate speeds, within a city where there are no height differences or considerable reliefs, the electric car would be ideal. Considering that its full charge can be completed overnight, the additional cost on the electric bill for each 0-100% charge is \$89.77; a much lower cost than filling the tank of a hybrid or gasoline car.
- While the electric car analysis full of fast charges is the lowest cost, the batteries are not designed to withstand fast charges as often. It is likely that before completing the run, the battery will reach its limit and stop working.
- The hybrid car is as recommendable as the internal combustion car for long trips. The purchase decision between a hybrid and a gasoline car depends purely on the customer's preference and budget, because although the hybrid car integrates more technologies and has a greater performance capacity than the gasoline car, it is also more than \$100,000 Mexican pesos more expensive than the gasoline model.

9.4 Annexes

Annex I

Table 9.10 Calculation of energy required by vehicles in each stretch.

Section		Energy required								
		Gasoline			Electric			Hybrid		
		Joules	kWh	km/kWh	Joules	kWh	km/kWh	Joules	kWh	km/kWh
Coahuila to Durango		2.37E+07	6.58	1.22	3.14E+07	8.713	0.92	2.84E+07	7.88	1.01
Durango to Zacatecas		3.37E+08	93.70	1.86	4.31E+08	119.739	1.45	3.94E+08	109.56	1.59
Zacatecas to Aguascalientes		4.93E+08	136.83	1.96	6.31E+08	175.243	1.53	5.77E+08	160.23	1.67
Aguascalientes to Jalisco		1.96E+08	54.37	1.86	2.51E+08	69.784	1.45	2.30E+08	63.77	1.58
Jalisco to Guanajuato		1.40E+08	38.99	2.05	1.79E+08	49.838	1.61	1.64E+08	45.60	1.75
Guanajuato to Querétaro		3.33E+08	92.54	1.86	4.24E+08	117.876	1.46	3.89E+08	107.97	1.59
Querétaro to Tlaxcala		4.45E+08	123.61	1.85	5.67E+08	157.466	1.45	5.19E+08	144.22	1.59
Tlaxcala to Puebla		1.42E+08	39.52	2.13	1.86E+08	51.735	1.62	1.69E+08	46.98	1.79
Totals			586.14	1.85		750.39	1.44		686.2	1.57

Source: Own elaboration

Annex II

Table 9.11 Gasoline vehicle route.

Section		Km Initial	Final Km	Initial Liters	Gasoline Consumption	Final Liters	Gasoline			No. of Stops	Time (hours)	Start Time	End Time
							Initial Energy (kWh)	Consumption (kWh)	Final Energy (kWh)				
Coahuila to Durango		0	8	41.00	0.7	40.3	369.00	6.58	362.4	0	0.2	06:00:00 a. m.	06:10:40 a. m.
Durango to Zacatecas		8	182	40.27	0.7	39.5	362.42	93.70	268.7	0	1.8	06:10:40 a. m.	08:00:06 a. m.
Zacatecas to Aguascalientes		182.00	450	39.54	29.5	10.0	355.84	136.83	219.0	1	3.0	08:00:06 a. m.	10:57:59 a. m.
Aguascalientes to Jalisco		450.00	557	41.00	15.2	25.8	369.00	54.37	314.6	0	1.2	10:57:59 a. m.	12:08:40 p. m.
Jalisco to Guanajuato		556.50	629	25.80	6.0	19.8	232.17	38.99	193.2	0	0.8	12:08:40 p. m.	12:56:44 p. m.
Guanajuato to Querétaro		628.92	819	19.76	10.3	9.5	177.80	92.54	85.3	1	2.1	12:56:44 p. m.	03:02:46 p. m.
Querétaro to Tlaxcala		818.81	1049	41.00	10.3	30.7	369.00	123.61	245.4	0	2.3	03:02:46 p. m.	05:22:05 p. m.
Tlaxcala to Puebla		1048.55	1122	30.72	4.4	26.3	276.46	39.52	236.9	0	1.3	05:22:05 p. m.	06:37:38 p. m.
Section							Totales	586.14	Totales	2	12.6		

Source: Own elaboration

Table 9.12 Hybrid vehicle route

Section		Initial Km	Final Km	Initial Liters	Gasoline Consumption	Final Liters	Gasoline			No. de Paradas	Time (hours)	Start time	End time
							Initial energy (kWh)	Consumption (kWh)	Final Energy (kWh)				
Coahuila to Durango		0	8	41.00	0.7	40.3	369.00	6.58	362.4	0	0.2	06:00:00 a. m.	06:10:40 a. m.
Durango to Zacatecas		8	182	40.27	0.7	39.5	362.42	93.70	268.7	0	1.8	06:10:40 a. m.	08:00:06 a. m.
Zacatecas to Aguascalientes		182.00	450	39.54	29.5	10.0	355.84	136.83	219.0	1	3.0	08:00:06 a. m.	10:57:59 a. m.
Aguascalientes to Jalisco		450.00	557	41.00	15.2	25.8	369.00	54.37	314.6	0	1.2	10:57:59 a. m.	12:08:40 p. m.
Jalisco to Guanajuato		556.50	629	25.80	6.0	19.8	232.17	38.99	193.2	0	0.8	12:08:40 p. m.	12:56:44 p. m.
Guanajuato to Querétaro		628.92	819	19.76	10.3	9.5	177.80	92.54	85.3	1	2.1	12:56:44 p. m.	03:02:46 p. m.
Querétaro to Tlaxcala		818.81	1049	41.00	10.3	30.7	369.00	123.61	245.4	0	2.3	03:02:46 p. m.	05:22:05 p. m.
Tlaxcala to Puebla		1048.55	1122	30.72	4.4	26.3	276.46	39.52	236.9	0	1.3	05:22:05 p. m.	06:37:38 p. m.
							Totales	586.14	Totales	2	12.6		

Source: Own elaboration

Table 9.13 Electric vehicle route, fast charges

Section		Initial Kilometer	Final Kilometer	Hybrid		Initial Energy (kWh)	Consumption (kWh)	Final Energy (kWh)	No. of stops	Time (hours)	Start time	End Time	
				Gasoline consumption	Final Liters								
Coahuila Durango	to	0	8	43	0.9	42.1	387.00	7.88	379.1	0	0.2	06:00:00 a. m.	06:10:40 a. m.
Durango Zacatecas	to	8	182	42.1	12.2	30.0	379.12	109.56	269.6	0	1.8	06:10:40 a. m.	08:00:06 a. m.
Zacatecas Aguascalientes	to	182	450	30.0	17.8	12.1	269.55	160.23	109.3	0	3.0	08:00:06 a. m.	10:57:59 a. m.
Aguascalientes Jalisco	to	450	551	12.1	7.1	5.1	109.32	63.77	45.6	1	1.5	10:57:59 a. m.	12:25:01 p. m.
Jalisco Guanajuato	to	551	631	43.0	5.1	37.9	387.00	45.60	341.4	0	0.9	12:25:01 p. m.	01:18:07 p. m.
Guanajuato Querétaro	to	631	803	37.9	27.9	10.0	341.40	107.97	233.4	1	2.1	01:18:07 p. m.	03:22:25 p. m.
Querétaro Tlaxcala	to	803	1032	43.0	16.0	27.0	387.00	144.22	242.8	0	2.3	03:22:25 p. m.	05:41:17 p. m.
Tlaxcala Puebla	to	1032	1116	27.0	16.0	11.0	242.78	46.98	195.8	0	1.4	05:41:17 p. m.	07:07:58 p. m.
Totales							686.21	Totales	2	13.1			

Source: Own elaboration

Table 9.14 Electric vehicle path, slow and fast loads

Section	Initial Kilometer	Final Kilometer	Carga Inicial	Battery Consumption	Final Charge	Initial Energy (kWh)	Consumption (kWh)	Final energy (kWh)	No. of stops	Time (hours)	Start time	End time
Coahuila to Durango	0	8	100%	28%	72%	31.40	8.71	22.69	0	0.18	06:00:00 a. m.	06:10:40 a. m.
Durango to Zacatecas	8	13	72%	62%	10%	22.69	19.55	3.14	1	0.98	06:10:40 a. m.	07:09:10 a. m.
	13	45	80%	70%	10%	25.12	21.98	3.14	1	1.69	07:09:10 a. m.	08:50:34 a. m.
	45	77	80%	70%	10%	25.12	21.98	3.14	1	1.69	08:50:34 a. m.	10:31:57 a. m.
	77	108	80%	70%	10%	25.12	21.98	3.14	1	1.69	10:31:57 a. m.	12:13:20 p. m.
	108	140	80%	70%	10%	25.12	21.98	3.14	1	1.69	12:13:20 p. m.	01:54:43 p. m.
	140	172	80%	70%	10%	25.12	21.98	3.14	1	1.69	01:54:43 p. m.	03:36:07 p. m.
Zacatecas to Aguascalientes	172	182	80%	21%	59%	25.12	6.59	18.53	0	0.21	03:36:07 p. m.	03:48:53 p. m.
	182	205	59%	49%	10%	18.53	15.39	3.14	1	1.21	03:48:53 p. m.	05:01:25 p. m.
	205	239	80%	70%	10%	25.12	21.98	3.14	1	1.73	05:01:25 p. m.	06:45:02 p. m.
	239	273	80%	70%	10%	25.12	21.98	3.14	1	1.73	06:45:02 p. m.	08:28:39 p. m.
	273	306	80%	70%	10%	25.12	21.98	3.14	1	1.73	08:28:39 p. m.	10:12:17 p. m.
	306	340	80%	70%	10%	25.12	21.98	3.14	1	1.73	10:12:17 p. m.	11:55:54 p. m.
	340	374	80%	70%	10%	25.12	21.98	3.14	1	1.73	11:55:54 p. m.	01:39:21 a. m.
	374	407	80%	70%	10%	25.12	21.98	3.14	1	1.73	01:39:21 a. m.	03:23:08 a. m.
Aguascalientes to Jalisco	407	441	80%	70%	10%	25.12	21.98	3.14	1	1.73	03:23:08 a. m.	05:06:45 a. m.
	441	450	80%	19%	61%	25.12	6.00	19.12	0	0.21	05:06:45 a. m.	05:19:03 a. m.
	450	473	61%	51%	10%	19.12	15.98	3.14	1	1.23	05:19:03 a. m.	06:32:39 a. m.
	473	505	80%	70%	10%	25.12	21.98	3.14	1	1.69	06:32:39 a. m.	08:13:52 a. m.
	505	537	80%	70%	10%	25.12	21.98	3.14	1	1.69	08:13:52 a. m.	09:55:05 a. m.
	537	551	80%	31%	49%	25.12	9.84	15.28	0	0.32	09:55:05 a. m.	10:14:05 a. m.
	551	570	49%	39%	10%	15.28	12.14	3.14	1	0.97	10:14:05 a. m.	11:12:32 a. m.
Jalisco to Guanajuato	570	606	80%	70%	10%	25.12	21.98	3.14	1	1.76	11:12:32 a. m.	12:58:22 p. m.
	606	631	80%	50%	30%	25.12	15.72	9.40	0	0.56	12:58:22 p. m.	01:32:01 p. m.
	631	640	30%	20%	10%	9.40	6.26	3.14	1	0.48	01:32:01 p. m.	02:00:56 p. m.
	640	672	80%	70%	10%	25.12	21.98	3.14	1	1.69	02:00:56 p. m.	03:42:30 p. m.
	672	704	80%	70%	10%	25.12	21.98	3.14	1	1.69	03:42:30 p. m.	05:24:04 p. m.
Guanajuato to Querétaro	704	736	80%	70%	10%	25.12	21.98	3.14	1	1.69	05:24:04 p. m.	07:05:38 p. m.
	736	768	80%	70%	10%	25.12	21.98	3.14	1	1.69	07:05:38 p. m.	08:47:12 p. m.
	768	800	80%	70%	10%	25.12	21.98	3.14	1	1.69	08:47:12 p. m.	10:28:45 p. m.
	800	803	80%	5%	75%	25.12	1.72	23.40	0	0.06	10:28:45 p. m.	10:32:06 p. m.
	803	833	75%	65%	10%	23.40	20.26	3.14	1	1.56	10:32:06 p. m.	12:05:44 a. m.
	833	865	80%	70%	10%	25.12	21.98	3.14	1	1.69	12:05:44 a. m.	01:47:17 a. m.
	865	897	80%	70%	10%	25.12	21.98	3.14	1	1.69	01:47:17 a. m.	03:28:51 a. m.
	897	929	80%	70%	10%	25.12	21.98	3.14	1	1.69	03:28:51 a. m.	05:10:25 a. m.
	929	961	80%	70%	10%	25.12	21.98	3.14	1	1.69	05:10:25 a. m.	06:51:59 a. m.
	961	993	80%	70%	10%	25.12	21.98	3.14	1	1.69	06:51:59 a. m.	08:33:32 a. m.
Querétaro to Tlaxcala	993	1025	80%	70%	10%	25.12	21.98	3.14	1	1.69	08:33:32 a. m.	10:15:06 a. m.
	1025	1032	80%	17%	63%	25.12	5.32	19.80	0	0.16	06:51:59 a. m.	07:01:19 a. m.
	1032	1056	63%	53%	10%	19.80	16.66	3.14	1	1.28	07:01:19 a. m.	08:13:17 a. m.
	1056	1088	80%	70%	10%	25.12	21.98	3.14	1	1.69	08:13:17 a. m.	09:59:51 a. m.
Tlaxcala to Puebla	1088	1116	80%	42%	38%	25.12	13.10	12.02	0	0.61	09:59:51 a. m.	10:36:40 a. m.
	Total Consumption							766.70	Total, fast loads	34	56.00	

Source: Own elaboration

9.5 Acknowledgments

We express our deep appreciation to the Instituto Tecnológico de la Laguna for their invaluable support in providing us with their facilities, which allowed us to carry out our research and writing effectively.

9.6 Funding

This work has been funded by CONACYT [CVU 1271712].

9.7 Conclusions

In this work, a comparative analysis of three types of automobiles: gasoline, hybrid and electric, was carried out with the objective of providing the average consumer with a purchase recommendation based on their individual needs. The study focused on highlighting the strengths and weaknesses of each option, considering both long-distance performance and environmental impact.

By selecting the best-selling cars of each type in Mexico, a detailed analysis of their characteristics was carried out and compared in terms of efficiency, autonomy and associated costs. In addition, a route of more than 1000 km was selected, from Torreón, Coahuila, to Puebla, Puebla, to evaluate the performance of the vehicles in real conditions.

The results obtained revealed that, compared to gasoline-powered cars, hybrid vehicles are an option with similar performance on long trips. On the other hand, electric cars were not recommended for this type of trips due to their limitations in terms of autonomy and the availability of charging points along the route.

In conclusion, this study provides consumers with a solid and objective comparison of the different types of cars available in the market, allowing them to make informed decisions based on their mobility needs and environmental considerations. However, it is important to keep in mind that electric vehicle technology is constantly evolving, and it is possible that some of the limitations identified in this study will be overcome in the future.

As future lines of research, it is suggested to extend the comparative analysis to other car models and explore the long-term economic and environmental impact of each option. In addition, it would be relevant to investigate the development of charging infrastructures for electric vehicles and their influence on the viability of these cars on long trips.

9.8 References

- I. Alfaro, D. C. (2022). *Vehículo Híbrido*. Mexico: Gobierno de Mexico.
- II. Antonio, R. O. (2022). *Qué es un coche híbrido y como funciona exactamente*. Barcelona : Car And Drive.
- III. AVSLD International. (2013). *Coefficient of Friction*. (AVSLD INTERNATIONAL) Recuperado el 20 de Junio de 2023, de <https://avslid.com.sg/coefficient-of-friction/>
- IV. AVSLD International. (2013). *Coefficient of Friction*. (AVSLD INTERNATIONAL) Obtenido de <https://avslid.com.sg/coefficient-of-friction/>
- V. Baysan Quality Blog. (12 de Mayo de 2019). *La evolución del automóvil*. Recuperado el 20 de Junio de 2023, de Baysan "moving fleetng": <https://baysanquality.com/blog/la-evolucion-del-automovil/>
- VI. Bonfiglioli Riduttr Industrial. (2019). *Motores Sincronos de Imanes Permanentes de CA*. Recuperado el 15 de Junio de 2023, de Bonfigliogli, BMD: https://www.bonfiglioli.com/BMD%20Motores%20Sincronos%20de%20Imanes%20Permanentes%20de%20CA_SPA_R02_2.pdf
- VII. Comisión Ambiental de la Megalópolis. (25 de Marzo de 2018). *El programa Hoy No Circula se mantiene operando de manera normal*. Obtenido de Gobierno de México: Comisión Ambiental de la Megalópolis : <https://www.gob.mx/comisionambiental/articulos/el-programa-hoy-no-circula-se-mantiene-operando-de-manera-normal?idiom=es>
- VIII. Comisión Federal de Electricidad. (2023). *CFE: Tarifas, Hogar*. Obtenido de <https://www.cfe.mx/hogar/tarifas/Pages/Acuerdosdetarifasant.aspx>
- IX. Díez González, P. (Junio de 2019). Principios Básicos del Vehículo Eléctrico. *Principios Básicos del Vehículo Eléctrico*. Valladolid, España: Universidad de Valladolid, PAG 23. Recuperado el 22 de Junio de 2023, de <https://core.ac.uk/download/pdf/222807924.pdf>
- X. Gasolina MX. (15 de Mayo de 2023). *Precio de la Gasolina en México (estados y localidades)*. Recuperado el 15 de Mayo de 2023, de <https://www.gasolinamx.com/precio-gasolina>

- XI. Gencel, M. I. (Enero-Abril de 2012). Sobre “fricción” en fluidos en movimiento y en su frontera sólida y sobre la energía “perdida”. *La Habana*, 33, 30-36. doi:ISSN 1680-0338
- XII. Gencel, M. I. (2012). Sobre “fricción” en fluidos en movimiento y en su frontera sólida y sobre la energía “perdida”. *La Habana*, 33, 30-36.
- XIII. Google Maps. (11 de Junio de 2023). *Maps, ruta: Torreón-Puebla*. (Google) Recuperado el 2023, de Google Maps: <https://www.google.com/maps/dir/Torre%C3%B3n,+Coahuila+de+Zaragoza/Puebla,+Pue./@22.7076923,-102.6215643,7z/data=!4m13!4m12!1m5!1m1!1s0x868fdb9bb45b3fb:0x8bcc7a9970aea01d!2m2!1d-103.4067861!2d25.5428443!1m5!1m1!1s0x85cfc0bd5ebc7a3b:0x48a6461de494ad95!2m2>
- XIV. IMCO, Instituto Mexicano para la Competitividad A.C. (2022). *México anuncia el incremento de sus compromisos climáticos en la COP 27*. Instituto Mexicano para la Competitividad A.C. Ciudad de México: Instituto Mexicano para la Competitividad A.C. Recuperado el 22 de Junio de 2023, de <https://imco.org.mx/mexico-anuncia-el-incremento-de-sus-compromisos-climaticos-en-la-cop-27/>
- XV. IMCO, Instituto Mexicano para la Competitividad. (5 de Febrero de 2016). *¿Cómo es el Mexicano Promedio? vía el País*. Recuperado el 11 de Junio de 2023, de Instituto Mexicano para la Competitividad, IMCO: <https://imco.org.mx/como-es-el-mexicano-promedio-via-el-pais/>
- XVI. JAC. (2022). *Manual de Usuario E10X*. Recuperado el 11 de Junio de 2023, de JAC: <https://img.jac.mx/assets/manuales/MANUALDEUSUARIO/ManualdeUsuarioE10X.pdf>
- XVII. Nissan. (2023). *Manuales y guías Nissan*. Recuperado el 12 de Junio de 2023, de Nissan: <https://www.nissan.com.mx/content/dam/Nissan/mexico/manuals-and-guides/versa/2023/nissan-2023-versa-manual.pdf>
- XVIII. Rodríguez, J. L. (2023). *Cómo funciona un vehículo híbrido*. Obtenido de *Cómo funciona*: <https://como-funciona.co/vehiculo-hibrido/>
- XIX. Secretaria de Energia de la República de Argentina. (2003). *Conceptos sobre Energía*. Argentina: Secretaría de Energía. Recuperado el 20 de Junio de 2023, de https://www.energia.gob.ar/contenidos/archivos/Reorganizacion/contenidos_didacticos/publicaciones/conceptos_energia.pdf

Importance of the development of companies that manage government administrative services in support of the senior citizens of Villa Guerrero

Importancia del desarrollo de empresas gestoras de servicios administrativos gubernamentales en apoyo a los adultos mayores de Villa Guerrero

SUAREZ-ARIZMENDI, Brenda Yazmín†*, GONZALEZ-GUTIERREZ, Martin Fernando, SANCHEZ-DIAZ, Magali Yazmín and GARCIA-CASTILLO, Karla Yazmín

Tecnológico Nacional de México TECNM, adscripción Tecnológico de Estudios Superiores de Villa Guerrero Licenciatura en Administración

ID 1st Author: *Brenda Yazmín, Suarez-Arizmendi* / **ORC ID:** 0009-0005-0775-3982

ID 1st Co-author: *Martin Fernando, González-Gutiérrez* / **ORC ID:** 0009-0003-5772-7235

ID 2nd Co-author: *Magali Yazmín, Sánchez-Díaz* / **ORC ID:** 0009-0003-8210-0127

ID 3rd Co-author: *Karla Yazmín, García-Castillo* / **ORC ID:** 0000-0002-5463-1794, **CVU CONAHCYT ID:** 556904

DOI: 10.35429/P.2023.1.107.116

B. Suarez, M. González, M. Sánchez and K. García

* karla.gc@villaguerrero.tecnm.mx

Á. Marroquín, L. Castillo, J. Olivares and A. Álvarez (AA. VV.). Young Researchers. Engineering Applications - Proceedings-©ECORFAN-México, Queretaro, 2023.

Abstract

A Gestoría of Asistencia Pública is understood as a company that offers services of issuance of procedures with benefit to society, some for profit and other non-profit, because, governmental and non-governmental institutions constantly launch calls for support and projects in order to benefit the most vulnerable sectors of society, including the elderly, which by their physical condition, among other factors, are those who need these supports and fail to obtain them due to the disadvantages with which they have economic, social and even academic. In view of this, it was intended to evaluate the feasibility of the creation of specialized Gestorías to support these people in the municipality of Villa Guerrero, State of Mexico and thus emphasize the importance of its development through a quantitative methodology with a descriptive and correlational approach, collecting information through a questionnaire of dichotomous and multiple choice questions to test the hypothesis of the project, which is to demonstrate that the creation of "Gestoría de Asistencia Pública" companies will help older adults in the municipality of Villa Guerrero to obtain the support that is directed to them through the services offered by these, encouraging an improvement in the quality of life of these.

Governmental, Correlational, Institutions, Villa Guerrero, Seniors

10 Introduction

The design of management of governmental and non-governmental social programs does not usually take into account the knowledge and resources of the sector to which it is directed, causing the wasting of the opportunities that arise in favor of them or that many times they lose, because they do not know them since they do not have a correct training to carry out these procedures by themselves.

Therefore, from the above arises the need to create specialized management companies, in charge of supporting and assisting the people to whom these supports are directed, emphasizing the sector of the elderly at national level, since this sector lacks knowledge and means to carry out the procedures that correspond to them in health, social and financial matters in an individual way, due to the fact that this sector lacks knowledge and means to carry out the procedures that correspond to them in health, social and financial matters in an individual way, due to the fact that this sector lacks knowledge and means to carry out the procedures that correspond to them in a social and financial way, However, this is not always the case, and in view of this, the creation of public assistance agencies to support this sector and thus take advantage of the subsidies destined to them is evident.

This is because, currently in the municipality of Villa Guerrero, State of Mexico there are no organizations that are responsible for supporting the management of specialized governmental and non-governmental administrative procedures and has been observed as an area of opportunity unattended since there is an increasing number of older adults in the town and surrounding localities which causes that these people are not beneficiaries and therefore cannot improve their quality of life, and similar companies that do not offer procedures that benefit the community, if not simple procedures, leaving once again exposed the need for these companies.

Therefore, it is intended to prove that if a public assistance management company is created focused on helping the elderly of the municipality through personalized counseling with small recovery fees, this sector will be encouraged to carry them out.

10.0.1 Public administration management

From the vision of Serra (1981), Public Administration is the action of the State aimed at achieving its goals and to administer is to provide through public services to the interests of a society, and contrasting what Gabriela Mistral says, as quoted in Euroinnova.mx, (2022), highlights that the management is carried out in public agencies that with their resources, watch over the interests of citizens in terms of actions, goods to generate a common good with legal regulations.

Therefore, according to the previous concepts obtained, the concept of public assistance management is translated as that which is part of the same management that is carried out in the agencies, institutions, or public entities, with economic resources by members of the government or the same in specific, all this activity aimed at facilitating the perpetuation of society and create capacities for the development of the elements belonging to the administration.

10.0.2 Catalog of procedures

The word catalog comes from the Latin term catálogos and this in turn from the Greek Catálogos, where, as mentioned by Martínez de Sousa, it is the "set of descriptions, according to certain rules, of the bibliographic entries of the books and documents of a library, with the indication of the place they occupy in it" and let us not forget the definition of Trámite, which according to the author, Guillermo Cabanellas de Torres, provided by the Diccionario Jurídico Elemental comes "from the Latin trames, tramitis, way, passage from one part to another part; change from one thing to another".

10.0.3 Digital tramits

According to Heredia Jerez (2019), digital transformation a the "Constant and permanent process in time, which allows to radically change the value for the client, based on changes in the business model", likewise indicating that this process involves intensive use of innovation, change from the current culture to digital culture and implementation of new technologies, This being a permanent process in time without any return, before this can be conceptualized as digital procedures, the action that a user performs through the use of information technology and communication, in relation to a document or administrative record, without being physically present, and any action that a user performs to respond to that document or file by electronic means.

10.0.4 Seniors

The third age is the term with which we refer to the last decades of a person's life, this period is usually characterized by a decline in the physical and cognitive functions of the person.

According to the WHO, people between 60 and 74 years of age are considered old, from 75 to 90 years old or elderly, and those who exceed 90 years of age are called old, or long-lived. Any individual over 60 years of age will be called indistinctly a senior citizen.

The third age is the stage of human life that begins at approximately 65 years of age or older. This mark may vary according to the health conditions and well-being of the person, as well as according to his or her state of mind. (GERONTOLOGICA.COM, 2022).

10.0.5 Consulting

The consulting process is carried out when it is requested by the company or person (those in charge of the organization or company) and according to Alvarez Lopez (2005), the consulting process is known as an activity carried out by the consultant and the client in which they seek to solve the problems posed by the organization.

Taking this into account, it can be determined that the consulting process is the activity that together the consultant and the client solve the problems presented by the company, applying changes desired or suggested by the same auditors, the same chosen to be applied by the top management.

10.0.6 Consulting in Mexico

Consulting in Mexico is of great importance because through these, the applicants benefit thanks to the fact that with the advice they are able to solve their problems in different specific areas of an organization. The consultancy can be provided by a professional expert in the requested field, fulfilling the work indicated by the client.

On the other hand, the author Cuevas (2011), mentions that:

"a consultancy is a professional service which owners or owners, business managers, public officials, and even a single person, can resort to if they need help or advice in solving internal or external problems with their environment and business or market turn".

Consulting in Mexico is recognized because the high competitiveness among the different companies makes it necessary for them to optimize their resources to the maximum. For this reason, they are usually recommended in various areas of work to squeeze business productivity and thus consulting (Torres, 2020).

Now, we can refer to consulting in Mexico as an indispensable service to optimize to the maximum the resources available to organizations. This makes it advisable for different types of organizations to improve productivity and business efficiency.

10.0.7 Consulting in Villa Guerrero

The consultancy in Villa Guerrero fulfills and exercises in many places, but where it stands out more in the H. City council and establishments on the part of the government that fulfill the function of working publicly, and other services related to it.

In addition, it is mentioned that consulting is not only exercised in the government sphere, but also by individuals or private companies, with a certain profession and specialty in it through a different variety of means.

Consulting in the municipality of Villa Guerrero, may not be very marked in a professional way, however, it exists in various activities, which are carried out by the residents of this municipality.

According to IEEM, Villa Guerrero:

"it is a municipality where the residents, seek to develop in all areas; economic, cultural, political among others, they are enterprising and proactive people, there are companies such as; consultancies, specialized service agencies and offices, cyber, stationery stores, among others where the consulting activity is provided".

According to the previous concept, a consultancy is of great importance, since through these more opportunities are taken advantage of and it is possible to highlight beneficial facts and growth in the different organizations of the municipality.

10.0.8 Consultancy administrative services

The administrative services in the consultancies comply with a great number of lists and variety depending on the branch they belong to.

According to Euroinnova (2022), it is mentioned that the administrative consultancy "is a consultancy performed so that a company can improve its capabilities and performance in a beneficial way, providing this service, as well as the same seeks to solve needs or problems determined by the company, institution or entity improving the quality of services and processes". On the other hand, we have as the administrative consulting services to the advice by specialists on issues of a company. This to provide solutions to present or potential conflicts.

10.0.9 Consultancy administrative services

The administrative services in the consultancies comply with a great number of lists and variety depending on the branch they belong to.

According to Euroinnova (2022), it is mentioned that administrative consultancy

"is a consultancy performed so that a company can improve its capabilities and performance in a beneficial way, providing this service, as well as the same seeks to solve needs or problems determined by the company, institution or entity improving the quality of services and processes".

On the other hand, we have as the administrative consulting services to the advice by specialists on issues of a company. This is in order to provide solutions to present or potential conflicts. With this we can affirm that a consultancy is of great help to those who need it, since it seeks to satisfy the needs of the client in the best way by solving their problems, affirming this with what Vsiconsulting, mentioned when it highlights that consultancy can help to improve a business and a person in many aspects since administrative services encompass different processes. Therefore, it can be said that the administrative services of consultancies are somewhat more complete and fulfill a broader function in terms of the client's request, solving their needs.

10.0.10 Access to digital media in communities

Access to digital media in communities today is the order of the day, as it is a fundamental element in many factors. According to ECLAC (2020), Information and Communication Technologies ICT are:

"tools that represent a set of technologies, to present and work information digitally use a code called bit. Within the framework of the information society, the level of penetration of goods and services linked to ICTs or information and communication technologies in households is undoubtedly the starting point for promoting public policies that encourage digital connectivity".

And it has been observed that in rural and indigenous communities there is little access to this type of tools however, this is already part of the daily life of those who live in these areas, since on the other hand, INFOTEC (2019), mentions that:

"despite the fact that rural and indigenous communities have little access to information and communication technologies (ICT), computers, cell phones and social networks are part of the daily lives of young students, influencing their social practices, their ways of relating and their collective and individual identities".

The use of ICT in communities is a favorable element for individual and collective development because making use of ICT in these, becomes an individual contribution that brings different positive factors in the social and emotional development of the individual, for many different reasons; but in relation to the participation of this process in the communities, the results generate collectively and integrally favorable elements in all the members who participate in it (Euroinnova 2022).

With the above information provided, it is possible to understand that access to digital media in the communities is of great importance and despite the distinctive features between one and the other, these media have perpetuated in most of the communities, have perpetuated in most of them since they are considered indispensable for certain types of activities.

10.0.11 Digital information in communities

The topic of digital information in the communities becomes a more complete topic as "digital community" since it should not be forgotten that thanks to technology the communication gap between people from different communities, states, countries, can be connected regardless of the distance, because its scope is very large. Currently, the Internet and ICTs have become indispensable in people's lives, a clear example is the Internet, which has become an undeniable force in everyday life and important efforts are made to bring access to the most remote communities and give them the opportunity to connect with the possibilities it offers in terms of knowledge, entertainment, and communication among others.

Digital information in communities in other terms is known as community digital literacy, giving way to digital inclusion, and with it the passage of digital information, so it can be summarized that digital information in communities is one that has been leaving a mark on the civilization of those involved, as it generates intellectual growth of the population and environment in which they develop.

10.0.12 Access to digital procedures for seniors

Currently, the management of various digital procedures is usually designed in an inclusive manner, for the benefit of different vulnerable sectors of society, such is the case of older adults who indirectly allow access to these, for their benefit, because the new technologies and platforms have been conceived and designed from an adult-centric perspective (Robles 2022).

Speaking of procedures and digitization, it is observed that they are usually carried out more easily by digital means, however, the elderly have some difficulty in relating to it. As mentioned by Honorable Concejo Deliberante (2022) "as users of information and communication technologies (ICT), older adults have needs and demands similar to those of people of other ages, i.e., that is to say, older adults are more likely to use digital technologies than those of people of other ages.

They require useful, functional, easy to handle and meaningful technology", to be able to use it for them, so the elderly must adapt to these digital media, because an important point is that they need to be able to adapt to these technologies.

Digital media, because an important point mentioned by Zambrano (2020), the sector of older adults is growing so it is necessary the growing and massive incorporation of ICT in society, so that they move in parallel and interact more, to the point of integration.

The objective is to address digital inclusion as a contributing alternative in the process of active aging, since this benefits in a notorious way to those who need it most, making their lives easier and more skillful. Incorporating the elderly into the information and knowledge societies.

10.1 Methodology to be developed

This study will make use of a mixed method since, as mentioned by Hernández (2002), it is a process that collects, analyzes, and pours quantitative and qualitative data in the same study. Therefore, this method will be used by employing interviews, surveys, documents and Internet pages. It will have a descriptive research approach since, according to Sampieri, descriptive research is a scientific procedure, a systematic process of inquiry, collection, organization, analysis and interpretation of information or data on a given topic. In view of this, information will be collected from the marginalized communities of the Municipality of Villa Guerrero where a record, analysis and interpretation of the current nature and the composition or processes of the phenomena will be made. Likewise, information on the nature and phenomena of the Municipality of Villa Guerrero will be analyzed.

In addition to using a correlational study which, according to Sampieri, is carried out when the treatment variables cannot be manipulated for different reasons, either physically, illegally or unethically, and this type of research starts from the fundamental in its operation and is related to variables in terms of the target, since it focuses on the elderly, and within its characteristics, it cannot lend itself to the analysis of the variables. of this analysis, it cannot lend itself to manipulation of their ways of being or simply their characteristics.

The population for this project is the municipality of Villa Guerrero and its neighboring towns, rancherías and communities such as Buenavista, Cantarranas, San Felipe, El progreso, La Finca, El Islote, San Lucas, Totolmajac, El Ejido, with an approximate population of 69,086 inhabitants according to the last census conducted by INEGI in 2020.

As for the sample, we only plan to apply the data collection instrument to the population made up of older adults aged 60 and over, which was obtained through simple random probability sampling using a statistical equation with an error of .5 and a degree of reliability of 95%, resulting in a sample of 382 people.

10.2 Results

To obtain data, an open-ended questionnaire of 12 questions was used, due to the target segment (older adults), which was analyzed by means of qualitative content analysis and a quantitative analysis in Excel and SPSS to facilitate the descriptive and correlational analyses that were carried out.

The results are presented below:

10.2.1 Descriptive analysis

The total number of respondents was 404 people of the ages of 60-64 years with 75 people, 65-69 years with 132 responses, 70-74 years with 137 and 75-79 with 52, where it was possible to visualize that the highest percentage is occupied by 33.9 percent with the ages of 70 to 74 years, which establishes the most prevalent age in the municipality of Villa Guerrero and the target segment for the Assistance Management Companies.

The highest percentage was 33.9 percent of respondents between the ages of 70 and 74, which establishes the most prevalent age group in the municipality of Villa Guerrero and the target segment for the public assistance management companies.

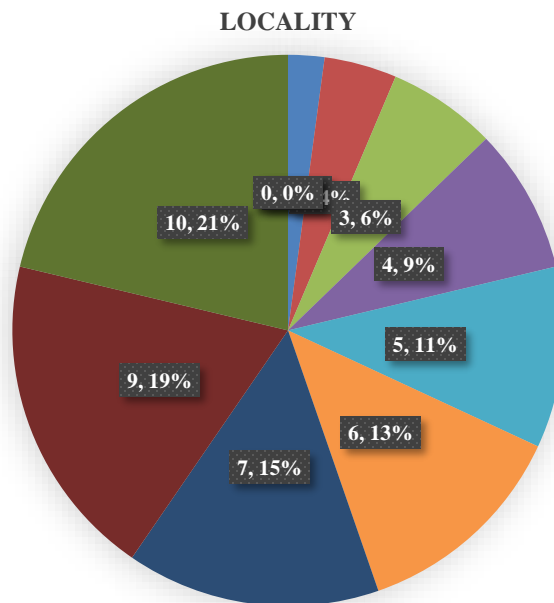
Table 10.1 Age

		AGE			
		Frequency	Percentage	Valid Percentage	Cumulative Percentage
Valid	60-64	75	18.6	18.9	18.9
	65-69	132	32.7	33.3	52.3
	70-74	137	33.9	34.6	86.9
	75-79	52	12.9	13.1	100.0
	Total	396	98.0	100.0	
Lost	System	8	2.0		
Total		404	100.0		

Source: Own elaboration

The localities of the municipality of Villa Guerrero that randomly participated were: the municipal seat with a result of 48 responses, as number two the locality of San Francisco with a result of 35 responses, number 3 Santiago with 48 responses, 4 San Felipe with 41 responses, 5 Buenavista with 96 responses with the highest rate of 23.8%, 6 Ejido de la Finca with 28 responses, the same tied with the locality of La Valenciana that occupies place 7, and highlighting the lowest localities with 22 responses to San Miguel and San Lucas occupying place 7. 8%, 6 Ejido de la Finca with 28 answers, same tied with the locality of La Valenciana that occupies the place 7 and highlighting the lowest localities with 22 answers to San Miguel and San Lucas occupying a percentage of 5.4% and as final part in other 50 answers with localities not named in the list.

Graphic 10.1 Localities



Source: Own elaboration

The results obtained to the question "Have you carried out a governmental procedure by yourself? with a percentage of 59.4% answered YES, taking into account the complete answer YES, giving examples of the most performed procedures are issuance of CURP, birth certificate and procedures related to INAPAM and the answer NO with 38.6%, resulting that most of the adults do perform this type of governmental procedures, obtaining as a result that 53.5% of the people of the localities of the municipality of Villa Guerrero DO have some governmental or other organization support and 44.6% of the people of the municipality of Villa Guerrero DO have some governmental or other organization support. This data reflects indicators of opportunity to cover 100% of older adults, who can be advised or accepted to obtain some type of support, considering the 44.6% who do not enjoy these opportunities, without neglecting those who already receive it.

In addition to highlighting that in the question "Do you turn to someone when you need to carry out a procedure?", it is evident that 80% of the sample of older adults DO turn to someone to carry out their procedures and 20% usually do it alone, which leads us to the next question where it was asked if in their community there is an organization in charge of supporting them in carrying out these procedures, which 54% answered NO, which opens the possibility of acceptance of the public assistance management companies.

This was reaffirmed with the last question, where it was asked, "If there were a company that provides the necessary help and assistance in terms of procedures and services to facilitate access to these, would you approach it?", with a positive indicator of 70.5% of answers with the term YES, which indicates acceptance and success for these companies.

10.2.2 Correlation analysis

Table 10.2 Positive correlations

CORRELACION		
		¿Is there any service in your area that provides assistance in carrying out any procedure?
¿Do you have any governmental or other organization support?	Pearson's Correlation	.417"
	Sig. (Bilateral)	
	N	
		¿ Do you turn to someone when you need to carry out a procedure?
If there were a company that provided the necessary help and assistance in terms of procedures and services to facilitate access to them, would you approach it?	Pearson's Correlation	.673"
	Sig. (Bilateral)	
	N	

Source: Own elaboration

In the previous table we can observe the significant correlations of some variables that are of utmost importance for the feasibility of the Public Assistance Management companies, using Pearson's correlation coefficient, which indicates that if there is a perfect positive correlation resulting in $r=1$, it indicates a total dependence between the two variables called direct relationship: when one of them increases, the other also increases in a constant proportion. But if $0 < r < 1$, then there is a positive correlation and if $r = 0$, then there is no linear relationship, but this does not necessarily imply that the variables are independent, if $-1 < r < 0$, there is a negative correlation and finally if $r = -1$, there is a perfect negative correlation. The index indicates a total dependence between the two variables called inverse relationship: when one of them increases, the other one decreases in constant proportion. (Vinuesa, 2016).

The result was that the question, "If there were a company that provided the necessary help and assistance in terms of procedures and services to facilitate access to them, would you approach it?" is directly related to the question, "Are you interested in professional help to assist you in making a registration or obtaining some support?" where a correlation of .673 was observed, which shows the interest of the older adult population in being attended with professional help, which is an indicator of opportunity for companies dedicated to providing public assistance services to older adults in the municipality.

On the other hand, the correlation .417 is obtained, referring to the following variables with bilateral correlation, do you have any governmental support or from another organization? and in your locality is there any service that offers help to carry out any procedure, which show the existence of organizations that offer advisory services with help in the elaboration of procedures, so that the adult population.

10.3 Conclusions

Regulating and guaranteeing equitable access to basic social processing services, as well as the assistance and adequate collection of documents should be the objective of governments for the execution of any procedure to be carried out, however it was observed that this is not the case, since there are vulnerable sectors such as the elderly who cannot access certain procedures that are usually government subsidies due to various factors, including lack of information, access to digital media, among others.

This opens a gap of opportunity for the creation of companies dedicated to offer public assistance services for the execution of various procedures that help to have a better quality of life to the mentioned sector, reaffirming with this research that resulted in the creation of such specialized companies would be accepted positively by this sector, with a degree of feasibility of more than 80%, to achieve that 100% of the sample studied achieve access to the subsidies offered by various entities, In addition, according to previous research, in a few years this sector will be the one with the highest population index, offering another reason to engage in this type of business and together to comply with one of the sustainable development goals of the 2030 agenda, which mentions that actions must be taken to reduce social inequalities, so here lies the importance of creating businesses that offer inclusion to vulnerable sectors of the population.

10.4 Funding

This work has been funded by TECNM Adscripción Tecnológico de Estudios Superiores de Villa Guerrero.

10.5 References

Alvarez López, L. F. (5 de junio de 2005). *El proceso de consultoría organizacional*. Obtenido de Gestipolis: <https://www.gestipolis.com/el-proceso-de-consultoria-organizacional/>

Arroyave Zambrano, P. M., Ocampo Arias, J., Sánchez Velásquez, S. P., & Antonio Vega, O. (2020). Digital Inclusion as a contributory alternative to active aging. *E-Ciencias de la Información*, 10(2), 123-136. doi:<https://doi.org/10.15517/eci.v10i2.39522>

CEPAL. (2020). *Revolución tecnológica e inclusión social*. Obtenido de CEPAL: https://www.cepal.org/sites/default/files/publication/files/45901/S2000401_es.pdf

Cuevas, M. R. (2011). *Definición de Consultoría*. Obtenido de Academia Comunidad Digital de Conocimiento: <https://revistaconsultoria.com.mx/que-es-consultoria/>

Euroinnova.mx. (23 de Noviembre de 2022). *Que es y para que sirve la gestion administrativa*. Obtenido de Euroinnova.mx: <https://www.euroinnova.mx/que-es-y-para-que-sirve-la-gestion-administrativa>

- GERONTOLOGICA.COM. (11 de octubre de 2022). *Tercera edad*. Obtenido de Genterologica: <https://www.gerontologica.com/articulo-interes/tercera-edad-concepto>
- Heredia Jerez, R. (2019). *Ecosistemas Digitales, la revolución de todas las industrias*. Digital Mart Ltda.
- Hernandez, R., & Fernandez Baptista, I. (2002). *Metodología de la Investigación*. Ciudad de México: Mc Graw Hill.
- Honorable Concejo Deliberante. (20 de Octubre de 2022). *RESOLUCIÓN N° 4.112 / 2.022*. Obtenido de Honorable Concejo Deliberante Junín Mendoza: <https://hcdjunin.gob.ar/wp-content/uploads/2023/04/res224112-Programa-Digital-Adultos.pdf>
- IEEM. (2019). *Plataforma Electoral Villa Guerrero*. Obtenido de IEEM: https://www.ieem.org.mx/maxima_publicidad/maxima17_18/InfGral/PLATAFORMAS-2018/docs/Plataformas_Mpales/PRI/114_Villa_Guerrero.pdf
- INEGI. (16 de marzo de 2020). *Censo Nacional de Población y Vivienda*. Obtenido de INEGI: <https://www.inegi.org.mx/programas/ccpv/2020/>
- Maximino, M. R., & Rodrigo, R. A. (2012). *Acceso y uso de las TIC en áreas rurales, periurbanas y urbano-marginales de México: Una perspectiva Antropologica* (Primera ed.). México: Fondo de Información y Documentación para la Industria (INFOTEC). Obtenido de <https://www.infotec.mx/work/models/Infotec/Publicaciones/Acceso-uso-de-TIC-areas-rurales-periurbanas-urbano-marginales-de-Mexico-una-perspectiva-antropologica.pdf>
- Organizacion Mundial de la Salud OMS. (1 de octubre de 2022). *Envejecimiento y salud*. Obtenido de Organizacion Mundial de la Salud OMS: <https://www.who.int/es/news-room/fact-sheets/detail/ageing-and-health>
- Robles, D. (25 de Agosto de 2022). *Se profundiza la brecha digital en la tercera edad*. Obtenido de Gaceta UNAM : <https://www.gaceta.unam.mx/se-profundiza-la-brecha-digital-en-la-tercera-edad/>
- Serra Rojas, A. (1981). *Derecho Administrativo*. Ciudad de México: porrua.
- Torres Paniagua, A. I. (13 de Septiembre de 2020). *IMPORTANCIA DE LA CONSULTORÍA EN MÉXICO, SU DESARROLLO Y APLICACIÓN EN LAS EMPRESAS PYMES*. Obtenido de Studocu: <https://www.studocu.com/es-mx/document/instituto-tecnologico-de-la-laguna/laboratorio-integral/ensayo-importancia-de-la-consultoria-en-mexico-su-desarrollo-y-aplicacion-en-las-empresas-pymes/9472140>
- Universidad Latina de Costa Rica. (8 de enero de 2023). *Importancia de la gestión administrativa en una empresa*. Obtenido de Universidad Latina de Costa Rica : <https://www.ulatina.ac.cr/articulos/importancia-de-la-gestion-administrativa-en-una-empresa>
- Vinuesa, P. (2016). Tema 8 - Correlación: teoría y práctica. En *Estadística*. Mexico: CCG-UNAM.
- VSI Consulting. (s.f.). *Qué es una Consultoría y qué servicios legales ofrece*. Obtenido de VSI Consulting Consultores en Internacionalización: <https://www.vsiconsulting.net/consultoria-y-sus-servicios-legales/>

Instructions for Scientific, Technological and Innovation Publication

[Title in Times New Roman and Bold Type No. 14 in English and Spanish]

Last Name (IN CAPITAL LETTERS), First Name of 1st Author†*, Last Name (IN CAPITAL LETTERS), First Name of 1st Co-Author, Last Name (IN CAPITAL LETTERS), First Name of 2nd Co-Author and Last Name (IN CAPITAL LETTERS), First Name of 3rd Co-Author.

Author's Institution of Affiliation including dependency (in Times New Roman No.12 and Italics)

International Identification of Science - Technology and Innovation

1st Author ID: (ORC ID - Researcher ID Thomson, arXiv Author ID - PubMed Author ID - Open ID) and CVU 1st Author: (Scholar-PNPC or SNI-CONAHCYT) (No.10 Times New Roman)

1st Co-author ID: (ORC ID - Researcher ID Thomson, arXiv Author ID - PubMed Author ID - Open ID) and CVU 1st Co-author: (Grantee-PNPC or SNI-CONAHCYT) (No.10 Times New Roman)

2nd Co-author ID: (ORC ID - Researcher ID Thomson, arXiv Author ID - PubMed Author ID - Open ID) and CVU 2nd Co-author: (Scholar-PNPC or SNI-CONAHCYT) (No.10 Times New Roman)

3rd Co-author ID: (ORC ID - Researcher ID Thomson, arXiv Author ID - PubMed Author ID - Open ID) and CVU 3rd Co-author: (Grantee-PNPC or SNI-CONAHCYT) (No.10 Times New Roman)

(Indicate Date of Submission: Month, Day, Year); Accepted (Indicate Date of Acceptance: Exclusive Use by ECORFAN)

Citation: First letter (IN CAPITAL LETTERS) of the Name of the 1st Author. Last Name, First Letter (IN CAPITAL LETTERS) of the 1st Co-author's Name. Last name, first letter (IN CAPITAL LETTERS) of the 2nd Co-author's name. Last Name, First Letter (IN CAPITAL LETTERS) of the Name of the 3rd Co-author. Last name

Institutional Mail [Times New Roman No.10].

First letter (IN CAPITAL LETTERS) of the Name Editors. Surname (eds.) *Title of the Proceeding [Times New Roman No.10]*, Selected Topics of the corresponding area ©ECORFAN-Filial, Year.

Abstract

Text written in Times New Roman No.12, single spaced, in English.

Indicate (3-5) keywords in Times New Roman and Bold No.12.

1 Introduction

Text written in Times New Roman No.12, single spaced.

Explanation of the topic in general and explain why it is important.

What is its added value with respect to other techniques?

Focus clearly on each of its characteristics.

Clearly explain the problem to be solved and the central hypothesis.

Explanation of the sections of the Chapter.

Development of Sections and Sections of the Chapter with subsequent numbering.

[Title in Times New Roman No.12, single space and Bold].

Development of Chapters in Times New Roman No.12, single space.

Inclusion of Graphs, Figures and Tables-Editables

In the content of the Chapter, all graphs, tables and figures must be editable in formats that allow modifying size, type and number of letters, for editing purposes, these must be in high quality, not pixelated and must be noticeable even if the image is reduced to scale.

[Indicating the title in the upper part with Times New Roman No.12 and Bold, indicating the font in the lower part centered with Times New Roman No. 10].

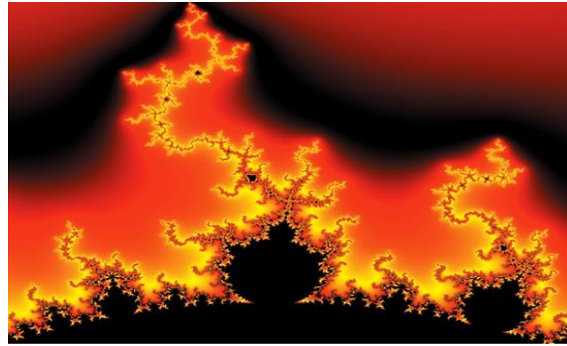
Table 1.1 Title

Variable	Description	Value
P ₁	Partition 1	481.00
P ₂	Partition 2	487.00
P ₃	Partition 3	484.00
P ₄	Partition 4	483.50
P ₅	Partition 5	484.00
P ₆	Partition 6	490.79
P ₇	Partition 7	491.61

Source:

(They should not be images, everything should be editable)

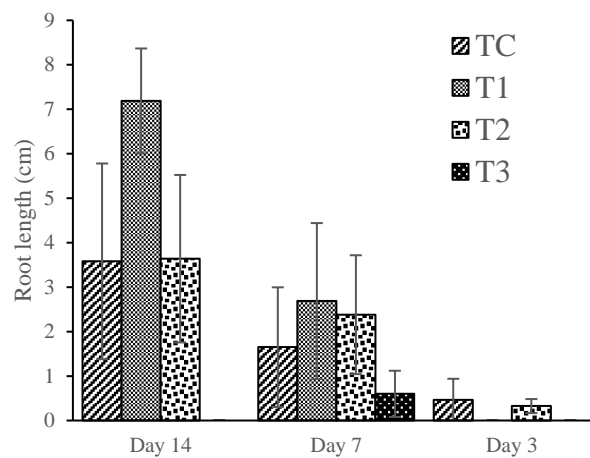
Figure 1.1 Title



Source:

(They should not be images, everything should be editable)

Graphic 1.1 Title



Source:

(They should not be images, everything should be editable)

Each Chapter should be presented separately in **3 Folders**: a) Figures, b) Graphs and c) Tables in .JPG format, indicating the number in Bold and the sequential Title.

For the use of Equations, indicate as follows:

$$\int_{lim^{-1}}^{lim^1} = \int \frac{lim^1}{lim^{-1}} = \left[\frac{1(-1)}{lim} \right]^2 = \frac{(0)^2}{lim} = \sqrt{lim} = 0 = 0 \rightarrow \infty \quad (1)$$

They should be editable and with numbering aligned on the far right.

Methodology to be developed

Give the meaning of the variables in linear wording and it is important to compare the criteria used.

Results

The results should be per section of the Chapter.

Annexes

Tables and appropriate sources.

Acknowledgements

Indicate if they were financed by any Institution, University or Company.

Conclusions

Clearly explain the results obtained and the possibilities for improvement.

References

Use the APA system. They should not be numbered or bulleted, however, if numbering is necessary, it will be because there is a reference or mention in some part of the Chapter.

Technical Data Sheet

Each Chapter should be presented in a Word document (.docx):

Name of the Handbook

Title of the Chapter

Abstract

Keywords

Sections of the Chapter, e.g:

1. *Introduction*
2. *Description of the method*
3. *Analysis based on demand curve regression*
4. *Results*
5. *Acknowledgement*
6. *Conclusions*
7. *References*

Name of Author(s)

Correspondence E-mail to Author

References

Intellectual Property Requirements for its edition:

- Author's and co-authors' autographic signature in blue colour of the originality form.
- Author's and co-authors' autographic signature in blue colour of the author and co-authors' acceptance form.
- Authentic Signature in blue colour of the Conflict of Interest Format of Author and Co-authors

Reservation to the Editorial Policy

ECORFAN Proceedings reserves the right to make any editorial changes required to bring the Scientific Work into compliance with the ECORFAN Proceedings Editorial Policy. Once the Scientific Work has been accepted in its final version, ECORFAN Proceedings will send the author the proofs for review. ECORFAN® will only accept the correction of errata and errors or omissions arising from the editing process of the journal, reserving in its entirety the rights of authorship and dissemination of content. Deletions, substitutions or additions that alter the formation of the Scientific Work will not be accepted.

Code of Ethics - Good Practices and Statement of Solution to Editorial Conflicts

Declaration of Originality and unpublished character of the Scientific Work, of Authorship, on the obtaining of data and interpretation of results, Acknowledgements, Conflict of interests, Assignment of rights and distribution.

The Management of ECORFAN-Mexico, S.C. claims to the Authors of the Scientific Work that its content must be original, unpublished and of Scientific, Technological and Innovation content in order to submit it for evaluation.

The Authors signing the Scientific Work must be the same who have contributed to its conception, realization and development, as well as to the obtaining of the data, the interpretation of the results, its writing and revision. The Corresponding Author of the proposed Scientific Work should fill in the following form.

Title of the Scientific Work:

- The submission of a Scientific Paper to ECORFAN Proceedings implies the author's commitment not to submit it simultaneously to the consideration of other serial publications. To do so, he/she must complete the Originality Form for his/her Scientific Paper, unless it is rejected by the Referee Committee, it may be withdrawn.
- None of the data presented in this Scientific Work has been plagiarized or invented. The original data are clearly distinguishable from those already published. And we are aware of the PLAGSCAN test, if a positive plagiarism level is detected, we will not proceed to refereeing.
- The references on which the information contained in the Scientific Work is based are cited, as well as theories and data from other previously published Scientific Works.
- The authors sign the Authorization Form for their Scientific Work to be disseminated by the means that ECORFAN-Mexico, S.C. in its Holding Mexico considers pertinent for the dissemination and diffusion of their Scientific Work, ceding their Scientific Work Rights.
- Consent has been obtained from those who have provided unpublished data obtained through verbal or written communication, and such communication and authorship are properly identified.
- The Author and Co-Authors signing this work have participated in its planning, design and execution, as well as in the interpretation of the results. Likewise, they critically reviewed the work, approved its final version and agree with its publication.
- No signature responsible for the work has been omitted and the criteria for Scientific Authorship have been met.
- The results of this Scientific Work have been interpreted objectively. Any results contrary to the views of the signatories are stated and discussed in the Scientific Work

Copyright and Access

The publication of this Scientific Work implies the assignment of the copyright to ECORFAN-Mexico, S.C. in its Holding Mexico for its ECORFAN Proceedings, which reserves the right to distribute on the Web the published version of the Scientific Work and the availability of the Scientific Work in this format implies for its Authors the compliance with the provisions of the Law of Science and Technology of the United Mexican States, regarding the obligation to allow access to the results of Scientific Research.

Title of the Scientific Work:

Name and surname(s) of Contact Author and Co-authors	Signature
1.	
2.	
3.	
4.	

Principles of Ethics and Editorial Conflict Resolution Statement

Editor's Responsibilities

The Editor undertakes to guarantee the confidentiality of the evaluation process, and may not reveal the identity of the Authors to the Referees, nor may he/she reveal the identity of the Referees at any time.

The Editor assumes the responsibility of duly informing the Author of the stage of the editorial process in which the submitted text is, as well as of the resolutions of the Double Blind Arbitration.

The Editor must evaluate manuscripts and their intellectual content without distinction of race, gender, sexual orientation, religious beliefs, ethnic origin, nationality, or political philosophy of the Authors.

The Editor and its editorial staff of ECORFAN® Holdings will not disclose any information about the submitted Scientific Work to anyone other than the corresponding Author.

The Editor must make fair and impartial decisions and ensure a fair peer review process.

Responsibilities of the Editorial Board

The description of the peer review process is made known by the Editorial Board so that the Authors are aware of the evaluation criteria and will always be ready to justify any controversy in the evaluation process. In case of Plagiarism Detection to the Scientific Work, the Committee notifies the Authors for Violation of the Right of Scientific, Technological and Innovation Authorship.

Responsibilities of the Referee Committee

The Referees undertake to notify any unethical conduct on the part of the Authors and to point out any information that may be a reason to reject the publication of the Scientific Work. In addition, they must undertake to keep confidential the information related to the Scientific Work they evaluate.

Any manuscript received for refereeing must be treated as a confidential document, not to be shown or discussed with other experts, except with the permission of the Editor.

Referees should conduct themselves in an objective manner; any personal criticism of the Author is inappropriate.

Referees should express their views clearly and with valid arguments that contribute to the Scientific, Technological and Innovation achievements of the Author.

Referees should not evaluate manuscripts in which they have conflicts of interest and which have been notified to the Editor before submitting the Scientific Work for evaluation.

Responsibilities of Authors

Authors must guarantee that their Scientific Works are the product of their original work and that the data have been obtained in an ethical manner.

Authors must guarantee that they have not been previously published or that they are not being considered in another serial publication.

Authors must strictly follow the rules for the publication of Scientific Works defined by the Editorial Board.

Authors should consider that plagiarism in all its forms constitutes unethical editorial conduct and is unacceptable; consequently, any manuscript that incurs in plagiarism will be eliminated and will not be considered for publication.

Authors should cite publications that have been influential in the nature of the Scientific Work submitted for refereeing.

Information Services

Indexing - Bases and Repositories

RESEARCH GATE (Germany)

MENDELEY (Bibliographic Reference Manager)

GOOGLE SCHOLAR (Citation Indexes-Google)

REDIB (Ibero-American Network of Innovation and Scientific Knowledge- CSIC)

Editorial Services

Citation Identification and H Index

Originality and Authorization Format Management

Proceedings Testing with PLAGSCAN

Evaluation of Scientific Work

Issuance of Referee Certificate

Scientific Work Editing

Web Layout

Indexing and Repository

Publication of Scientific Work

Scientific Work Certificate

Invoicing for Publishing Services

Editorial Policy and Administration

Park Pedregal Business. 3580 – Adolfo Ruiz Cortines Boulevard – CP.01900. San Jerónimo Aculco – Álvaro Obregón, Mexico City. Tel: +52 1 55 6159 2296, +52 1 55 1260 0355, +52 1 55 6034 9181; E-mail: contact@ecorfan.org www.ecorfan.org.

ECORFAN®

Editor in Chief

VARGAS-DELGADO, Oscar. PhD

Executive Director

RAMOS-ESCAMILLA, María. PhD

Editorial Director

PERALTA-CASTRO, Enrique. MsC

Web Designer

ESCAMILLA-BOUCHAN, Imelda. PhD

Web Diagrammer

LUNA-SOTO, Vladimir. PhD

Editorial Assistant

TREJO-RAMOS, Iván. BsC

Philologist

RAMOS-ARANCIBIA, Alejandra. BsC

Advertising and Sponsorship

(ECORFAN® - Mexico – Bolivia – Spain – Ecuador – Cameroon – Colombia - El Salvador – Guatemala – Nicaragua – Peru – Paraguay - Democratic Republic of The Congo - Taiwan), sponsorships@ecorfan.org

Site Licenses

03-2010-032610094200-01-For printed material, 03-2010-031613323600-01-For electronic material, 03-2010-032610105200-01-For photographic material, 03-2010-032610115700-14-For Compilation of Data, 04 -2010-031613323600-01-For its Web page, 19502-For Ibero-American and Caribbean Indexing, 20-281 HB9-For Latin American Indexing in the Social Sciences and Humanities, 671-For Indexing in Electronic Scientific Journals in Spain and Latin America, 7045008-For dissemination and publication in the Ministry of Education and Culture-Spain, 25409-For its repository in the University Library-Madrid, 16258-For its indexing in Dialnet, 20589-For Indexing in the Directory in the countries of Iberoamerica and the Caribbean, 15048-For the international registration of Congresses and Colloquia. financingprograms@ecorfan.org

Management Offices

Park Pedregal Business. 3580 – Adolfo Ruiz Cortines Boulevard – CP.01900. San Jerónimo Aculco – Álvaro Obregón, Mexico City.

21 Santa Lucia, CP-5220. Libertadores -Sucre - Bolivia.

38 Matacerquillas, CP-28411. Moralzarzal -Madrid-Spain.

18 Marcial Romero, CP-241550. Avenue, Salinas I - Santa Elena-Ecuador.

1047 Avenida La Raza - Santa Ana, Cusco-Peru.

Boulevard de la Liberté, Immeuble Kassap, CP-5963.Akwa- Douala-Cameroon.

Avenida Suroeste, San Sebastian - León-Nicaragua.

31 Kinshasa 6593- Republique Démocratique du Congo.

Avenida San Quentin, R 1-17 Miralvalle - San Salvador-El Salvador.

16 kilometers, U.S. highway, Terra Alta house, D7 Mixco Zone 1-Guatemala.

105 Alberdi Rivarola Capitán, CP-2060. Luque City- Paraguay.

69 Street YongHe District, Zhongxin. Taipei-Taiwan.

43 Street # 30 -90 B. El Triunfo CP.50001. Bogotá-Colombia.



9 7 8 6 0 7 8 9 4 8 1 6 1

ISBN 978-607-8948-16-1



www.ecorfan.org